

Project Number: MA-RYL-1314

Mathematical Modeling of Influenza Viruses

A Major Qualifying Project

submitted to the Faculty

of the

WORCESTER POLYTECHNIC INSTITUTE

in partial fulfillment of the requirements for the

Degree of Bachelor of Science

by

Linan Zhang

Tianyu Li

Zhaokun Xue

March 14, 2014

Approved

Professor Roger Y. Lui
Major Advisor

Abstract

This Major Qualifying Project can be divided into three parts. We first start with the simplest SIR model to describe the transmission of communicable disease through individuals. We analyze the SIR model and the SEIR model with periodic transmission rates. With a constant transmission rate in the SIR or SEIR model, the occurrence of an epidemic outbreak depends on the Basic Reproduction Number of the model. But with a periodic transmission rate, small amplitude periodic solutions exhibiting a sequence of period-doubling bifurcations may appear. Then we focus on the two-strain SIR model with constant transmission rate. The two-strain model displays three basic relationships between the two viruses: coexistence, replacement, and periodic alternation between coexistence and replacement. These relationships are determined by the existence and stability of each equilibrium point. If there is no stable equilibrium point, the two-strain model has periodic solutions. We also study the two-strain SIR model with periodic transmission rate. The last part of this project concerns patterns observed from data downloaded from the World Health Organization (WHO) on the infective individuals of H1N1(77), H1N1(09), and H3N2(68) viruses.

Acknowledgments

We would like to thank Professor Roger Lui of the Mathematical Sciences Department for his continuous advice and assistance throughout this project. We would also like to thank Professor Daihai He of the Applied Mathematics Department, Hong Kong Polytechnic University, who assisted us in building the two-strain SIR model and downloading data from WHO.

Contents

1	Introduction	7
1.1	Biology Background	7
1.1.1	Classification of Influenza Viruses	7
1.1.2	Influenza Pandemic	8
1.1.3	Antigenic Drift	10
1.1.4	Antigenic Shift	11
1.2	The One-Strain SIR Model	11
2	The One-Strain Influenza Models with Periodic Transmission Rate	14
2.1	Analysis of the SIR Model	14
2.2	Analysis of the SEIR Model	19
2.3	Effective Infectee Number of the SEIR Model	24
3	The Two-Strain Influenza Model	27
3.1	Introduction	27
3.2	Analyses of the Equilibrium Points	28
3.2.1	Analysis of \mathbf{E}_1	29
3.2.2	Analysis of \mathbf{E}_2	29
3.2.3	Analysis of \mathbf{E}_3	31
3.2.4	Analysis of \mathbf{E}_4	33
4	Stability of Interior Equilibrium Points	35
4.1	Analyses of the Model when $F_0 < 1$	35
4.1.1	$0 < \beta < \gamma \left(1 + \frac{\delta_1}{\delta_2}\right)$	36
4.1.2	$\gamma \left(1 + \frac{\delta_1}{\delta_2}\right) < \beta < 2\gamma$	36
4.1.3	$2\gamma < \beta < \gamma \left(1 + \frac{\delta_2}{\delta_1}\right)$	38
4.1.4	$\gamma \left(1 + \frac{\delta_2}{\delta_1}\right) < \beta < (2 + \delta_2 - \delta_1)\gamma + (\delta_2 - \delta_1)$	39
4.2	Analyses of the Model when $F_0 > 1$	40
4.2.1	Stability of \mathbf{E}_4	40
4.2.2	Stability of \mathbf{E}_1	42
4.2.3	Existence and Stability of \mathbf{E}_2 and \mathbf{E}_3	42

5	Effects of Transmission Rate in the Two-strain Model	47
5.1	Two-strain SIR Model with Constant Transmission Rate	47
5.1.1	Coexistence	48
5.1.2	Replacement	48
5.1.3	Periodic and Alternating Coexistence and Replacement	48
5.2	Two-strain SIR Model with Periodic Transmission Rate	50
5.2.1	Coexistence	50
5.2.2	Replacement	51
5.2.3	Periodic and Alternating Coexistence and Replacement	51
6	Analysis of the WHO Data	57
6.1	Downloading Data from FluNet	57
6.2	Interpolation of the Data	58
6.3	Interpretation of the Data	58
6.3.1	Replacement of H1N1(77) by H1N1(09)	58
6.3.2	Coexistence of H1N1 and H3N2(68)	60
6.3.3	Skips of H1N1(09) and H3N2(68)	61
7	Conclusion	64
A	List of Symbols	69
B	Matlab Scripts	70
B.1	SIRperiodic.m	70
B.2	SEIRstable.m	71
B.3	SIRSIR.m	72
B.4	SIRSIRplot.m	78
B.5	simulateE4.m	82
B.6	E4root.m	84

List of Figures

1.1	Trajectories of the SIR Model with $\gamma = 1$ and $\beta = 2$	13
2.1	Trajectories of the SIR Model with $\gamma = 1$ and $\beta = 3$ and $\mu = 1$	16
2.2	$-\log(I)$ vs. t and $-\log(I)$ vs. $-\log(S)$ of the SIR Model with $\kappa = 0.07$	17
2.3	$-\log(I)$ vs. t and $-\log(I)$ vs. $-\log(S)$ of the SIR Model with $\kappa = 0.08$	17
2.4	$-\log(I)$ vs. t and $-\log(I)$ vs. $-\log(S)$ of the SIR Model with $\kappa = 0.0875$	18
2.5	$-\log(I)$ vs. t and $-\log(I)$ vs. $-\log(S)$ of the SIR Model with $\kappa = 0.09$	18
2.6	$-\log(I)$ vs. t and $-\log(I)$ vs. $-\log(S)$ of the SEIR Model with $\kappa = 0.03$	21
2.7	$-\log(I)$ vs. t and $-\log(I)$ vs. $-\log(S)$ of the SEIR Model with $\kappa = 0.05$	22
2.8	$-\log(I)$ vs. t and $-\log(I)$ vs. $-\log(S)$ of the SEIR Model with $\kappa = 0.05$	22
2.9	$-\log(I)$ vs. t and $-\log(I)$ vs. $-\log(S)$ of the SEIR Model with $\kappa = 0.08$	23
2.10	$-\log(I)$ vs. t and $-\log(I)$ vs. $-\log(S)$ with $\kappa = 0.1$	23
2.11	$-\log(I)$ vs. t and $-\log(I)$ vs. $-\log(S)$ of the SEIR Model with $\kappa = 0.15$	24
2.12	$-\log(I)$ vs. t and $-\log(I)$ vs. $-\log(S)$ of the SEIR Model with $\kappa = 0.25$	24
2.13	$-\log(I)$ vs. t and $-\log(I)$ vs. $-\log(S)$ of the SEIR Model with $\kappa = 0.26$	25
2.14	$-\log(I)$ vs. t and $-\log(I)$ vs. $-\log(S)$ of the SEIR Model with $\kappa = 0.27$	25
4.1	\mathbf{E}_1 is stable; \mathbf{E}_2 , \mathbf{E}_3 , and \mathbf{E}_4 do not exist	37
4.2	\mathbf{E}_1 is unstable; \mathbf{E}_3 is stable; \mathbf{E}_2 and \mathbf{E}_4 do not exist	38
4.3	\mathbf{E}_1 and \mathbf{E}_2 are unstable; \mathbf{E}_3 is stable; \mathbf{E}_4 does not exist	40
4.4	\mathbf{E}_1 and \mathbf{E}_3 are unstable; \mathbf{E}_2 does not exist; \mathbf{E}_4 is stable	43
4.5	\mathbf{E}_1 , \mathbf{E}_3 , and \mathbf{E}_4 are unstable; \mathbf{E}_2 does not exist	44
4.6	\mathbf{E}_1 , \mathbf{E}_2 , and \mathbf{E}_3 are unstable; \mathbf{E}_4 is stable	45
4.7	\mathbf{E}_1 , \mathbf{E}_2 , \mathbf{E}_3 , and \mathbf{E}_4 are all unstable	46
5.1	Coexistence between virus 1 and virus 2	48
5.2	Replacement of virus 2 by virus 1	49
5.3	Periodic alternation between coexistence and replacement	49
5.4	Coexistence between virus 1 and virus 2 with $\kappa = 0.1$ and $\kappa = 0.4$	50
5.5	Replacement of virus 2 by virus 1 with $\kappa = 0.1$ and $\kappa = 0.4$	52
5.6	Periodic and alternating coexistence and replacement with $\kappa = 0.1$	53
5.7	Periodic and alternating coexistence and replacement with $\kappa = 0.2$	54
5.8	Periodic and alternating coexistence and replacement with $\kappa = 0.3$	55
5.9	Periodic and alternating coexistence and replacement with $\kappa = 0.4$	56
6.1	Replacement of H1N1(77) by H1N1(09) in some European and Asian regions	59
6.2	Coexistence of H1N1(77) and H3N2(68) in the American regions	61

6.3	Coexistence of H1N1(09) and H3N2(68) in the American regions (Due to the magnitude, the peaks of H3N2(68) are hard to see)	62
6.4	Skips of H1N1(09) and H3N2(68) in the European regions	63

Chapter 1

Introduction

Influenza, commonly known as "flu", is an infectious disease of birds and mammals caused by RNA viruses of the family Orthomyxoviridae, the influenza viruses (Urban, 2009). It can cause mild to severe illness. Serious outcomes of flu infection can result in hospitalization or death. Some people, such as the old, the young, and those with certain health conditions, are at high risk for serious flu complications (Unknown, 2013a).

Epidemiologists use systems of differential equations to model the number of people infected with a virus in a closed population over time. The simplest system is the Kermack-McKendrick model.

1.1 Biology Background

1.1.1 Classification of Influenza Viruses

In virus classification, influenza viruses are RNA viruses that make up three of the five genera of the family Orthomyxoviridae: Influenzavirus A, Influenzavirus B, and Influenzavirus C. The type A Influenza viruses are the most virulent human pathogens among the three influenza types and cause the severest disease. The influenza A virus can be subdivided into 11 different serotypes based on the antibody response to hemagglutinin and neuraminidase which form the basis of the H and N. These serotypes are: H1N1, H2N2, H3N2, H5N1, H7N7, H1N2, H9N2, H7N2, H7N3, H10N7, H7N9, (Hay et al., 2001)(Hilleman, 2002). Wild aquatic birds are the natural hosts for a large variety of influenza A (Mettenleiter and Sobrino, 2008). As for influenza B virus, it almost exclusively infects humans and is less common than influenza A (Hay et al., 2001). The only other animals known to be susceptible to influenza B infection are the seal (Osterhaus et al., 2000) and the ferret (Jakeman et al., 1994). Influenza C virus, which infects humans, dogs, and pigs, sometimes causing both severe illness and local epidemics, is less common than the other types (Matsuzaki et al., 2002)(Taubenberger and Morens, 2008).

1.1.2 Influenza Pandemic

A pandemic is a worldwide disease outbreak. It is determined by how the disease spreads not how many deaths it causes. When an influenza virus especially influenza A virus emerges, an influenza pandemic can occur (Unknown, 2013e).

Influenza pandemics usually occur when a new strain of the influenza virus is transmitted to humans from another animal species. Pigs, chickens, and ducks are thought to be important in the emergence of new human strains. Influenza A viruses can occasionally be transmitted from wild birds to other species, which causes outbreaks in domestic poultry and gives rise to human influenza pandemics (Kawaoka, 2006)(Mettenleiter and Sobrino, 2008). WHO has produced a six-phase classification that describes the process by which a novel influenza virus moves from the first few infections in humans through to a pandemic. These six phases also reflect WHO's risk assessment of the global situation regarding each influenza virus with pandemic potential that infects humans (Unknown, 2013b). These six phases are followed by post-peak period and post-pandemic period (Unknown, 2009b).

Phase 1: No viruses circulating among animals have been reported to cause infections in humans.

Phase 2: An animal influenza virus circulating among domesticated or wild animals is known to have caused infection in humans, and is therefore considered a potential pandemic threat.

Phase 3: An animal or human-animal influenza reassortant virus has caused sporadic cases or small clusters of disease in people, but has not resulted in human-to-human transmission sufficient to sustain community-level outbreaks.

Phase 4: This phase is characterized by verified human-to-human transmission of an animal or human-animal influenza reassortant virus able to cause community-level outbreaks. The ability to cause sustained disease outbreaks in a community marks a significant upwards shift in the risk for a pandemic.

Phase 5: Characterized by human-to-human spread of the virus into at least two countries in one WHO region.

Phase 6: Characterized by community level outbreaks in at least one other country in a different WHO region in addition to the criteria defined in Phase 5.

Post-Peak Period: During the post-peak period, pandemic disease levels in most countries with adequate surveillance will have dropped below peak observed levels.

Post-Pandemic Period: In the post-pandemic period, influenza disease activity will have returned to levels normally seen for seasonal influenza.

Until now, four main influenza pandemics have occurred throughout history:

1918 - 1920

1918 flu pandemic (January 1918 - December 1920) was an unusually deadly influenza pandemic. And it was the first of the two pandemics involving H1N1 influenza virus (the second being the 2009 flu pandemic) (Taubenberger and Morens, 2006). At that time, to maintain morale, wartime censors minimized early reports of illness and mortality in Germany, Britain, France, and the United States; but papers were free to report the epidemic's effects in neutral Spain (such as the grave illness of King Alfonso XIII), creating a false impression of Spain as especially hard hit, thus the pandemic's nickname Spanish flu (Galvin). On the U.S. Department of Health & Human Services website's 1918 flu pandemic report, it announces that approximately 20% to 40% of the worldwide population became ill, around 50 million people died, and nearly 675,000 people died in the United States (Unknown, 2013f).

1957 - 1958

1957 flu pandemic is also called the Asian flu, which is the H2N2 subtype of influenza A. Asian flu pandemic outbreak originated in China in early 1956, and lasted until 1958 (Greene, 2006). Estimates of worldwide deaths vary widely depending on source, ranging from 1 million to 4 million, with WHO settling on "about two million." Death toll in the US was approximately 69,800 (Greene and Moline, 2006). The elderly people had the highest rates of death. The Asian flu strain later evolved via antigenic shift into H3N2, which caused a milder pandemic from 1968 to 1969 (Hong, 2006).

1968 - 1969

The 1968-70 pandemic or Hong Kong flu was also relatively mild compared to the Spanish flu (Unknown, 2013d). The Hong Kong flu was a category 2 flu pandemic. It was caused by an H3N2 strain of influenza A virus which descended from H2N2. The Hong Kong flu affected mainly the elderly and killed approximately one million people in the world (Mandel, 2009)(Paul, 2008)(Unknown, 2009a). In the US, there were about 33,800 deaths (Unknown, 2013c).

2009 - 2010

The most recent one is 2009 flu pandemic or swine flu which is the second pandemic involving H1N1 influenza virus (the first one is the 1918 flu pandemic). On June 11, 2009, Dr. Margaret Chan, the director of WHO, announced that the world now at the start of 2009 influenza pandemic. By that time, nearly 30,000 confirmed cases have been reported in 74 countries (Chan, 2009). According to the data on the U.S. Department of Health & Human Services website, by November 2009, 48 states in the United States had reported cases of H1N1, mostly in young people. The Centers of Disease Control and Prevention (CDC) announced that approximately 43 million to 89 million people had H1N1 between April 2009 and April 2012 and estimated between 8,870 and 18,300 H1N1 related deaths. On August 10, 2010 WHO declared an end to the global H1N1 flu pandemic (Chan, 2009).

Influenza pandemics have caused tremendous impacts on society and economy. The 1918 influenza pandemic claimed 40 million deaths worldwide over 18 months; 675,000 of those

deaths occurred in the United States. The 1918 influenza also estimated of its overall economic impact range from a 4.25 to a 5.5 percent annual decline in GDP in the US. In addition, the deaths of the 1918 Influenza were aged 18 to 40. Such a sudden and irreversible decline in the labor force would likely produce negative economic consequences in the following years (Ott, 2008).

Not only the 1918 influenza pandemic led to such huge social and economic impacts to the United States and the world, but every severe pandemic in the history did lead similarly disasters on both society and economy to the whole world. Therefore, it is really valuable for us to work on our project, "Mathematical Modeling of Influenza Viruses". Studying on this project could help us get better understanding of behaviors among two or more influenza viruses. In the future, our analysis might help us predict possible outcomes and trends of influenza viruses outbreaks in advance. This could help us prepare the prevention work early and reduce the loss as much as possible.

1.1.3 Antigenic Drift

Two processes drive the antigens to change: antigenic drift and antigenic shift. These are small changes in the virus that happen continually over time, and antigenic drift is more common than the other. (Earn et al., 2002).

Antigenic drift is the mechanism for variation in viruses that involves the accumulation of mutations within the genes that code for antibody-binding sites. This results in a new strain of virus particles which cannot be inhibited as effectively by the antibodies that were originally targeted against previous strains, making it easier for the virus to spread throughout a partially immune population (Earn et al., 2002). This process works as follows: a person infected with a particular flu virus strain develops antibody against that virus. As newer virus strains appear, the antibodies against the older strains no longer recognize the newer virus, and reinfection can occur. This is one of the main reasons why people can get the flu more than one time (Unknown, 2011a). Antigenic drift occurs in both influenza A and influenza B viruses (Earn et al., 2002). The process of antigenic drift is best characterized in influenza type A viruses, and the emergence of a new strain of influenza A due to antigenic drift can cause an influenza epidemic or pandemic (Rogers, 2007).

The rate of antigenic drift is dependent on two characteristics: the duration of the epidemic and the strength of host immunity. A longer epidemic allows for selection pressure to continue over an extended period of time and stronger host immune responses increase selection pressure for development of novel antigens (Earn et al., 2002).

Antigenic drift is also known to occur in HIV (human immunodeficiency virus), which causes AIDS, and in certain rhinoviruses, which cause common colds in humans. It also has been suspected to occur in some cancer-causing viruses in humans. Antigenic drift of such viruses is believed to enable the viruses to escape destruction by immune cells, thereby promoting virus survival and facilitating cancer development (Rogers, 2007).

1.1.4 Antigenic Shift

Of greater public health concern is the process of antigenic shift also called reassortment. Antigenic shift is the process by which two or more different strains of a virus, or strains of two or more different viruses, combine to form a new subtype having a mixture of the surface antigens of the two or more original strains. The term is often applied specifically to influenza (Narayan and Griffin, 1977). Unlike Antigenic drift which can occur in all kinds of influenza, antigenic shift only occurs in influenza virus A because it can infect not only humans, but also other mammals and birds (Treanor, 2004) (Zambon, 1999).

Antigenic shift results in a new influenza A subtype or a virus with a hemagglutinin or a hemagglutinin and neuraminidase combination that has emerged from an animal population that is so different from the same subtype in humans that most people do not have immunity to the new virus. Such a shift occurred in the spring of 2009, when a new H1N1 virus with a new combination of genes emerged to infect people and quickly spread, causing a pandemic.(Unknown, 2011b)

1.2 The One-Strain SIR Model

The SIR model is an epidemiological model that computes the theoretical number of people infected with a contagious illness in a closed population over time. One of the basic one strain SIR models is Kermack-McKendrick Model. The Kermack-McKendrick Model is used to explain the rapid rise and fall in the number of infective patients observed in epidemics. It assumes that the population size is fixed (i.e., no births, no deaths due to disease nor by natural causes), incubation period of the infectious agent is instantaneous, and duration of infectivity is the same as the length of the disease. It also assumes a completely homogeneous population with no age, spatial, or social structure.

The model consists of a system of three coupled nonlinear ordinary differential equations:

$$\dot{S} = -\beta SI \tag{1.1a}$$

$$\dot{I} = \beta SI - \gamma I \tag{1.1b}$$

$$\dot{R} = \gamma I \tag{1.1c}$$

where S , I and R are the number of susceptible, infectious and recovered/immunized individuals respectively. β is the transmission rate, γ is the recovery rate, and $\dot{}$ denotes the derivative with respect to time t . Let N denote the population size. Clearly,

$$N = S + I + R,$$

and $\dot{N} = \dot{S} + \dot{I} + \dot{R} = 0$.

Applying phase-plane analysis to the first two equations, set

$$\dot{S} = -\beta SI = 0, \quad (1.2a)$$

$$\text{and } \dot{I} = (\beta S - \gamma)I = 0. \quad (1.2b)$$

Therefore, the S-nullclines are

$$S = 0, \quad (1.3a)$$

$$I = 0; \quad (1.3b)$$

and the I-nullclines are

$$S = \frac{\gamma}{\beta}, \quad (1.4a)$$

$$I = 0. \quad (1.4b)$$

These three nullclines form a triangle with vertices $(0, 0)$, $(N, 0)$ and $(0, N)$ on the SI -plane. This triangle is an invariant region of steady states. A trajectory always starts from the line $S + I = N$, since $R(0) = 0$. A point is an equilibrium point if and only if $\dot{S} = \dot{I} = \dot{R} = 0$. Thus, any trajectory will converge to a point $(S, 0)$ where $0 \leq S \leq N$.

If $S(0) = S_0 < \frac{\gamma}{\beta}$, both $S(t)$ and $I(t)$ decreases and converges to a point on the S -axis.

There is no outbreak. If $S_0 > \frac{\gamma}{\beta}$, $I(t)$ first increases in the region $\left(\frac{\gamma}{\beta}, 1\right)$ and then decreases to 0. In this case, an outbreak occurs. See Figure 1.1.

Starting from $(S_1(0), I_1(0))$, both $S(t)$ and $I(t)$ decreases to an equilibrium point on the S -axis. There is no outbreak. In the contrast, starting from $(S_2(0), I_2(0))$, $I(t)$ first increases, hitting its maximum where $S(t) = \frac{\gamma}{\beta}$, and then decreases to 0. Thus, an outbreak occurs.

In conclusion, there is a threshold value $\frac{\gamma}{\beta}$. Define the basic reproduction number (epidemiological threshold) of this model:

$$R_0 = \frac{N\beta}{\gamma} \approx \frac{S_0\beta}{\gamma}. \quad (1.5)$$

Then

$$S_0 > \frac{\gamma}{\beta} \iff R_0 > 1, \quad (1.6)$$

$$\text{and } S_0 < \frac{\gamma}{\beta} \iff R_0 < 1. \quad (1.7)$$

When $R_0 < 1$, each person who contracts to the disease will infect less than one person before dying or recovering. When $R_0 > 1$, the opposite occurs and there will be a outbreak of disease.

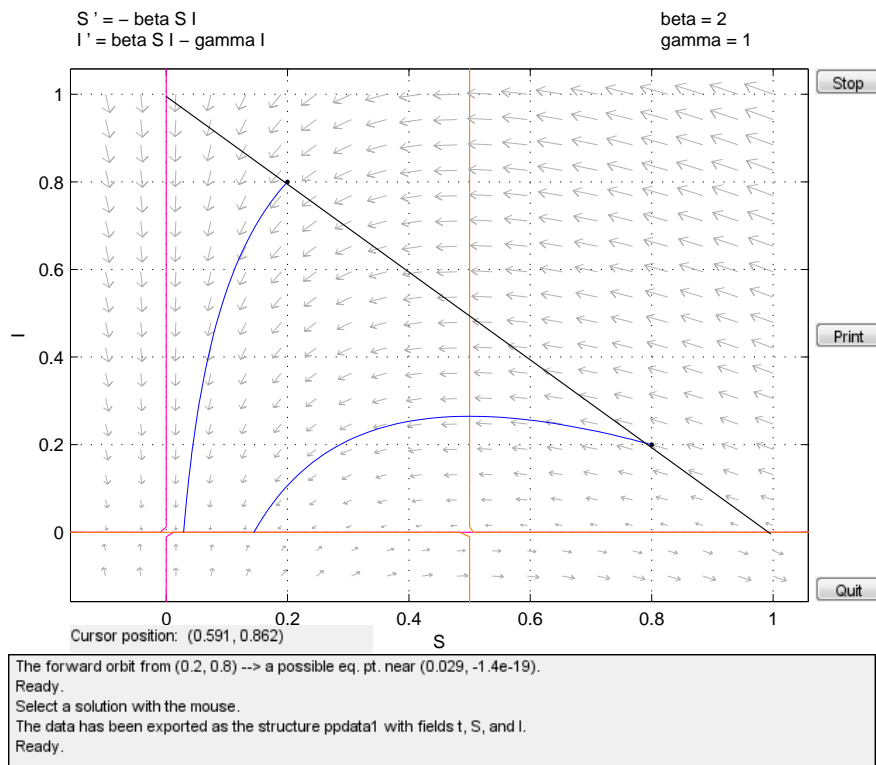


Figure 1.1: Trajectories of the SIR Model with $\gamma = 1$ and $\beta = 2$
 $(S_1(0), I_1(0)) = (0.2, 0.8)$. $(S_2(0), I_2(0)) = (0.8, 0.2)$.
 Magenta curve: S-nullcline; orange curves: I-nullclines.
 Blue curves: trajectories; black curve: invariant line.

Chapter 2

The One-Strain Influenza Models with Periodic Transmission Rate

2.1 Analysis of the SIR Model

In Chapter 1, we introduced the SIR model (1.1) in which birth rate and death rate are not taken into account, and the transmission rate β is considered as a constant. Now we assume (1) that new susceptible are introduced at a constant birth rate μ , (2) that the infectious and recovered classes experience the same constant birth rate μ , and (3) that all the three classes experience the same constant death rate, equal to the birth rate μ . The third assumption ensures that the population size is fixed. For simplicity, set $N = 1$, which can be achieved by non-dimensionalization. The new SIR model is:

$$\dot{S} = \mu - \mu S - \beta SI \quad (2.1a)$$

$$\dot{I} = \beta SI - (\mu + \gamma)I \quad (2.1b)$$

$$\dot{R} = \gamma I - \mu R \quad (2.1c)$$

Applying phase-plane analysis to the first two equations, set

$$\dot{S} = \mu - \mu S - \beta SI = 0, \quad (2.2a)$$

$$\text{and } \dot{I} = (\beta S - \mu - \gamma)I = 0. \quad (2.2b)$$

Therefore, the S-nullcline is

$$I = \frac{\mu}{\beta} \left(\frac{1}{S} - 1 \right), \quad (2.3)$$

and the I-nullclines are

$$S = \frac{\mu + \gamma}{\beta}, \quad (2.4a)$$

$$I = 0. \quad (2.4b)$$

These three nullclines form a triangle with vertices $(0, 0)$, $(1, 0)$ and $(0, 1)$ on the SI -plane. This triangle is an invariant region of steady states. A trajectory always starts from the line

$S + I = N = 1$, since $R(0) = 0$. The point $\mathbf{P}_1 = (S_1^*, I_1^*) = (1, 0)$ is always an equilibrium point, which is a solution of

$$\text{S-nullcline: } I = \frac{\mu}{\beta} \left(\frac{1}{S} - 1 \right), \quad (2.5a)$$

$$\text{I-nullcline: } I = 0. \quad (2.5b)$$

The other equilibrium point $\mathbf{P}_2 = (S_2^*, I_2^*)$ is the solution of

$$\text{S-nullcline: } I = \frac{\mu}{\beta} \left(\frac{1}{S} - 1 \right), \quad (2.6a)$$

$$\text{I-nullcline: } S = \frac{\mu + \gamma}{\beta}. \quad (2.6b)$$

Substitute $S_2^* = \frac{\mu + \gamma}{\beta}$ into (2.2a) and solve for I_2^* .

$$\begin{aligned} 0 &= \mu - \mu S_2^* - \beta S_2^* I_2^* \\ 0 &= \mu - \mu \frac{\mu + \gamma}{\beta} - \beta \frac{\mu + \gamma}{\beta} I_2^* \\ (\mu + \gamma) I_2^* &= \mu - \mu \frac{\mu + \gamma}{\beta} \\ I_2^* &= \frac{\mu}{\mu + \gamma} - \frac{\mu}{\beta} \end{aligned}$$

Therefore, the equilibrium point

$$\mathbf{P}_2 = \left(\frac{\mu + \gamma}{\beta}, \frac{\mu}{\mu + \gamma} - \frac{\mu}{\beta} \right) \quad (2.7)$$

exists if $\beta > \mu + \gamma$. Moreover, using Maple, it is not hard to see that the Jacobian of System (2.1) evaluated at \mathbf{P}_2 has no positive eigenvalues. Thus, if \mathbf{P}_2 exists, it must be stable.

If $S(0) = S_0 < \frac{\mu + \gamma}{\beta}$, then $S(t)$ increases and $I(t)$ decreases, converging to the equilibrium point. There is no outbreak. If $S_0 > \frac{\mu + \gamma}{\beta}$, $I(t)$ first increases, and then decreases to I_2^* . In this case, an outbreak occurs. See Figure 2.1.

Starting from $(S_1(0), I_1(0))$, $S(t)$ increases and $I(t)$ decreases to the equilibrium point. There is no outbreak. In the contrast, starting from $(S_2(0), I_2(0))$, $I(t)$ first increases, hitting its maximum where $S(t) = \frac{\mu + \gamma}{\beta}$, and then decreases to I_2^* . Thus, an outbreak occurs.

In conclusion, there is a threshold value $\frac{\mu + \gamma}{\beta}$. Define the basic reproduction number (epidemiological threshold) of this model:

$$R_0 = \frac{\beta}{\mu + \gamma} S_0. \quad (2.8)$$

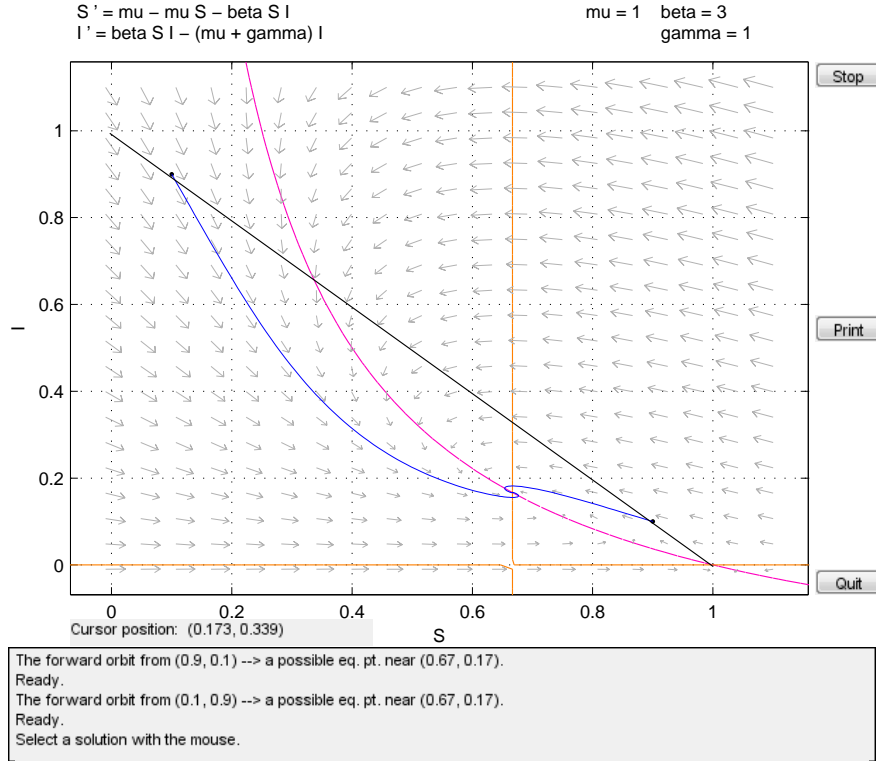


Figure 2.1: Trajectories of the SIR Model with $\gamma = 1$ and $\beta = 3$ and $\mu = 1$
 $(S_1(0), I_1(0)) = (0.1, 0.9)$. $(S_2(0), I_2(0)) = (0.9, 0.1)$.
Magenta curve: S-nullcline; orange curves: I-nullclines.
Blue curves: trajectories; black curve: invariant line.
Trajectory on the left, starting from (0.1,0.9), shows no outbreak.
Trajectory on the right, starting from (0.9,0.1), shows outbreak.

Then

$$S_0 > \frac{\mu + \gamma}{\beta} \iff R_0 > 1, \quad (2.9)$$

$$\text{and } S_0 < \frac{\mu + \gamma}{\beta} \iff R_0 < 1. \quad (2.10)$$

When $R_0 < 1$, each person who contracts to the disease will infect less than one person before dying or recovering. When $R_0 > 1$, there will be a outbreak of disease.

Now assume that the contact rate β is seasonally varying in time (with period 1 year), and use a simple sinusoidal form to model it:

$$\beta(t) = \beta_0(1 + \kappa \cos(2\pi t)), \quad (2.11)$$

where κ is called the degree of seasonality and $0 \leq \kappa \leq 1$.

Let $S_0 = 0.7$, $I_0 = 0.3$. Fix $\mu = 0.02$, $\gamma = 100$, and $\beta = 1800$. The following series of figures (Figure 2.2 - 2.5) displays the negation of logarithm of infective, $-\log(I)$, as a function of time and as a function of $-\log(S)$ for periodic solutions of System (2.1). The corresponding Matlab code can be found in Appendix B.1.

For κ very small, a stable periodical orbit having period 1 emerges from the endemic equilibrium point \mathbf{P}_2 . See Figure 2.2 with $\kappa = 0.07$.

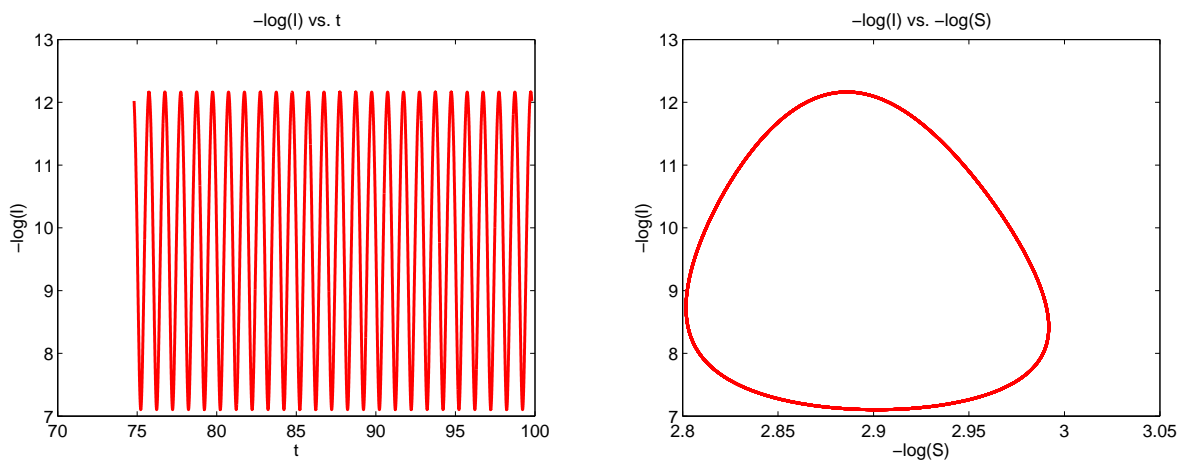


Figure 2.2: $-\log(I)$ vs. t and $-\log(I)$ vs. $-\log(S)$ of the SIR Model with $\kappa = 0.07$
Stable periodical solutions. There is no bifurcation.

As κ increases, past a critical value, the period 1 orbit becomes unstable and a stable biennial orbit appears. See Figure 2.3 with $\kappa = 0.08$ and Figure 2.4 with $\kappa = 0.0875$.

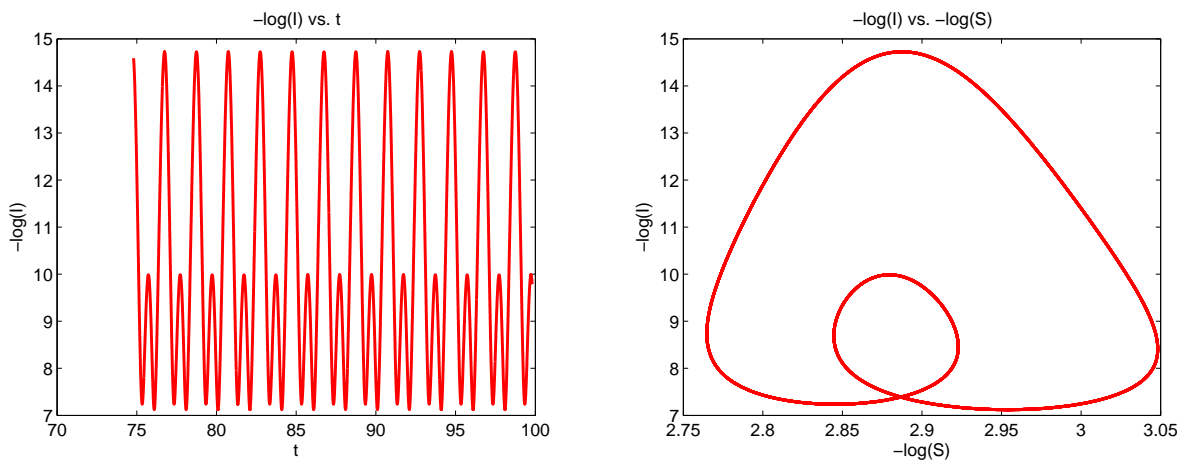


Figure 2.3: $-\log(I)$ vs. t and $-\log(I)$ vs. $-\log(S)$ of the SIR Model with $\kappa = 0.08$
Unstable periodical solutions. Period doubling bifurcation occurs.

An important feature of the biennial outbreak, or bifurcation, is that alternating years of high and low incidence, or effective infectee number, begin to appear, represented as inner and outer cycles respectively in Figure 2.3. Further information on effective infectee number and its derivation can be found in Section 2.3.

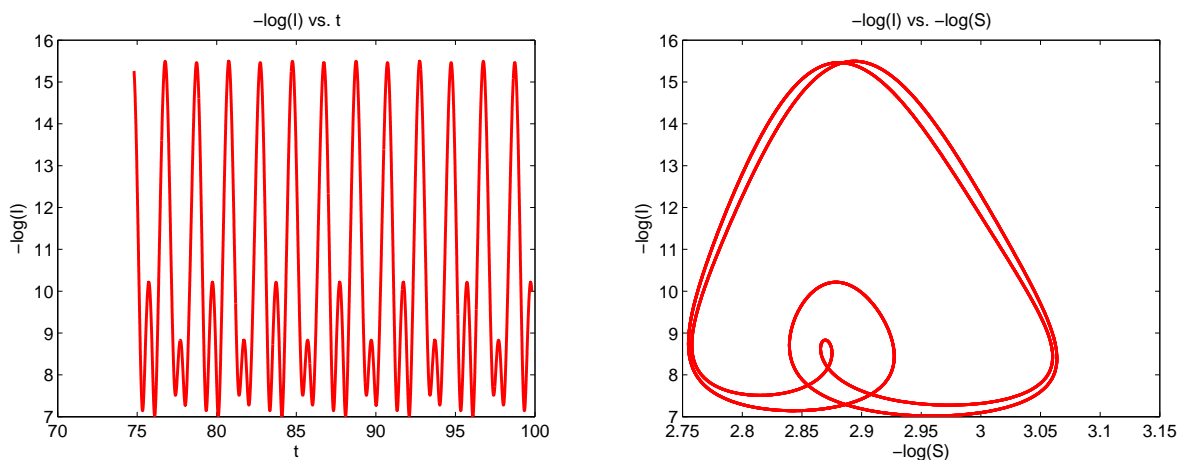


Figure 2.4: $-\log(I)$ vs. t and $-\log(I)$ vs. $-\log(S)$ of the SIR Model with $\kappa = 0.0875$ Unstable periodical solutions. Period doubling bifurcation occurs.

Further increments in κ yield chaotic period doubling bifurcation. In (Keeling et al., 2001), it is explained that nonlinear effects of the system play a stronger role than periodic behavior of seasonality. See Figure 2.5 with $\kappa = 0.09$.

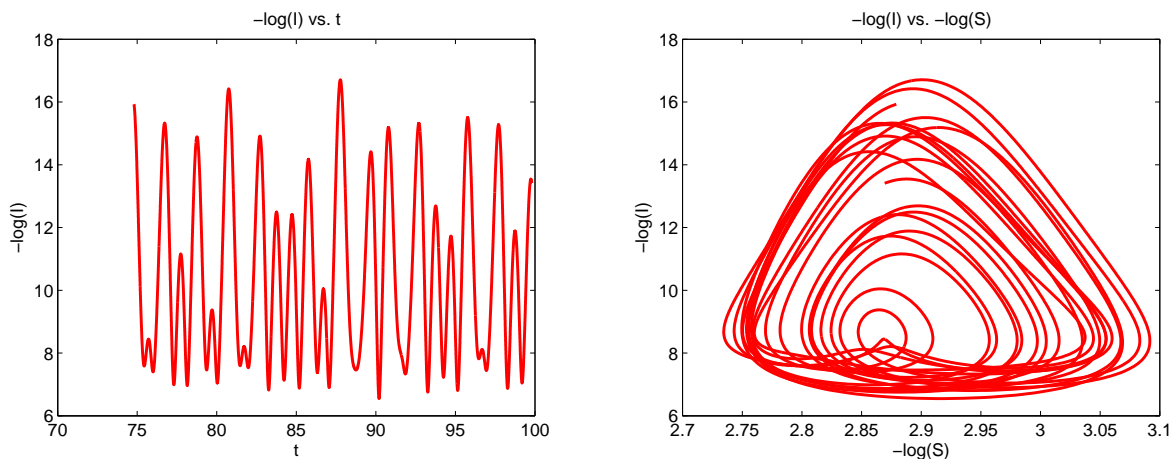


Figure 2.5: $-\log(I)$ vs. t and $-\log(I)$ vs. $-\log(S)$ of the SIR Model with $\kappa = 0.09$ Unstable periodical solutions. Bifurcation becomes chaotic.

In conclusion, for κ very small, a stable periodical orbit having period 1 emerges from the nontrivial equilibrium point \mathbf{P}_2 . As κ increases, past a critical value, the period 1 orbit becomes unstable and a stable biennial orbit appears, where occurs the period doubling bifurcation. Further increments in κ yield chaotic period doubling bifurcation.

2.2 Analysis of the SEIR Model

Now consider the population with constant size consisting of the fourth class of individuals: the exposed, denoted as E . Then $S + E + I + R = 1$. Assume that exposed individuals become infective at a rate α , which leads the SIR model (2.1) to:

$$\dot{S} = \mu - \mu S - \beta SI \quad (2.12a)$$

$$\dot{E} = \beta SI - (\mu + \alpha)E \quad (2.12b)$$

$$\dot{I} = \alpha E - (\mu + \gamma)I \quad (2.12c)$$

$$\dot{R} = \gamma I - \mu R \quad (2.12d)$$

Applying phase-plane analysis to the first three equations, set

$$\dot{S} = \mu - \mu S - \beta SI = 0, \quad (2.13a)$$

$$\dot{E} = \beta SI - (\mu + \alpha)E = 0, \quad (2.13b)$$

$$\text{and } \dot{I} = \alpha E - (\mu + \gamma)I = 0. \quad (2.13c)$$

Therefore, the S-nullcline is

$$I = \frac{\mu}{\beta} \left(\frac{1}{S} - 1 \right), \quad (2.14)$$

the E-nullcline is

$$E = \frac{\beta}{\mu + \alpha} SI, \quad (2.15)$$

and the I-nullcline is

$$E = \frac{\mu + \gamma}{\alpha} I, \quad (2.16)$$

These three nullclines form a tetrahedron with vertices $(0, 0, 0)$, $(1, 0, 0)$, $(0, 1, 0)$ and $(0, 0, 1)$ on the SEI -plane. This tetrahedron is an invariant region of steady states. A trajectory always starts from the plane $S + E + I = N = 1$, since $R(0) = 0$. The point $\mathbf{Q}_1 = (S_1^*, E_1^*, I_1^*) = (1, 0, 0)$ is always an equilibrium point, which clearly satisfies Equation (2.13).

The other equilibrium point $\mathbf{Q}_2 = (S_2^*, E_2^*, I_2^*)$ can be derived as the following:

$$\begin{aligned}\frac{\beta}{\mu + \alpha} S_2^* I_2^* &= \frac{\mu + \gamma}{\alpha} I_2^* \\ S_2^* &= \frac{(\mu + \gamma)(\mu + \alpha)}{\alpha\beta} \\ I_2^* &= \frac{\mu}{\beta} \left(\frac{1}{S_2^*} - 1 \right) = \frac{\mu\alpha}{(\mu + \gamma)(\mu + \alpha)} - \frac{\mu}{\beta} \\ E_2^* &= \frac{\mu + \gamma}{\alpha} I_2^* = \frac{\mu}{\mu + \alpha} - \frac{\mu(\mu + \gamma)}{\alpha\beta}\end{aligned}$$

Therefore, the equilibrium point

$$\mathbf{Q}_2 = (S_2^*, E_2^*, I_2^*) = \left(\frac{(\mu + \gamma)(\mu + \alpha)}{\alpha\beta}, \frac{\mu}{\mu + \alpha} - \frac{\mu(\mu + \gamma)}{\alpha\beta}, \frac{\mu\alpha}{(\mu + \gamma)(\mu + \alpha)} - \frac{\mu}{\beta} \right) \quad (2.17)$$

exists if $\beta > \frac{(\mu + \gamma)(\mu + \alpha)}{\alpha}$.

The Jacobian of System (2.12) evaluated at \mathbf{Q}_2 is

$$DF(\mathbf{Q}_2) = \begin{pmatrix} -\mu - \frac{\beta\mu}{\mu + \alpha} + \frac{\mu(\mu + \gamma)}{\alpha} & 0 & -\frac{(\mu + \gamma)(\mu + \alpha)}{\alpha} & 0 \\ \frac{\beta\mu}{\mu + \alpha} - \frac{\mu(\mu + \gamma)}{\alpha} & -\mu - \alpha & \frac{(\mu + \gamma)(\mu + \alpha)}{\alpha} & 0 \\ 0 & \alpha & -\mu - \gamma & 0 \\ 0 & 0 & \gamma & -\mu \end{pmatrix}. \quad (2.18)$$

In (Schwartz and Smith, 1983), it has been proved that \mathbf{Q}_2 must be asymptotically stable if it exists. The corresponding Matlab code that computes the stability of \mathbf{Q}_2 can be found in Appendix B.2.

If $S(0) = S_0 < \frac{(\mu + \gamma)(\mu + \alpha)}{\alpha\beta}$, then $I(t)$ always decreases, converging to the equilibrium point. There is no outbreak. If $S_0 > \frac{(\mu + \gamma)(\mu + \alpha)}{\alpha\beta}$, $I(t)$ first increases, and then decreases to I_2^* .

In conclusion, there is a threshold value $\frac{(\mu + \gamma)(\mu + \alpha)}{\alpha\beta}$. Define the basic reproduction number (epidemiological threshold) of this model:

$$R_0 = \frac{\alpha\beta}{(\mu + \gamma)(\mu + \alpha)} S_0. \quad (2.19)$$

Then

$$S_0 > \frac{(\mu + \gamma)(\mu + \alpha)}{\alpha\beta} \iff R_0 > 1, \quad (2.20)$$

$$\text{and } S_0 < \frac{(\mu + \gamma)(\mu + \alpha)}{\alpha\beta} \iff R_0 < 1. \quad (2.21)$$

When $R_0 < 1$, each person who contracts to the disease will infect less than one person before dying or recovering. When $R_0 > 1$, there will be an outbreak of disease.

Now assume that the contact rate β is seasonally varying in time, same as what has been done in Section 2.1,

$$\beta(t) = \beta_0(1 + \kappa \cos(2\pi t)).$$

Let $S_0 = 0.7$, $E_0 = 0.2$, $I_0 = 0.1$. Fix $\mu = 0.02$, $\gamma = 100$, $\alpha = 35.8$, and $\beta = 1800$. The following series of figures (Figure 2.6 - 2.14) displays the negation of logarithm of infective, $-\log(I)$, as a function of time and as a function of $-\log(S)$ for periodic solutions of System (2.12). The corresponding Matlab code is almost identical to Appendix B.1.

For κ very small, a stable periodical orbit having period 1 emerges from the endemic equilibrium point \mathbf{Q}_2 . See Figure 2.6 with $\kappa = 0.03$.

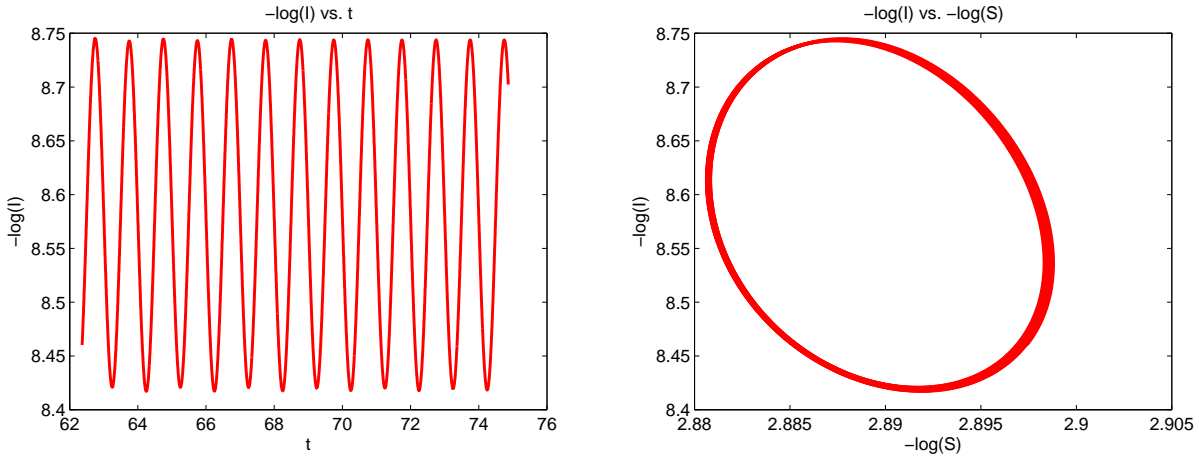


Figure 2.6: $-\log(I)$ vs. t and $-\log(I)$ vs. $-\log(S)$ of the SEIR Model with $\kappa = 0.03$
Stable periodical solutions. There is no bifurcation.

As κ increases, past a critical value, the period 1 orbit becomes unstable and a stable biennial orbit appears. See Figure 2.7 with $\kappa = 0.05$.

However, as t as to infinity, the period 2 orbit turns back to a stable period 1 orbit. See Figure 2.8 with $\kappa = 0.05$.

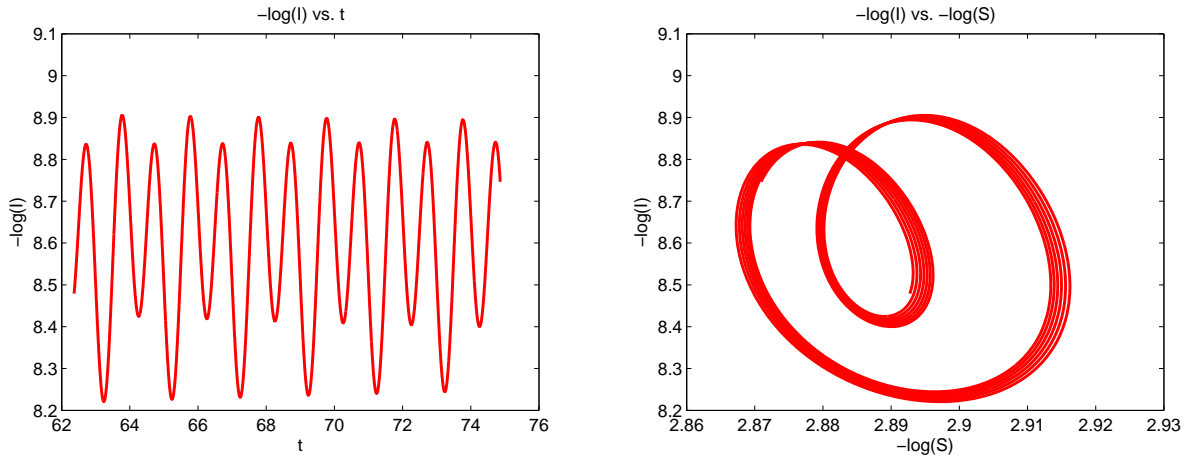


Figure 2.7: $-\log(I)$ vs. t and $-\log(I)$ vs. $-\log(S)$ of the SEIR Model with $\kappa = 0.05$ From $t = 62.5$ to $t = 75$. Unstable periodical solutions. Period doubling bifurcation.

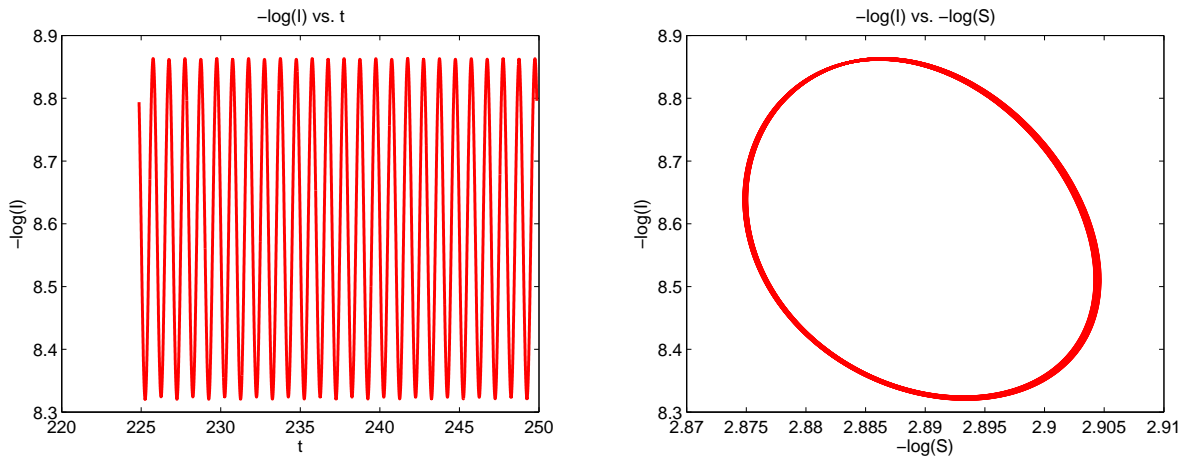


Figure 2.8: $-\log(I)$ vs. t and $-\log(I)$ vs. $-\log(S)$ of the SEIR Model with $\kappa = 0.05$ From $t = 225$ to $t = 250$. Stable periodical solutions. No bifurcation.

Figure 2.9 with $\kappa = 0.08$ is an example of stable period doubling bifurcation.

However, when κ increases to some critical value, the orbit becomes triennial. See Figure 2.10 with $\kappa = 0.1$.

Then the trajectory becomes biennial again. See Figure 2.11 with $\kappa = 0.15$.

Further increments in κ yield chaotic bifurcation. See a regular period doubling bifurcation in Figure 2.12 with $\kappa = 0.25$.

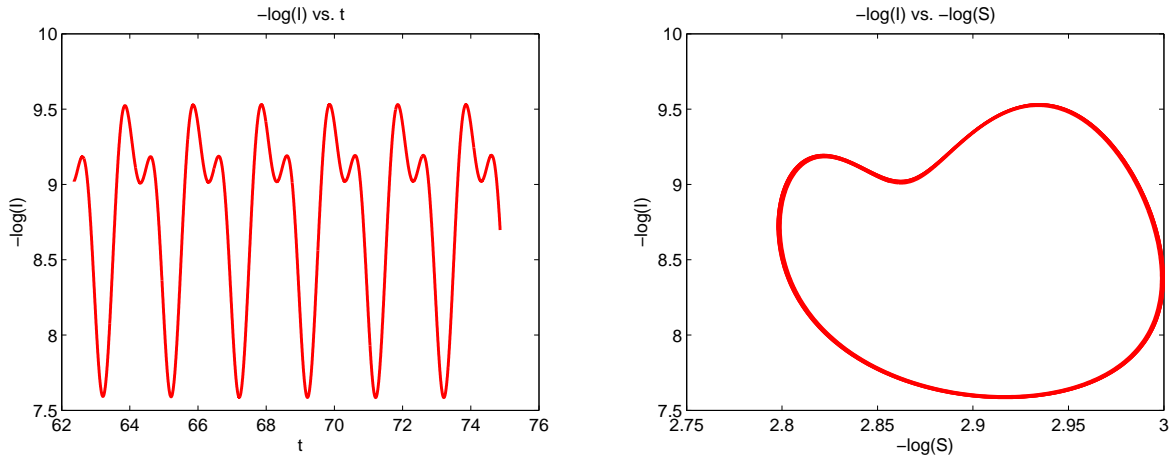


Figure 2.9: $-\log(I)$ vs. t and $-\log(I)$ vs. $-\log(S)$ of the SEIR Model with $\kappa = 0.08$ Stable periodical solutions. Period doubling bifurcation.

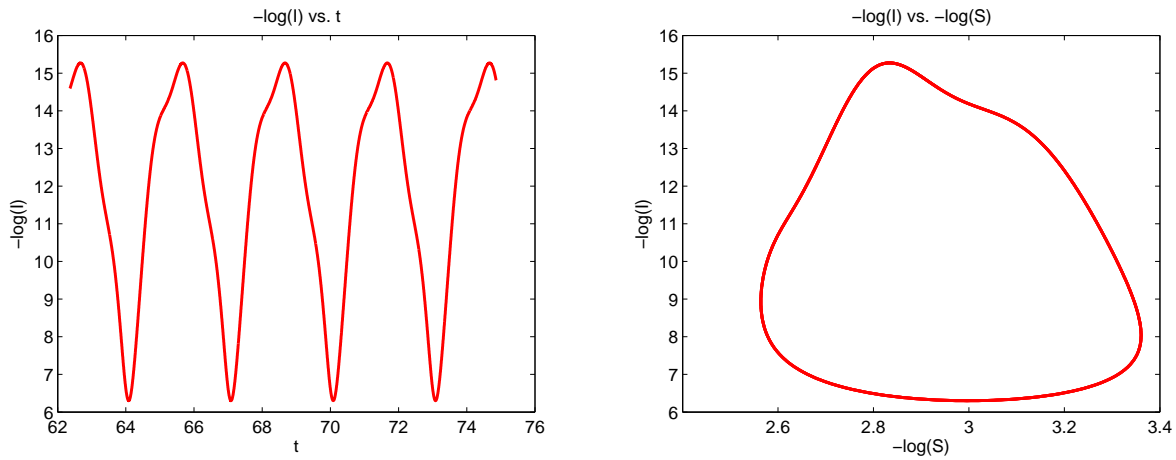


Figure 2.10: $-\log(I)$ vs. t and $-\log(I)$ vs. $-\log(S)$ with $\kappa = 0.1$ Stable periodical solutions. Period tripling bifurcation.

See a chaotic period tripling bifurcation in Figure 2.13 with $\kappa = 0.26$.

See a chaotic period doubling bifurcation in Figure 2.14 with $\kappa = 0.27$.

In conclusion, different from the direct relationship between period of the orbit and β , there is one unanticipated result in the simulation of the SEIR model. For κ very small, a stable periodical orbit having period 1 emerges from the nontrivial equilibrium point \mathbf{Q}_2 . As κ increases, past a critical value, the period 1 orbit becomes unstable and a stable biennial orbit appears, where occurs the period doubling bifurcation. However, when κ increases to

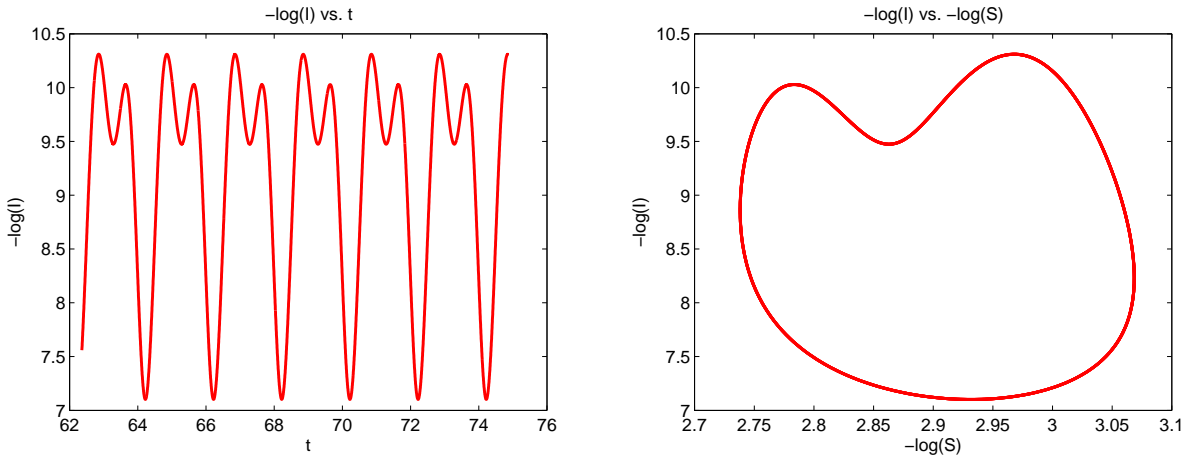


Figure 2.11: $-\log(I)$ vs. t and $-\log(I)$ vs. $-\log(S)$ of the SEIR Model with $\kappa = 0.15$. Stable periodical solutions. Period doubling bifurcation.

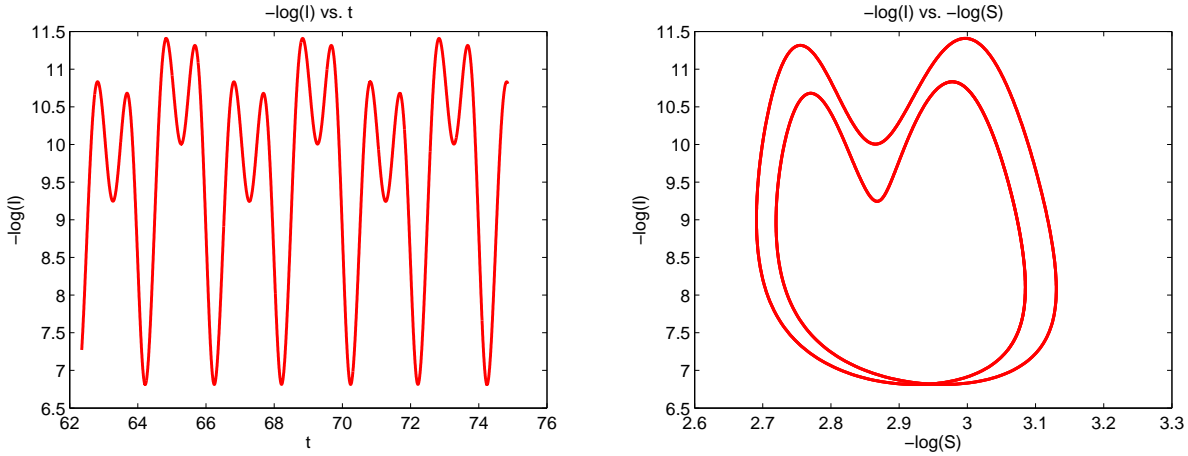


Figure 2.12: $-\log(I)$ vs. t and $-\log(I)$ vs. $-\log(S)$ of the SEIR Model with $\kappa = 0.25$. Regular period doubling bifurcation.

some critical value, the orbit becomes triennial, and then turns back to biennial. Chaotic period doubling bifurcations occur with further increments in κ .

2.3 Effective Infectee Number of the SEIR Model

Define the effective infectee number to be the average number of cases produced per average infective in one infectious period (Aron and Schwartz, 1984). The effective infectee number approaches unity if the system approaches an equilibrium.

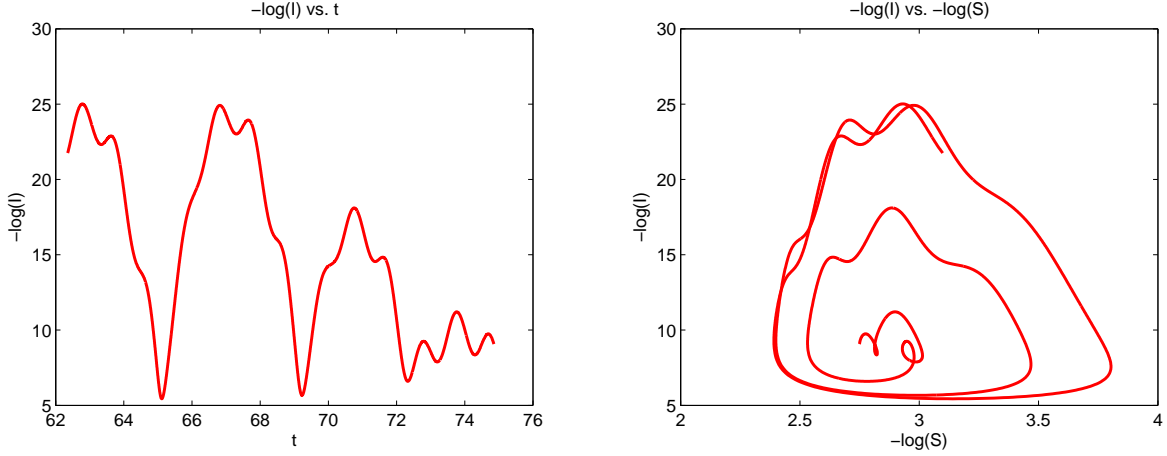


Figure 2.13: $-\log(I)$ vs. t and $-\log(I)$ vs. $-\log(S)$ of the SEIR Model with $\kappa = 0.26$ Chaotic period tripling bifurcation.

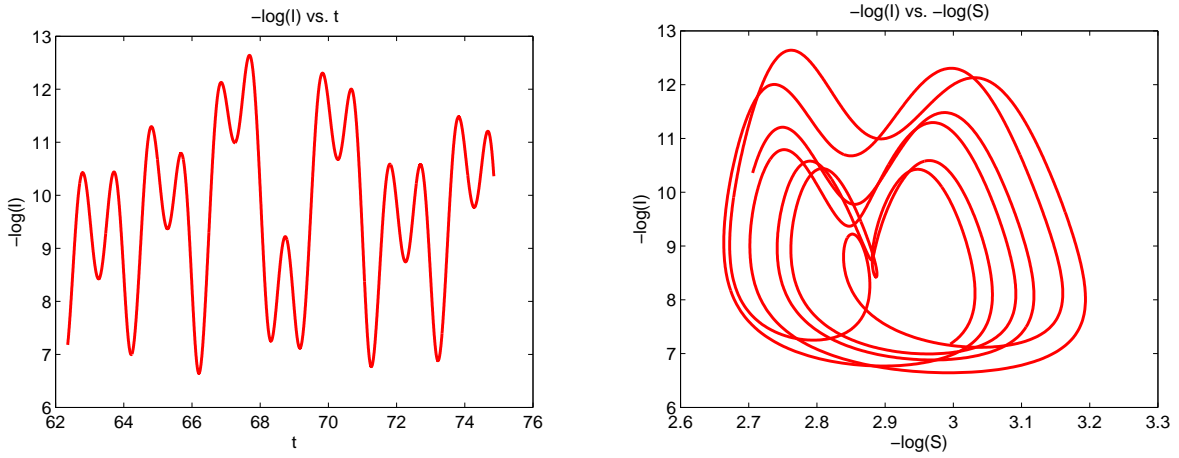


Figure 2.14: $-\log(I)$ vs. t and $-\log(I)$ vs. $-\log(S)$ of the SEIR Model with $\kappa = 0.27$ Chaotic period doubling bifurcation.

Define

$$C[a, b] = \eta \frac{\int_a^b \beta(t) S(t) I(t) dt}{\int_a^b I(t) dt}, \quad (2.22)$$

where $\eta = \frac{\alpha}{(\mu + \gamma)(\mu + \alpha)}$. $\frac{C[a, b]}{\eta}$ is the ratio of the average incidence to the average number of infective in time interval $[a, b]$. If

$$(S(t), E(t), I(t)) = (S(t + p), E(t + p), I(t + p)), \quad (2.23)$$

where p is an integer greater than or equal to unity, then $C[0, p]$ is the effective infectee number along a periodic orbit having period p .

Based on equations (2.12), (2.22), and (2.23), the numerator of $C[0, p]$ can be simplified as following:

$$\begin{aligned}
\int_0^p \beta(t)S(t)I(t) dt &= \int_0^p [\mu - \dot{S}(t) - \mu S(t)] dt \\
&= \mu \int_0^p [1 - S(t)] dt \\
&= \mu \int_0^p [E(t) + I(t) + R(t)] dt \\
&= \mu \int_0^p \left[E(t) + \frac{\alpha}{\mu + \gamma} E(t) + \frac{\gamma}{\mu} \frac{\alpha}{\mu + \gamma} E(t) \right] dt \\
&= \mu \int_0^p \left[\left(1 + \frac{\alpha}{\mu} \right) E(t) \right] dt \\
&= (\mu + \alpha) \int_0^p E(t) dt
\end{aligned}$$

The denominator of $C[0, p]$ is simplified as following:

$$\begin{aligned}
\int_0^p I(t) dt &= (\mu + \gamma)^{-1} \int_0^p [\alpha E(t) - \dot{I}(t)] dt \\
&= (\mu + \gamma)^{-1} \int_0^p \alpha E(t) dt \\
&= (\mu + \gamma)^{-1} \int_0^p (\mu + \gamma) I(t) dt
\end{aligned}$$

Thus,

$$\begin{aligned}
C[0, p] &= \frac{\alpha}{(\mu + \gamma)(\mu + \alpha)} \frac{(\mu + \alpha) \int_0^p E(t) dt}{(\mu + \gamma)^{-1} \int_0^p (\mu + \gamma) I(t) dt} \\
&= \frac{\int_0^p \alpha E(t) dt}{\int_0^p (\mu + \gamma) I(t) dt} \\
&= \frac{\int_0^p \dot{I}(t) dt + \int_0^p (\mu + \gamma) I(t) dt}{(\mu + \gamma)^{-1} \int_0^p (\mu + \gamma) I(t) dt} \\
&= 1
\end{aligned}$$

Therefore, if a periodic orbit having period p is asymptotically stable, the effective infectee number approaches unity.

Chapter 3

The Two-Strain Influenza Model

3.1 Introduction

In this research, the following model (3.1) is used to understand the replacement and coexistence of two influenza viruses.

$$\dot{S}_1 = g_2 R_2 - \beta(t) S_1 I_1 - \delta_1 S_1 + \delta_2 S_2 \quad (3.1a)$$

$$\dot{I}_1 = \beta(t) S_1 I_1 - \gamma I_1 \quad (3.1b)$$

$$\dot{R}_1 = \gamma I_1 - g_1 R_1 \quad (3.1c)$$

$$\dot{S}_2 = g_1 R_1 - \beta(t) S_2 I_2 - \delta_2 S_2 + \delta_1 S_1 \quad (3.1d)$$

$$\dot{I}_2 = \beta(t) S_2 I_2 - \gamma I_2 \quad (3.1e)$$

$$\dot{R}_2 = \gamma I_2 - g_2 R_2 \quad (3.1f)$$

where S_i , I_i and R_i are the susceptible, infectious and recovered individuals associated with strain $i = 1, 2$. The two strains share the same transmission rate β (which is a periodic function with period of 1 year) and recovery rate γ (where $\gamma^{-1} = 3$ days). For simplicity, the latent period ($\frac{1}{\alpha}$, which is about 1 day) is not taken into consideration. Parameters δ_1 and δ_2 reflect the evolution and competition of these two strains. In addition, the assumptions on fixed population size and homogeneous population are still applied.

The key part of this model is the way to model loss-of-immunity and cross-immunity.

Assume that an individual leaves the recovered class of a strain at a rate g_i , $i = 1, 2$, then moves to the susceptible pool of the other strain. This assumption is based on the general biological understanding. However, the two susceptible pools also exchange individuals at some rates (or, they 'steal' individuals from each other). It is allowed that an individual can be infected alternatively by the two strains (no double infection). Due to the exchange of susceptible of the two strains, it is also possible in this model that an individual can be infected by one type of strain repeatedly without being infected by the other strain first. However, being alternatively infected is more biologically reasonable, since direct-protection should be more reliable than cross-protection. Thus, this model grasps the key ecology features.

3.2 Analyses of the Equilibrium Points

In system (3.1), it is easy to see that the total population size $N = \sum_{i=1}^2 S_i + I_i + R_i$ is a constant. We assume that the transmission rate $\beta(t) = \beta$ is a constant and $g_1 = g_2 = g$. Then system (2.1) can be non-dimensionalized to the following system with $N = 1$ and $g = 1$.

$$\dot{S}_1 = R_2 - \beta S_1 I_1 - \delta_1 S_1 + \delta_2 S_2 \quad (3.2a)$$

$$\dot{I}_1 = \beta S_1 I_1 - \gamma I_1 \quad (3.2b)$$

$$\dot{R}_1 = \gamma I_1 - R_1 \quad (3.2c)$$

$$\dot{S}_2 = R_1 - \beta S_2 I_2 - \delta_2 S_2 + \delta_1 S_1 \quad (3.2d)$$

$$\dot{I}_2 = \beta S_2 I_2 - \gamma I_2 \quad (3.2e)$$

$$\dot{R}_2 = \gamma I_2 - R_2 \quad (3.2f)$$

Using Maple, four equilibrium points are found, $(S_{i,1}^*, I_{i,1}^*, R_{i,1}^*, S_{i,2}^*, I_{i,2}^*, R_{i,2}^*)$, $i = 1, 2, 3, 4$, which are used to represent different states of four different kinds of viruses:

$$\mathbf{E}_1 = \left(\frac{\delta_2}{\delta_1 + \delta_2}, 0, 0, \frac{\delta_1}{\delta_1 + \delta_2}, 0, 0 \right), \quad (3.3a)$$

$$\mathbf{E}_2 = \left(\frac{\gamma(\beta - \gamma + \delta_2 + \delta_2\gamma)}{\beta(\gamma + \delta_1 + \gamma\delta_1)}, 0, 0, \frac{\gamma}{\beta}, I_{2,2}^*, \gamma I_{2,2}^* \right), \quad (3.3b)$$

$$\mathbf{E}_3 = \left(\frac{\gamma}{\beta}, I_{3,1}^*, \gamma I_{3,1}^*, \frac{\gamma(\beta - \gamma + \delta_1 + \delta_1\gamma)}{\beta(\gamma + \delta_2 + \gamma\delta_2)}, 0, 0 \right), \quad (3.3c)$$

$$\mathbf{E}_4 = \left(\frac{\gamma}{\beta}, \frac{R_{4,1}^*}{\gamma}, R_{4,1}^*, \frac{\gamma}{\beta}, \frac{R_{4,2}^*}{\gamma}, R_{4,2}^* \right), \quad (3.3d)$$

where

$$I_{2,2}^* = \frac{\beta\delta_1 - \delta_1\gamma - \delta_2\gamma}{\beta(\gamma + \delta_1 + \gamma\delta_1)},$$

$$I_{3,1}^* = \frac{\beta\delta_2 - \delta_2\gamma - \delta_1\gamma}{\beta(\gamma + \delta_2 + \gamma\delta_2)},$$

$$R_{4,1}^* = \frac{\gamma}{2\beta(1 + \gamma)} ((\beta - 2\gamma) + (\delta_2 - \delta_1)(\gamma + 1)),$$

$$R_{4,2}^* = \frac{\gamma}{2\beta(1 + \gamma)} ((\beta - 2\gamma) + (\delta_1 - \delta_2)(\gamma + 1)).$$

The Jacobian matrix of $\mathbf{F}(S_1, I_1, R_1, S_2, I_2, R_2)$ at an equilibrium point is

$$J\mathbf{F} = \begin{pmatrix} -\beta I_1^* - \delta_1 & -\beta S_1^* & 0 & \delta_2 & 0 & 1 \\ \beta I_1^* & \beta S_1^* - \gamma & 0 & 0 & 0 & 0 \\ 0 & \gamma & -1 & 0 & 0 & 0 \\ \delta_1 & 0 & 1 & -\beta I_2^* - \delta_2 & -\beta S_2^* & 0 \\ 0 & 0 & 0 & \beta I_2^* & \beta S_2^* - \gamma & 0 \\ 0 & 0 & 0 & 0 & \gamma & -1 \end{pmatrix}. \quad (3.4)$$

If \mathbf{E}_2 or \mathbf{E}_3 exist and only one of them is stable, then replacement occurs between viruses. Else, if \mathbf{E}_4 exists and is stable or if all existing equilibrium points are unstable in which case we shall see later that there are limit cycles, then coexistence occurs between viruses.

The corresponding Matlab code that computes the existence and stability of each equilibrium point can be found in Appendix B.3.

3.2.1 Analysis of \mathbf{E}_1

As shown in the beginning of this section,

$$\mathbf{E}_1 = \left(\frac{\delta_2}{\delta_1 + \delta_2}, 0, 0, \frac{\delta_1}{\delta_1 + \delta_2}, 0, 0 \right). \quad (3.5)$$

Clearly, \mathbf{E}_1 always exists. \mathbf{E}_1 has positive coordinates $S_{1,1}^*$ and $S_{1,2}^*$, and zeros elsewhere. If \mathbf{E}_1 is stable, both viruses will vanish, leaving only the susceptible of both viruses in the population.

The Jacobian matrix $J\mathbf{F}_1$ evaluated at \mathbf{E}_1 is

$$J\mathbf{F}(\mathbf{E}_1) = \begin{pmatrix} -\delta_1 & -\beta S_{1,1}^* & 0 & \delta_2 & 0 & 1 \\ 0 & \beta S_{1,1}^* - \gamma & 0 & 0 & 0 & 0 \\ 0 & \gamma & -1 & 0 & 0 & 0 \\ \delta_1 & 0 & 1 & -\delta_2 & -\beta S_{1,2}^* & 0 \\ 0 & 0 & 0 & 0 & \beta S_{1,2}^* - \gamma & 0 \\ 0 & 0 & 0 & 0 & \gamma & -1 \end{pmatrix}. \quad (3.6)$$

The eigenvalues are

$$\lambda_{11} = \beta S_{1,2}^* - \gamma, \quad (3.7a)$$

$$\lambda_{12} = \beta S_{1,1}^* - \gamma, \quad (3.7b)$$

$$\lambda_{13} = 0, \quad (3.7c)$$

$$\lambda_{14} = -(\delta_1 + \delta_2), \quad (3.7d)$$

$$\lambda_{15} = -1, \quad (3.7e)$$

$$\lambda_{16} = -1. \quad (3.7f)$$

We only need to worry about the eigenvalues λ_{11} and λ_{12} . If they are both negative, \mathbf{E}_1 is stable; otherwise, it is unstable.

3.2.2 Analysis of \mathbf{E}_2

As shown in the beginning of this section,

$$\mathbf{E}_2 = \left(\frac{\gamma(\beta - \gamma + \delta_2 + \delta_2\gamma)}{\beta(\gamma + \delta_1 + \gamma\delta_1)}, 0, 0, \frac{\gamma}{\beta}, I_{2,2}^*, \gamma I_{2,2}^* \right), \quad (3.8)$$

where

$$I_{2,2}^* = \frac{\beta\delta_1 - \delta_1\gamma - \delta_2\gamma}{\beta(\gamma + \delta_1 + \gamma\delta_1)}.$$

The necessary and sufficient conditions for \mathbf{E}_2 to exist are:

$$\beta - \gamma + \delta_2(1 + \gamma) > 0, \quad (3.9)$$

$$\text{and } \beta\delta_1 - \gamma(\delta_1 + \delta_2) > 0. \quad (3.10)$$

However,

$$\begin{aligned} \beta\delta_1 - \gamma(\delta_1 + \delta_2) > 0 &\implies \beta > \gamma \left(1 + \frac{\delta_2}{\delta_1}\right) \\ &\implies \beta - \gamma + \delta_2(1 + \gamma) > 0 \end{aligned}$$

For existence of \mathbf{E}_2 , we only need to check condition (3.10).

If \mathbf{E}_2 exists, it has positive coordinates $S_{2,1}^*$, $S_{2,2}^*$, $I_{2,2}^*$, and $R_{2,2}^*$. Thus, if \mathbf{E}_2 is stable, virus 2 will replace virus 1 as time goes to infinity, leaving only the susceptible of virus 1 in the population.

The Jacobian matrix $J\mathbf{F}_2$ evaluated at \mathbf{E}_2 is

$$J\mathbf{F}(\mathbf{E}_2) = \begin{pmatrix} -\delta_1 & -\beta S_{2,1}^* & 0 & \delta_2 & 0 & 1 \\ 0 & \beta S_{2,1}^* - \gamma & 0 & 0 & 0 & 0 \\ 0 & \gamma & -1 & 0 & 0 & 0 \\ \delta_1 & 0 & 1 & -\beta I_{2,2}^* - \delta_2 & -\gamma & 0 \\ 0 & 0 & 0 & \beta I_{2,2}^* & 0 & 0 \\ 0 & 0 & 0 & 0 & \gamma & -1 \end{pmatrix}. \quad (3.11)$$

The characteristic polynomial is

$$\lambda (\lambda + 1) (\lambda - \beta S_{2,1}^* + \gamma) (\lambda^3 + a_1\lambda^2 + a_2\lambda + a_3), \quad (3.12)$$

where

$$a_1 = 1 + \beta I_{2,2}^* + \delta_1 + \delta_2, \quad (3.13a)$$

$$a_2 = (\gamma + 1 + \delta_1)\beta I_{2,2}^* + \delta_1 + \delta_2, \quad (3.13b)$$

$$a_3 = \beta I_{2,2}^*(\gamma + \delta_1 + \gamma\delta_1) = \beta\delta_1 - \gamma\delta_1 - \gamma\delta_2. \quad (3.13c)$$

The eigenvalues of $J\mathbf{F}_2$ are

$$\lambda_{21} = \beta S_{2,1}^* - \gamma, \quad (3.14a)$$

$$\lambda_{22} = 0, \quad (3.14b)$$

$$\lambda_{23} = -1, \quad (3.14c)$$

and $\lambda_{24}, \lambda_{25}, \lambda_{26}$, which are the roots of the polynomial $\lambda^3 + a_1\lambda^2 + a_2\lambda + a_3 = 0$. Since the coefficients of this polynomial are all positive, there is no positive real root and there must be at least one negative real root. It follows from Routh-Hurwitz criterion that the remaining two roots have negative real parts if and only if $a_1a_2 > a_3$.

$$\begin{aligned} a_1a_2 - a_3 &= (\beta I_{2,2}^* + 1 + \delta_1 + \delta_2)[(\gamma + 1 + \delta_1)\beta I_{2,2}^* + \delta_1 + \delta_2] - \beta I_{3,1}^*(\gamma + \delta_1 + \gamma\delta_1) \\ &= (\gamma + 1 + \delta_1)(\beta I_{2,2}^*)^2 + M(\beta I_{2,2}^*) + (1 + \delta_1 + \delta_2)(\delta_1 + \delta_2), \end{aligned}$$

where

$$\begin{aligned} M &= (1 + \delta_1 + \delta_2)(\gamma + 1 + \delta_1) + \delta_1 + \delta_2 - (\gamma + \delta_1 + \gamma\delta_1) \\ &= 1 + 2\delta_1 + 2\delta_2 + \delta_1^2 + \delta_2\gamma + \delta_1\delta_2 > 0. \end{aligned}$$

Therefore, $a_1a_2 - a_3 > 0$ if $I_{2,2}^*$ exists. We only need to worry about the eigenvalue λ_{21} . If it is negative, \mathbf{E}_2 is stable; otherwise, it is unstable.

3.2.3 Analysis of \mathbf{E}_3

As shown in the beginning of this section,

$$\mathbf{E}_3 = \left(\frac{\gamma}{\beta}, I_{3,1}^*, \gamma I_{3,1}^*, \frac{\gamma(\beta - \gamma + \delta_1 + \delta_1\gamma)}{\beta(\gamma + \delta_2 + \gamma\delta_2)}, 0, 0 \right), \quad (3.15)$$

where

$$I_{3,1}^* = \frac{\beta\delta_2 - \delta_2\gamma - \delta_1\gamma}{\beta(\gamma + \delta_2 + \gamma\delta_2)}.$$

The necessary and sufficient conditions for \mathbf{E}_3 to exist are:

$$\beta - \gamma + \delta_1(1 + \gamma) > 0 \quad (3.16)$$

$$\text{and } \beta\delta_2 - \gamma(\delta_1 + \delta_2) > 0. \quad (3.17)$$

However,

$$\begin{aligned} \beta\delta_2 - \gamma(\delta_1 + \delta_2) > 0 &\implies \beta > \gamma \left(1 + \frac{\delta_1}{\delta_2} \right) \\ &\implies \beta - \gamma + \delta_1(1 + \gamma) > 0 \end{aligned}$$

Thus, we only need to check condition (3.17).

If \mathbf{E}_3 exists, it has positive coordinates $S_{3,1}^*, I_{3,1}^*, R_{3,1}^*$, and $S_{3,2}^*$. Thus, if \mathbf{E}_3 is stable, virus 1 will replace virus 2 as time goes to infinity, leaving only the susceptible of virus 2 in the population.

The Jacobian matrix $J\mathbf{F}_3$ evaluated at \mathbf{E}_3 is

$$J\mathbf{F}(\mathbf{E}_3) = \begin{pmatrix} -\beta I_{3,1}^* - \delta_1 & -\gamma & 0 & \delta_2 & 0 & 1 \\ \beta I_{3,1}^* & 0 & 0 & 0 & 0 & 0 \\ 0 & \gamma & -1 & 0 & 0 & 0 \\ \delta_1 & 0 & 1 & -\delta_2 & -\beta S_{3,2}^* & 0 \\ 0 & 0 & 0 & 0 & \beta S_{3,2}^* - \gamma & 0 \\ 0 & 0 & 0 & 0 & \gamma & -1 \end{pmatrix}. \quad (3.18)$$

The characteristic polynomial of $J\mathbf{F}(\mathbf{E}_3)$ is

$$\lambda(\lambda + 1)(\lambda - \beta S_{3,2}^* + \gamma)(\lambda^3 + b_1\lambda^2 + b_2\lambda + b_3), \quad (3.19)$$

where

$$b_1 = 1 + \beta I_{3,1}^* + \delta_1 + \delta_2, \quad (3.20a)$$

$$b_2 = (\gamma + 1 + \delta_2)\beta I_{3,1}^* + \delta_1 + \delta_2, \quad (3.20b)$$

$$b_3 = \beta I_{3,1}^*(\gamma + \delta_2 + \gamma\delta_2) = \beta\delta_2 - \gamma\delta_2 - \gamma\delta_1. \quad (3.20c)$$

The eigenvalues of $J\mathbf{F}_3$ are

$$\lambda_{31} = \beta S_{3,2}^* - \gamma, \quad (3.21a)$$

$$\lambda_{32} = 0, \quad (3.21b)$$

$$\lambda_{33} = -1, \quad (3.21c)$$

and $\lambda_{34}, \lambda_{35}, \lambda_{36}$, which are the roots of the polynomial $\lambda^3 + b_1\lambda^2 + b_2\lambda + b_3 = 0$. Similar to the analysis of \mathbf{E}_2 , since the coefficients of this polynomial are all positive, there is no positive real root and there must be at least one negative real root. The remaining two roots have negative real parts if and only if $b_1b_2 > b_3$.

$$\begin{aligned} b_1b_2 - b_3 &= (\beta I_{3,1}^* + 1 + \delta_1 + \delta_2)[(\gamma + 1 + \delta_2)\beta I_{3,1}^* + \delta_1 + \delta_2] - \beta I_{3,1}^*(\gamma + \delta_2 + \gamma\delta_2) \\ &= (\gamma + 1 + \delta_2)(\beta I_{3,1}^*)^2 + N(\beta I_{3,1}^*) + (1 + \delta_1 + \delta_2)(\delta_1 + \delta_2), \end{aligned}$$

where

$$\begin{aligned} N &= (1 + \delta_1 + \delta_2)(\gamma + 1 + \delta_2) + \delta_1 + \delta_2 - (\gamma + \delta_2 + \gamma\delta_2) \\ &= 1 + 2\delta_1 + 2\delta_2 + \delta_2^2 + \delta_1\gamma + \delta_1\delta_2 > 0. \end{aligned}$$

Therefore, $b_1b_2 - b_3 > 0$ if $I_{3,1}^*$ exists. We only need to worry about the eigenvalue λ_{31} . If it has negative real part, \mathbf{E}_3 is stable; otherwise, it is unstable.

3.2.4 Analysis of \mathbf{E}_4

As shown in the beginning of this section,

$$\mathbf{E}_4 = \left(\frac{\gamma}{\beta}, \frac{R_{4,1}^*}{\gamma}, R_{4,1}^*, \frac{\gamma}{\beta}, \frac{R_{4,2}^*}{\gamma}, R_{4,2}^* \right), \quad (3.22)$$

where

$$R_{4,1}^* = \frac{\gamma}{2\beta(1+\gamma)} ((\beta - 2\gamma) + (\delta_2 - \delta_1)(\gamma + 1)), \quad (3.23)$$

$$R_{4,2}^* = \frac{\gamma}{2\beta(1+\gamma)} ((\beta - 2\gamma) + (\delta_1 - \delta_2)(\gamma + 1)). \quad (3.24)$$

$$(3.25)$$

A necessary and sufficient condition for \mathbf{E}_4 to exist is $R_{4,1}^*$ and $R_{4,2}^*$ are positive; that is

$$F_0 := \frac{(\beta - 2\gamma)}{|\delta_1 - \delta_2|(\gamma + 1)} > 1. \quad (3.26)$$

The above inequality is equivalent to

$$\beta - 2\gamma + |\delta_1 - \delta_2|(\gamma + 1) > 0. \quad (3.27)$$

If \mathbf{E}_4 exists, all its six coordinates are positive. Thus, if \mathbf{E}_4 is stable, two viruses will coexist.

The Jacobian matrix $J\mathbf{F}_4$ evaluated at \mathbf{E}_4 is

$$J\mathbf{F}(\mathbf{E}_4) = \begin{pmatrix} -\frac{\beta R_{4,1}^*}{\gamma} - \delta_1 & -\gamma & 0 & \delta_2 & 0 & 1 \\ \frac{\beta R_{4,1}^*}{\gamma} & 0 & 0 & 0 & 0 & 0 \\ 0 & \gamma & -1 & 0 & 0 & 0 \\ \delta_1 & 0 & 1 & -\frac{\beta R_{4,2}^*}{\gamma} - \delta_2 & -\gamma & 0 \\ 0 & 0 & 0 & \frac{\beta R_{4,2}^*}{\gamma} & 0 & 0 \\ 0 & 0 & 0 & 0 & \gamma & -1 \end{pmatrix}. \quad (3.28)$$

The characteristic polynomial of above matrix is

$$\lambda(\lambda^5 + c_1\lambda^4 + c_2\lambda^3 + c_3\lambda^2 + c_4\lambda + c_5), \quad (3.29)$$

where

$$\begin{aligned}
c_1 &= \frac{2\gamma + \beta R_{4,2}^* + \delta_2\gamma + \beta R_{4,1}^* + \delta_1\gamma}{\gamma} \\
&= (2 + \delta_1 + \delta_2) + (R_1 + R_2), \\
c_2 &= \frac{1}{\gamma^2} \{ (2\delta_2 + 2\delta_1 + 1)\gamma^2 + (2\gamma\beta + \delta_2\gamma\beta + \beta\gamma^2)R_{4,1}^* + (2\beta\gamma + \beta\delta_1\gamma + \beta\gamma^2)R_{4,2}^* + \beta^2 R_{4,1}^* R_{4,2}^* \} \\
&= (1 + 2\delta_1 + 2\delta_2) + (2 + \delta_2 + \gamma)R_1 + (2 + \delta_1 + \gamma)R_2 + R_1 R_2, \\
c_3 &= \frac{1}{\gamma^2} \{ \gamma^2(\delta_1 + \delta_2) + [2\gamma\beta\delta_2 + 2\beta\gamma^2 + \gamma\beta + \delta_2\gamma^2\beta]R_{4,1}^* \} \\
&\quad + \frac{1}{\gamma^2} \{ [2\beta\gamma^2 + \beta\gamma + \beta\gamma^2\delta_1 + 2\beta\delta_1\gamma]R_{4,2}^* + 2\beta^2(1 + \gamma)R_{4,1}^* R_{4,2}^* + \gamma^2(\delta_1 + \delta_2) \} \\
&= (\delta_1 + \delta_2) + [2\delta_2 + 2\gamma + 1 + \delta_2\gamma]R_1 + [2\delta_1 + 2\gamma + 1 + \delta_1\gamma]R_2 + (1 + \gamma)R_1 R_2, \\
c_4 &= \frac{\beta}{\gamma^2} \{ (\delta^2\gamma + \delta_2\gamma^2 + \gamma^2)R_{4,1}^* + (\gamma^2 + \delta_1\gamma + \gamma^2\delta_1)R_{4,2}^* + (4\beta\gamma + \beta + \beta\gamma^2)R_{4,1}^* R_{4,2}^* \} \\
&= (\delta_2 + \gamma + \delta_2\gamma)R_1 + (\delta_1 + \gamma + \delta_1\gamma)R_2 + (4\gamma + 1 + \gamma^2)R_1 R_2, \\
c_5 &= \frac{2}{\gamma}\beta^2(1 + \gamma)R_{4,1}^* R_{4,2}^* \\
&= 2\gamma(1 + \gamma)R_1 R_2,
\end{aligned}$$

where

$$\begin{aligned}
R_1 &= \frac{\beta}{\gamma}R_{4,1}^* = \frac{\beta - 2\gamma + (\delta_2 - \delta_1)(\gamma + 1)}{2(1 + \gamma)}, \\
R_2 &= \frac{\beta}{\gamma}R_{4,2}^* = \frac{\beta - 2\gamma + (\delta_1 - \delta_2)(\gamma + 1)}{2(1 + \gamma)}.
\end{aligned}$$

Due to the complication of the coefficients of (3.29), further analysis of \mathbf{E}_4 requires Hopf Bifurcation theory which we will not include in our report.

Chapter 4

Stability of Interior Equilibrium Points

In Section 3.2.4, it is showed that \mathbf{E}_4 exists if and only if $F_0 > 1$, where

$$F_0 = \frac{(\beta - 2\gamma)}{|\delta_1 - \delta_2|(\gamma + 1)}.$$

To examine the existence and stability of each equilibrium point, we first assume that $F_0 < 1$ and then $F_0 > 1$.

4.1 Analyses of the Model when $F_0 < 1$

Under this condition, \mathbf{E}_4 does not exist. Thus, only \mathbf{E}_1 , \mathbf{E}_2 , and \mathbf{E}_3 will be considered. Without loss of generality, one can assume that $\delta_2 > \delta_1$. Due to the symmetry of \mathbf{E}_2 and \mathbf{E}_3 , in the opposite case, just switch the existence and stability of \mathbf{E}_2 and \mathbf{E}_3 .

Given that $\delta_2 > \delta_1$, inequality (3.27) is equivalent to

$$\beta - 2\gamma + (\delta_1 - \delta_2)(\gamma + 1) > 0. \quad (4.1)$$

A partition for of the positive real line is either

$$0 < \gamma \left(1 + \frac{\delta_1}{\delta_2}\right) < 2\gamma < \gamma \left(1 + \frac{\delta_2}{\delta_1}\right) < (2 + \delta_2 - \delta_1)\gamma + (\delta_2 - \delta_1), \quad (4.2)$$

or

$$0 < \gamma \left(1 + \frac{\delta_1}{\delta_2}\right) < (2 + \delta_2 - \delta_1)\gamma + (\delta_2 - \delta_1) < \gamma \left(1 + \frac{\delta_2}{\delta_1}\right). \quad (4.3)$$

4.1.1 $0 < \beta < \gamma \left(1 + \frac{\delta_1}{\delta_2}\right)$

\mathbf{E}_1 is stable since:

$$\begin{aligned}\lambda_{11} &= \beta S_{1,2}^* - \gamma = \beta \frac{\delta 2}{\delta 1 + \delta 2} - \gamma < \gamma \left(\frac{\delta 2}{\delta 1 + \delta 2} \cdot \frac{\delta_1 + \delta_2}{\delta_2} - 1 \right) = 0 \\ \lambda_{12} &= \beta S_{1,1}^* - \gamma = \beta \frac{\delta 1}{\delta 1 + \delta 2} - \gamma < \gamma \left(\frac{\delta 1}{\delta 1 + \delta 2} \cdot \frac{\delta_1 + \delta_2}{\delta_2} - 1 \right) < 0\end{aligned}$$

\mathbf{E}_2 does not exist by condition (3.10) and \mathbf{E}_3 does not exist by condition (3.17).
Given the initial conditions

$$S_{1,0} = 0.2, \tag{4.4a}$$

$$I_{1,0} = 0.01, \tag{4.4b}$$

$$R_{1,0} = 0.4, \tag{4.4c}$$

$$S_{2,0} = 0.2, \tag{4.4d}$$

$$I_{2,0} = 30^{-1}, \tag{4.4e}$$

$$R_{2,0} = 1 - S_{1,0} - I_{1,0} - R_{1,0} - S_{2,0} - I_{2,0}, \tag{4.4f}$$

Figure 4.1 plots a trajectory of population under this case. Red stars represent the initial points; Cyan, black, green, and magenta dots represent, respectively, \mathbf{E}_1 , \mathbf{E}_2 , \mathbf{E}_3 , and \mathbf{E}_4 . In this case, \mathbf{E}_1 is stable; \mathbf{E}_2 , \mathbf{E}_3 , and \mathbf{E}_4 do not exist. The trajectory converges to \mathbf{E}_1 ; that is, as time goes to infinity, there are only the susceptible of both viruses in the population. Neither replacement nor coexistence occurs.

The corresponding Matlab code that plots the trajectory under given parameter values and initial conditions can be found in Appendix B.4.

4.1.2 $\gamma \left(1 + \frac{\delta_1}{\delta_2}\right) < \beta < 2\gamma$

\mathbf{E}_1 is unstable since:

$$\begin{aligned}\lambda_{11} &= \beta S_{1,2}^* - \gamma = \beta \frac{\delta 2}{\delta 1 + \delta 2} - \gamma > \gamma \left(\frac{\delta 2}{\delta 1 + \delta 2} \cdot \frac{\delta_1 + \delta_2}{\delta_2} - 1 \right) = 0 \\ \lambda_{12} &= \beta S_{1,1}^* - \gamma = \beta \frac{\delta 1}{\delta 1 + \delta 2} - \gamma < 2\gamma \frac{\delta 1}{\delta 1 + \delta 2} - \gamma = \frac{\delta_1 - \delta_2}{\delta_1 + \delta_2} \gamma < 0\end{aligned}$$

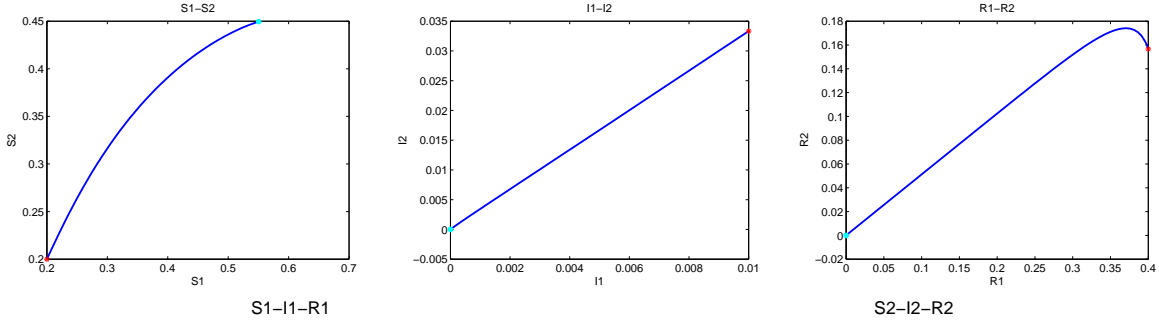


Figure 4.1: \mathbf{E}_1 is stable; \mathbf{E}_2 , \mathbf{E}_3 , and \mathbf{E}_4 do not exist
The trajectory converges to \mathbf{E}_1 (0.5505, 0, 0, 0.4495, 0, 0).
 $\gamma = 17.5047$, $\delta_1 = 0.7801$, $\delta_2 = 0.9553$, $\beta = 27.7309$.
No replacement or coexistence.

\mathbf{E}_2 does not exist by condition (3.10). \mathbf{E}_3 is stable since:

$$\begin{aligned}
\lambda_{31} &= \beta S_{3,2}^* - \gamma \\
&= \gamma \left(\frac{\beta - \gamma + \delta_1(1 + \gamma)}{\gamma + \delta_2 + \gamma\delta_2} - 1 \right) \\
&= \frac{\gamma}{\gamma + \delta_2 + \gamma\delta_2} (\beta - \gamma + \delta_1(1 + \gamma) - \gamma - \delta_2(1 + \gamma)) \\
&= \frac{\gamma}{\gamma + \delta_2 + \gamma\delta_2} (\beta - 2\gamma + (\delta_1 - \delta_2)(1 + \gamma)) < 0
\end{aligned}$$

Figure 4.2 plots a trajectory of population under this case. In this case, \mathbf{E}_1 is unstable; \mathbf{E}_3 is stable; \mathbf{E}_2 and \mathbf{E}_4 do not exist. The trajectory converges to \mathbf{E}_3 . As time goes to infinity, virus 1 replaces virus 2.

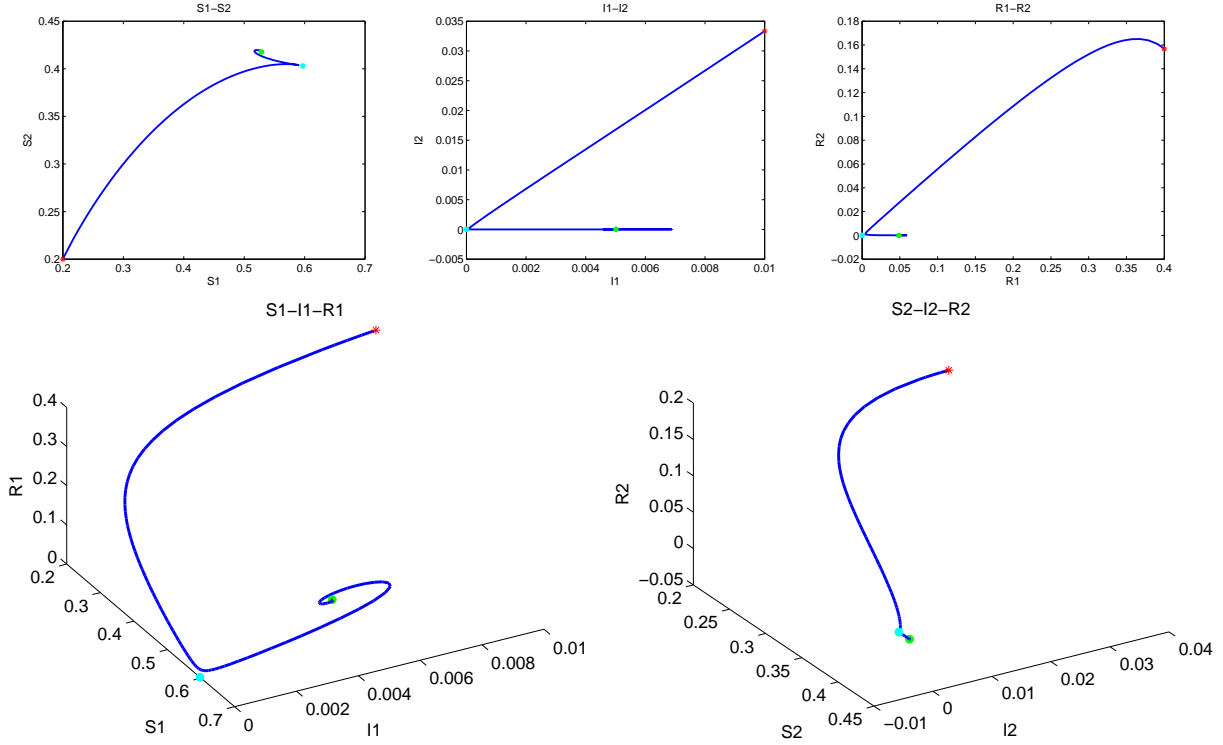


Figure 4.2: \mathbf{E}_1 is unstable; \mathbf{E}_3 is stable; \mathbf{E}_2 and \mathbf{E}_4 do not exist
 The trajectory converges to \mathbf{E}_3 (0.5285, 0.0050, 0.0488, 0.4177, 0, 0).
 $\gamma = 9.7299$, $\delta_1 = 0.5402$, $\delta_2 = 0.8004$, $\beta = 18.4108$.
 Replacement occurs. Virus 1 replaces virus 2.

4.1.3 $2\gamma < \beta < \gamma \left(1 + \frac{\delta_2}{\delta_1}\right)$

There are two subcases:

$$(1) \quad 2\gamma < \beta < \gamma \left(1 + \frac{\delta_2}{\delta_1}\right) < (2 + \delta_2 - \delta_1)\gamma + (\delta_2 - \delta_1),$$

$$(2) \quad 2\gamma < \beta < (2 + \delta_2 - \delta_1)\gamma + (\delta_2 - \delta_1) < \gamma \left(1 + \frac{\delta_2}{\delta_1}\right).$$

Nevertheless, same conclusions as in Section 4.1.2 can be drawn.

\mathbf{E}_1 is unstable since:

$$\lambda_{11} = \beta S_{1,2}^* - \gamma = \beta \frac{\delta_2}{\delta_1 + \delta_2} - \gamma > 2\gamma \frac{\delta_2}{\delta_1 + \delta_2} - \gamma = \gamma \frac{\delta_2 - \delta_1}{\delta_2 + \delta_1} > 0$$

$$\lambda_{12} = \beta S_{1,1}^* - \gamma = \beta \frac{\delta_1}{\delta_1 + \delta_2} - \gamma < \gamma \frac{\delta_1 + \delta_2}{\delta_1} \frac{\delta_1}{\delta_1 + \delta_2} - \gamma < 0$$

\mathbf{E}_2 does not exist by condition (3.10). \mathbf{E}_3 is stable since:

$$\begin{aligned}
\lambda_{31} &= \beta S_{3,2}^* - \gamma \\
&= \gamma \left(\frac{\beta - \gamma + \delta_1(1 + \gamma)}{\gamma + \delta_2 + \gamma\delta_2} - 1 \right) \\
&= \frac{\gamma}{\gamma + \delta_2 + \gamma\delta_2} (\beta - \gamma + \delta_1(1 + \gamma) - \gamma - \delta_2(1 + \gamma)) \\
&= \frac{\gamma}{\gamma + \delta_2 + \gamma\delta_2} (\beta - 2\gamma + (\delta_1 - \delta_2)(1 + \gamma)) < 0
\end{aligned}$$

4.1.4 $\gamma \left(1 + \frac{\delta_2}{\delta_1} \right) < \beta < (2 + \delta_2 - \delta_1)\gamma + (\delta_2 - \delta_1)$

\mathbf{E}_1 is unstable since:

$$\begin{aligned}
\lambda_{11} &= \beta S_{1,2}^* - \gamma = \beta \frac{\delta_2}{\delta_1 + \delta_2} - \gamma > \left(\frac{\delta_1 + \delta_2}{\delta_1} \frac{\delta_2}{\delta_1 + \delta_2} - 1 \right) \gamma = \gamma \frac{\delta_2}{\delta_1} > 0 \\
\lambda_{12} &= \beta S_{1,2}^* - \gamma = \beta \frac{\delta_1}{\delta_1 + \delta_2} - \gamma > \left(\frac{\delta_1 + \delta_2}{\delta_1} \frac{\delta_1}{\delta_1 + \delta_2} - 1 \right) \gamma = 0
\end{aligned}$$

\mathbf{E}_2 is unstable since:

$$\begin{aligned}
\lambda_{21} &= \beta S_{2,1}^* - \gamma \\
&= \gamma \left(\frac{\beta - \gamma + \delta_2(1 + \gamma)}{\gamma + \delta_1 + \gamma\delta_1} - 1 \right) \\
&= \frac{\gamma}{\gamma + \delta_1 + \gamma\delta_1} (\beta - \gamma + \delta_2(1 + \gamma) - \gamma - \delta_1(1 + \gamma)) \\
&= \frac{\gamma}{\gamma + \delta_2 + \gamma\delta_2} (\beta - 2\gamma + (\delta_2 - \delta_1)(1 + \gamma)) > 0
\end{aligned}$$

\mathbf{E}_3 is stable since:

$$\begin{aligned}
\lambda_{31} &= \beta S_{3,2}^* - \gamma \\
&= \gamma \left(\frac{\beta - \gamma + \delta_1(1 + \gamma)}{\gamma + \delta_2 + \gamma\delta_2} - 1 \right) \\
&= \frac{\gamma}{\gamma + \delta_2 + \gamma\delta_2} (\beta - \gamma + \delta_1(1 + \gamma) - \gamma - \delta_2(1 + \gamma)) \\
&= \frac{\gamma}{\gamma + \delta_2 + \gamma\delta_2} (\beta - 2\gamma + (\delta_1 - \delta_2)(1 + \gamma)) < 0
\end{aligned}$$

Figure 4.3 plots a trajectory of population under this case. In this case, \mathbf{E}_1 and \mathbf{E}_2 are unstable; \mathbf{E}_3 is stable; \mathbf{E}_4 does not exist. The trajectory converges to \mathbf{E}_3 . As time goes to infinity, virus 1 replaces virus 2.

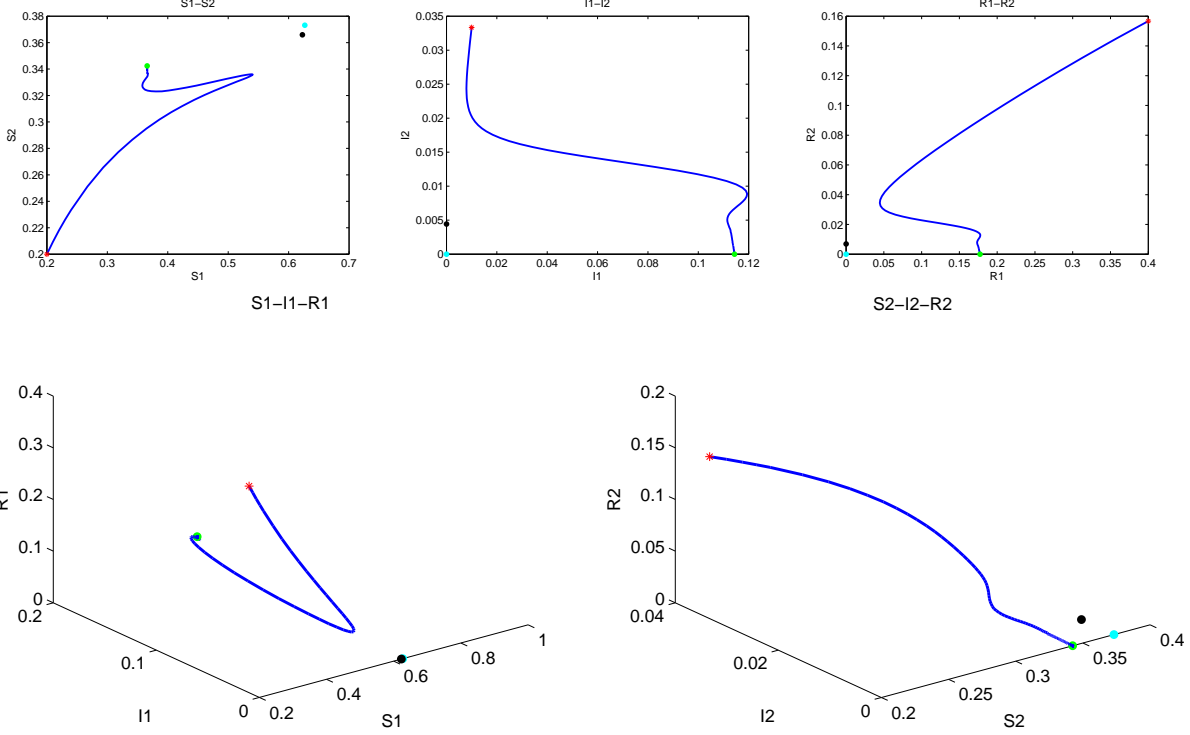


Figure 4.3: \mathbf{E}_1 and \mathbf{E}_2 are unstable; \mathbf{E}_3 is stable; \mathbf{E}_4 does not exist
The trajectory converges to \mathbf{E}_3 (0.3659, 0.1144, 0.1774, 0.3424, 0, 0).
 $\gamma = 1.5499$, $\delta_1 = 0.8473$, $\delta_2 = 1.4234$, $\beta = 4.2359$.
Replacement occurs. Virus 1 replaces virus 2.

4.2 Analyses of the Model when $F_0 > 1$

The condition $F_0 > 1$ implies that \mathbf{E}_4 exists but it may or may not be stable. In any case, when \mathbf{E}_4 exists, all other equilibrium points exist and must be unstable.

4.2.1 Stability of \mathbf{E}_4

Referring to Section 3.22, set the characteristic polynomial (3.29) to be 0.

$$\lambda^5 + c_1\lambda^4 + c_2\lambda^3 + c_3\lambda^2 + c_4\lambda + c_5 = 0, \quad (4.5)$$

where

$$c_1 = (2 + \delta_1 + \delta_2) + (R_1 + R_2), \quad (4.6a)$$

$$c_2 = (1 + 2\delta_1 + 2\delta_2) + (2 + \delta_2 + \gamma)R_1 + (2 + \delta_1 + \gamma)R_2 + R_1R_2, \quad (4.6b)$$

$$c_3 = (\delta_1 + \delta_2) + (2\delta_2 + 2\gamma + 1 + \delta_2\gamma)R_1 + (2\delta_1 + 2\gamma + 1 + \delta_1\gamma)R_2 + (1 + \gamma)R_1R_2, \quad (4.6c)$$

$$c_4 = (\delta_2 + \gamma + \delta_2\gamma)R_1 + (\delta_1 + \gamma + \delta_1\gamma)R_2 + (4\gamma + 1 + \gamma^2)R_1R_2, \quad (4.6d)$$

$$c_5 = 2\gamma(1 + \gamma)R_1R_2, \quad (4.6e)$$

where

$$R_1 = \frac{\beta - 2\gamma + (\delta_2 - \delta_1)(\gamma + 1)}{2(1 + \gamma)}, \quad (4.7a)$$

$$R_2 = \frac{\beta - 2\gamma + (\delta_1 - \delta_2)(\gamma + 1)}{2(1 + \gamma)}. \quad (4.7b)$$

To find signs of the real parts of all roots of equation (4.5), which reflect the stability of \mathbf{E}_4 , the Routh-Hurwitz stability criterion is applied. The Hurwitz Matrix of the 5th order polynomial related to equation (4.5) is

$$H(p) = \begin{bmatrix} c_1 & c_3 & c_5 & 0 & 0 \\ 1 & c_2 & c_4 & 0 & 0 \\ 0 & c_1 & c_3 & c_5 & 0 \\ 0 & 1 & c_2 & c_4 & 0 \\ 0 & 0 & c_1 & c_3 & c_5 \end{bmatrix} \quad (4.8)$$

All its roots have strictly negative real part if and only if all the leading principal minors of the matrix minors $\Delta(p)$ are positive; that is:

$$\Delta_1(p) = |c_1| = c_1 > 0 \quad (4.9a)$$

$$\Delta_2(p) = \begin{vmatrix} c_1 & c_3 \\ 1 & c_2 \end{vmatrix} = c_1 c_2 - c_3 > 0 \quad (4.9b)$$

$$\Delta_3(p) = \begin{vmatrix} c_1 & c_3 & c_5 \\ 1 & c_2 & c_4 \\ 0 & c_1 & c_3 \end{vmatrix} = c_1(c_5 - c_1 c_4) + c_3 \Delta_2(p) > 0 \quad (4.9c)$$

$$\Delta_4(p) = \begin{vmatrix} c_1 & c_3 & c_5 & 0 \\ 1 & c_2 & c_4 & 0 \\ 0 & c_1 & c_3 & c_5 \\ 0 & 1 & c_2 & c_4 \end{vmatrix} = c_5(c_1 c_4 - c_5) - c_5 c_2 \Delta_2(p) + c_4 \Delta_3(p) > 0 \quad (4.9d)$$

$$\Delta_5(p) = \begin{vmatrix} c_1 & c_3 & c_5 & 0 & 0 \\ 1 & c_2 & c_4 & 0 & 0 \\ 0 & c_1 & c_3 & c_5 & 0 \\ 0 & 1 & c_2 & c_4 & 0 \\ 0 & 0 & c_1 & c_3 & c_5 \end{vmatrix} = c_5 \Delta_4(p) > 0 \quad (4.9e)$$

Therefore, \mathbf{E}_4 is stable if and only if

$$c_1, c_5 > 0, \quad (4.10a)$$

$$c_1 c_2 - c_3 > 0, \quad (4.10b)$$

$$c_1(c_5 - c_1 c_4) > c_3(c_3 - c_1 c_2), \quad (4.10c)$$

$$\text{and } c_5(c_1 c_4 - c_5) > (c_5 c_2 - c_3 c_4)(c_1 c_2 - c_3) - c_1 c_4(c_5 - c_1 c_4). \quad (4.10d)$$

Using Matlab, we found that \mathbf{E}_4 can be either stable or unstable if it exists. Moreover, the stability of \mathbf{E}_4 is independent on the partition of γ .

4.2.2 Stability of \mathbf{E}_1

It can be shown that \mathbf{E}_1 is locally unstable if $F_0 > 1$. According to condition (3.26),

$$F_0 = \frac{(\beta - 2\gamma)}{|\delta_1 - \delta_2|(\gamma + 1)} > 1 \implies \beta - 2\gamma > 0$$

$$\begin{aligned} \lambda_{11} + \lambda_{12} &= \beta S_{1,2}^* - \gamma + \beta S_{1,1}^* - \gamma \\ &= \beta(S_{1,2}^* + S_{1,1}^*) - 2\gamma \\ &= \beta - 2\gamma > 0 \end{aligned}$$

Therefore, at least one of $\lambda_{11}, \lambda_{12}$ must be positive, and thus \mathbf{E}_1 is locally unstable if \mathbf{E}_4 exists.

4.2.3 Existence and Stability of \mathbf{E}_2 and \mathbf{E}_3

Once Again, one can assume that $\delta_2 > \delta_1$ without loss of generality. There are three inequalities related to β that ensure, respectively, the existence of $\mathbf{E}_2, \mathbf{E}_3,$ and \mathbf{E}_4 .

$$\begin{aligned} \beta &> \left(1 + \frac{\delta_2}{\delta_1}\right) \\ \beta &> \left(1 + \frac{\delta_1}{\delta_2}\right) \\ \beta &> (2 + |\delta_2 - \delta_1|)\gamma + |\delta_2 - \delta_1| \end{aligned}$$

A partition for β is either

$$\left(1 + \frac{\delta_1}{\delta_2}\right) < 2\gamma < (2 + \delta_2 - \delta_1)\gamma + (\delta_2 - \delta_1) < \left(1 + \frac{\delta_2}{\delta_1}\right),$$

or

$$\left(1 + \frac{\delta_1}{\delta_2}\right) < 2\gamma < \left(1 + \frac{\delta_2}{\delta_1}\right) < (2 + \delta_2 - \delta_1)\gamma + (\delta_2 - \delta_1).$$

If

$$(2 + \delta_2 - \delta_1)\gamma + (\delta_2 - \delta_1) < \beta < \left(1 + \frac{\delta_2}{\delta_1}\right),$$

\mathbf{E}_2 does not exist by condition (3.10).

$$\begin{aligned} \lambda_{31} &= \beta S_{3,2}^* - \gamma \\ &= \gamma \left(\frac{\beta - \gamma + \delta_1(1 + \gamma)}{\gamma + \delta_2 + \gamma\delta_2} - 1 \right) \\ &= \frac{\gamma}{\gamma + \delta_2 + \gamma\delta_2} (\beta - \gamma + \delta_1(1 + \gamma) - \gamma - \delta_2(1 + \gamma)) \\ &= \frac{\gamma}{\gamma + \delta_2 + \gamma\delta_2} (\beta - 2\gamma + (\delta_1 - \delta_2)(1 + \gamma)) > 0 \end{aligned}$$

\mathbf{E}_3 is unstable, since λ_{31} is positive by condition (3.27).

Figure 4.4 plots a trajectory of population under this case when \mathbf{E}_4 is stable. In the figure set, \mathbf{E}_1 and \mathbf{E}_3 are unstable, \mathbf{E}_2 does not exist, and \mathbf{E}_4 is stable. The trajectory converges to \mathbf{E}_4 ; that is, coexistence between two viruses occurs.

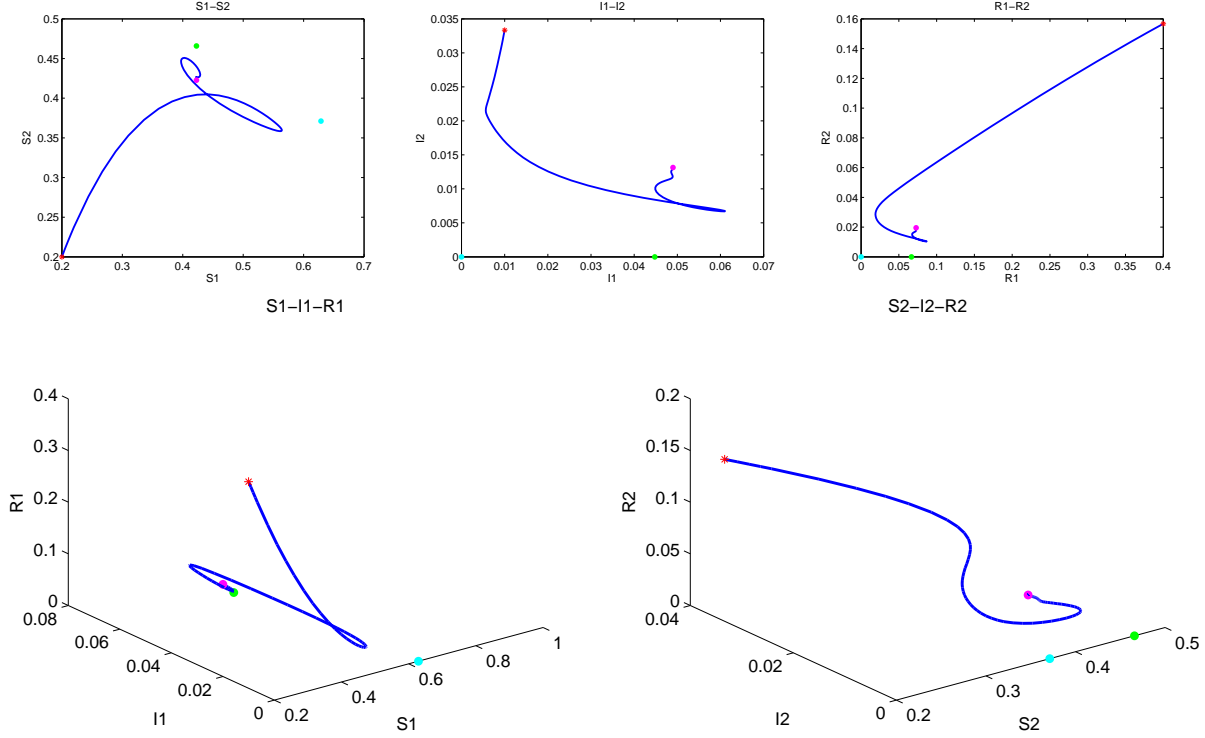


Figure 4.4: \mathbf{E}_1 and \mathbf{E}_3 are unstable; \mathbf{E}_2 does not exist; \mathbf{E}_4 is stable
 The trajectory converges to \mathbf{E}_4 (0.4156, 0.0490, 0.0729, 0.4156, 0.0131, 0.0195).
 $\gamma = 1.4878$, $\delta_1 = 0.1818$, $\delta_2 = 0.3080$, $\beta = 3.5196$.
 Coexistence occurs.

Figure 4.5 also plots a trajectory of population under this case but with \mathbf{E}_4 unstable. In the figure set, \mathbf{E}_1 and \mathbf{E}_3 are unstable, \mathbf{E}_2 does not exist, and \mathbf{E}_4 is unstable. The trajectory converges to a limit cycle as time goes to infinity. Coexistence and replacement occur alternatively and periodically.

If either

$$(2 + \delta_2 - \delta_1)\gamma + (\delta_2 - \delta_1) < \left(1 + \frac{\delta_2}{\delta_1}\right) < \beta,$$

or

$$\left(1 + \frac{\delta_2}{\delta_1}\right) < (2 + \delta_2 - \delta_1)\gamma + (\delta_2 - \delta_1) < \beta,$$

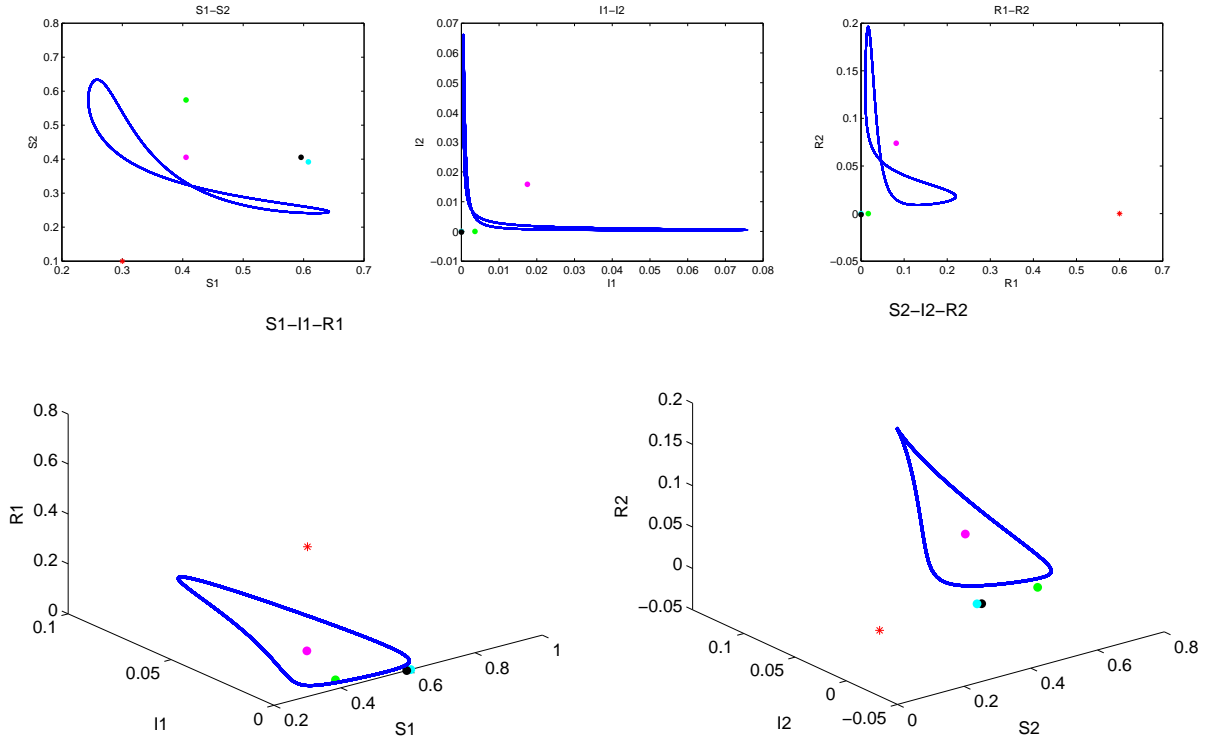


Figure 4.5: \mathbf{E}_1 , \mathbf{E}_3 , and \mathbf{E}_4 are unstable; \mathbf{E}_2 does not exist
 There appears limit cycles.
 $\gamma = 4.6681$, $\delta_1 = 0.0347$, $\delta_2 = 0.0538$, $\beta = 11.5110$.
 Coexistence and replacement occur alternatively and periodically.

referring to Section 4.1.4, both \mathbf{E}_2 and \mathbf{E}_3 are unstable.

Figure 4.6 plots a trajectory of population under this case when \mathbf{E}_4 is stable. In the figure set, \mathbf{E}_1 , \mathbf{E}_2 , and \mathbf{E}_3 are unstable, while \mathbf{E}_4 is stable. The trajectory converges to \mathbf{E}_4 ; that is, coexistence between two viruses occurs.

Figure 4.7 also plots a trajectory of population under this case but with \mathbf{E}_4 unstable. In the figure set, all four equilibrium points are unstable. The trajectory converges to a limit cycle as time goes to infinity. Coexistence and replacement occur alternatively and periodically.

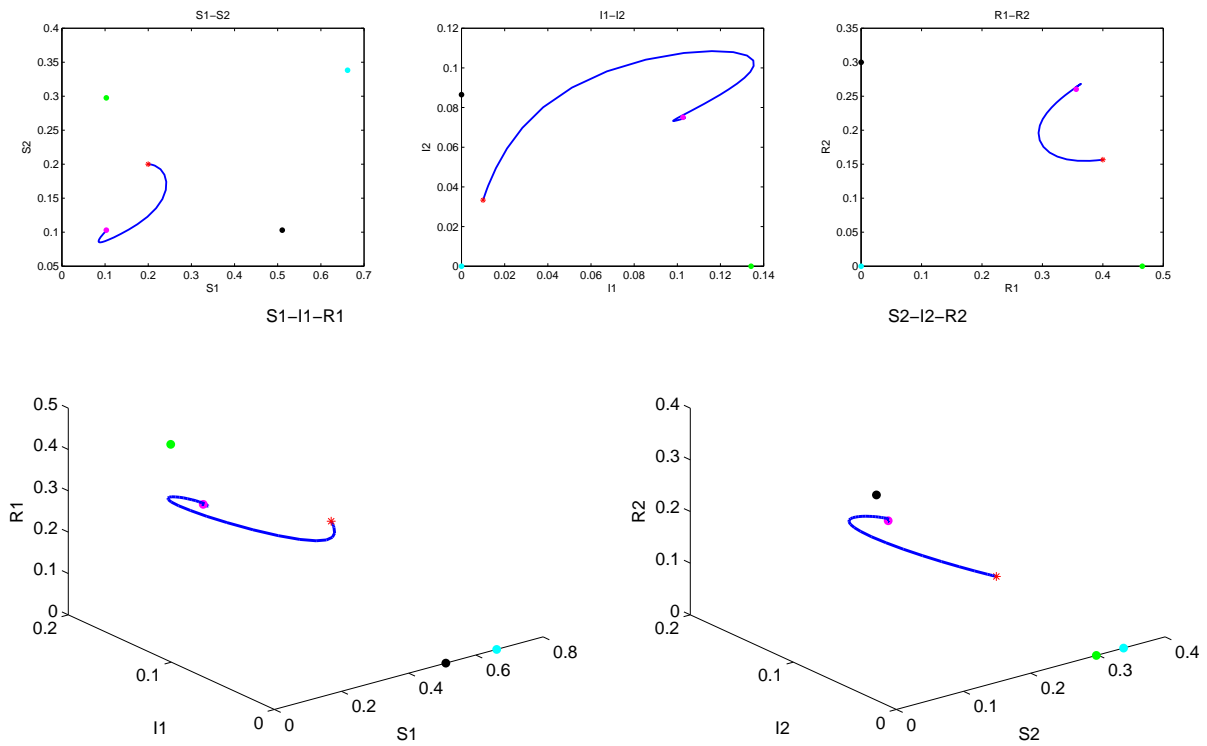


Figure 4.6: E_1 , E_2 , and E_3 are unstable; E_4 is stable
 The trajectory converges to E_4 (0.1030, 0.1027, 0.3560, 0.1030, 0.0751, 0.3603).
 $\gamma = 3.4675$, $\delta_1 = 0.9706$, $\delta_2 = 1.8996$, $\beta = 33.6607$.
 Coexistence occurs.

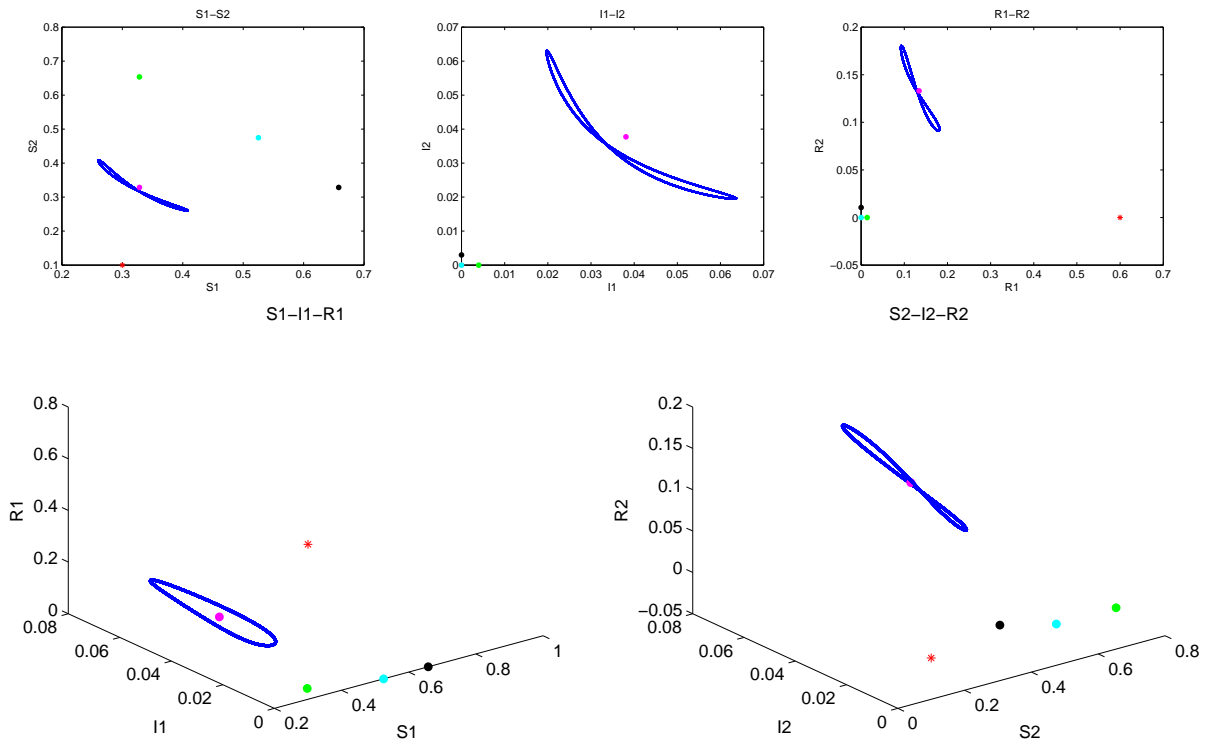


Figure 4.7: \mathbf{E}_1 , \mathbf{E}_2 , \mathbf{E}_3 , and \mathbf{E}_4 are all unstable
 There appears limit cycles.
 $\gamma = 3.5244$, $\delta_1 = 0.0356$, $\delta_2 = 0.0394$, $\beta = 10.7309$.
 Coexistence and replacement occur alternatively and periodically.

Chapter 5

Effects of Transmission Rate in the Two-strain Model

5.1 Two-strain SIR Model with Constant Transmission Rate

In Chapter 3, the following system was introduced to understand the replacement and coexistence of two influenza viruses.

$$\begin{aligned}\dot{S}_1 &= R_2 - \beta(t)S_1I_1 - \delta_1S_1 + \delta_2S_2 \\ \dot{I}_1 &= \beta(t)S_1I_1 - \gamma I_1 \\ \dot{R}_1 &= \gamma I_1 - R_1 \\ \dot{S}_2 &= R_1 - \beta(t)S_2I_2 - \delta_2S_2 + \delta_1S_1 \\ \dot{I}_2 &= \beta(t)S_2I_2 - \gamma I_2 \\ \dot{R}_2 &= \gamma I_2 - R_2\end{aligned}$$

where $\beta(t) = \beta$ is a constant and we assume that $\delta_2 > \delta_1$.

In Chapter 4, the existence and stability of each equilibrium point of the above system was studied. The results can be divided into three classes, each of which implies a relationship between the two viruses.

- Two viruses coexist, cf. Figure 4.6.
- One virus is replaced by the other, cf. Figure 4.3.
- Coexistence and replacement occur alternatively and periodically, cf. Figure 4.5.

The following series of figures are introduced to display I_1 and I_2 as functions of time.

5.1.1 Coexistence

If \mathbf{E}_4 is stable, then two viruses coexist. See Figure 5.1. I_1 and I_2 have almost the same trend. Both of them burgeon at the very beginning and then decrease simultaneously. After around $t = 4$, they both reach their steady states.

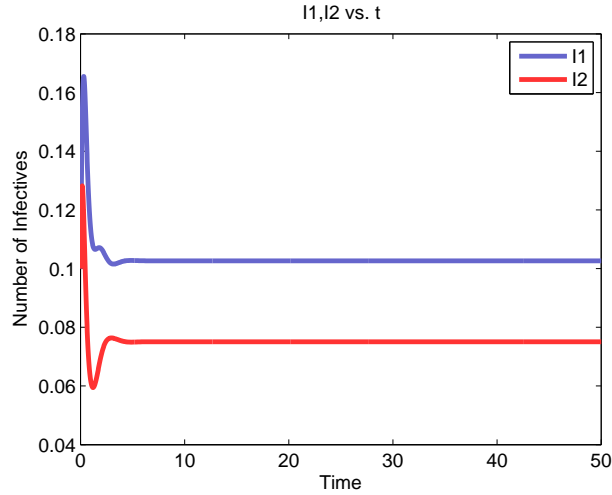


Figure 5.1: Coexistence between virus 1 and virus 2
 $\gamma = 3.4675$, $\delta_1 = 0.9706$, $\delta_2 = 1.8996$, $\beta = 33.6607$.

5.1.2 Replacement

If \mathbf{E}_3 is stable, then virus 2 will be replaced by virus 1. See Figure 5.2. As I_1 increases, I_2 drops dramatically. I_2 vanishes at around $t = 25$, while I_1 reaches its steady state.

\mathbf{E}_4 does not exist in this case, because otherwise \mathbf{E}_3 is not stable, cf. Section 4.2.3.

5.1.3 Periodic and Alternating Coexistence and Replacement

If there is no stable equilibrium point, then coexistence and replacement of two viruses occur alternatively and periodically. See Figure 5.3. I_1 and I_2 have the same period differed by a phase, which is called anti-phase. After $t = 40$, the minimum of each oscillation drops to zero. Thus, one virus replaces the other alternatively.

In Chapter 2, a simple sinusoidal form is introduced to model the periodic transmission rate.

$$\beta(t) = \beta_0(1 + \kappa \cos(2\pi t))$$

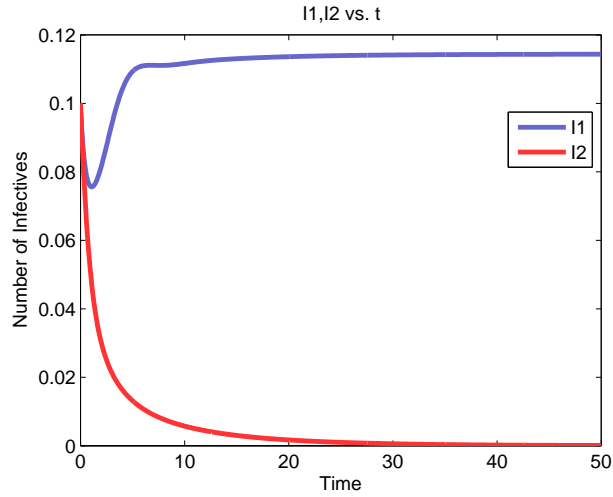


Figure 5.2: Replacement of virus 2 by virus 1
 $\gamma = 1.5499$, $\delta_1 = 0.8473$, $\delta_2 = 1.4234$, $\beta = 4.2359$.

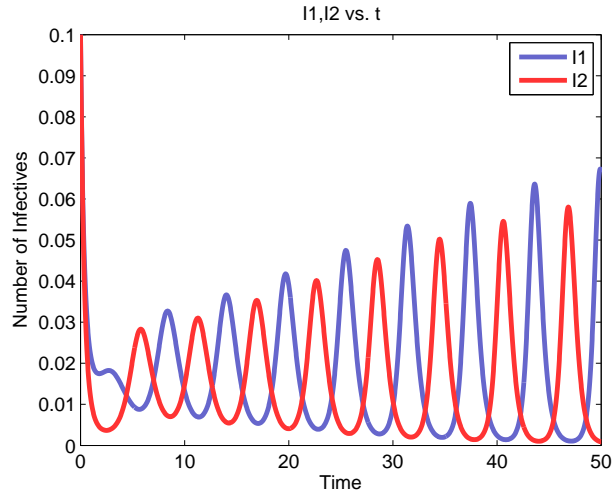


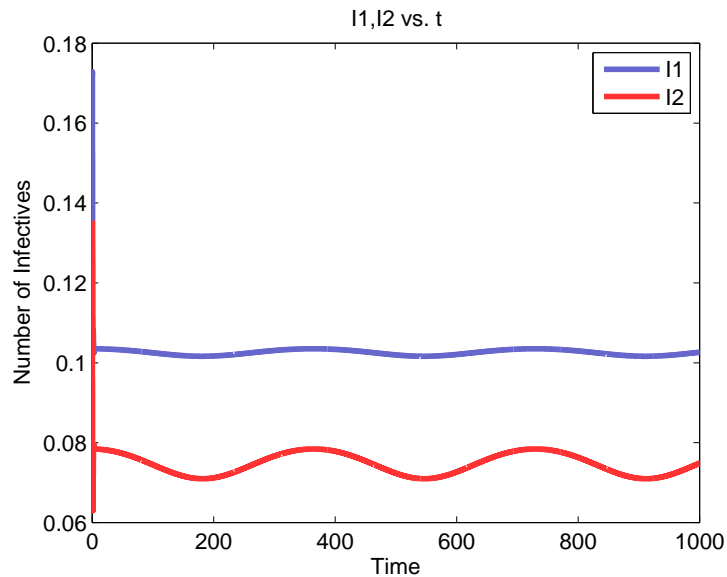
Figure 5.3: Periodic alternation between coexistence and replacement
 $\gamma = 4.6681$, $\delta_1 = 0.0347$, $\delta_2 = 0.0538$, $\beta = 11.5110$.

The effect of a periodic transmission rate defined as above on the infective number in the two-strain model (3.1) will be discussed in the next section. The corresponding Matlab code is a combination of Appendix B.1 and B.4.

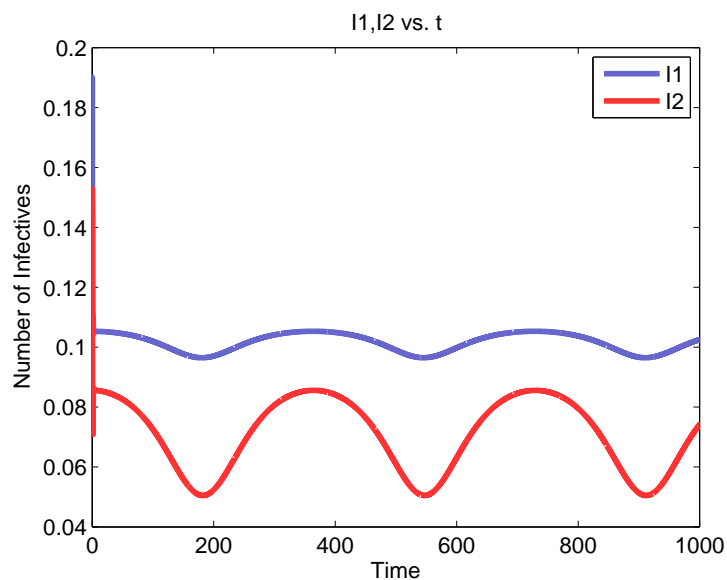
5.2 Two-strain SIR Model with Periodic Transmission Rate

5.2.1 Coexistence

Fixing $\gamma = 3.4675$, $\delta_1 = 0.9706$, $\delta_2 = 1.8996$, $\beta = 33.6607$, the case that two viruses coexist, I_1 and I_2 are plotted as a function of time. See Figure 5.4.



(a) $\kappa=0.1$



(b) $\kappa=0.4$

Figure 5.4: Coexistence between virus 1 and virus 2 with $\kappa = 0.1$ and $\kappa = 0.4$

Two graphs in Figure 5.4 are almost the same except for the amplitude of oscillations of both viruses. In both figures, I_1 is above I_2 . When $\kappa = 0.1$, the curve of I_1 is relatively flat, and I_2 has an amplitude $A_2 \approx 0.01$. When $\kappa = 0.4$, both curves are stretched, with $A_1 \approx 0.01$ and $A_2 \approx 0.03$, respectively.

5.2.2 Replacement

Fixing $\gamma = 1.5499$, $\delta_1 = 0.8473$, $\delta_2 = 1.4234$, $\beta = 4.2359$, the case that virus 2 is replaced by virus 1, I_1 and I_2 are plotted as a function of time. See Figure 5.5.

Two graphs in Figure 5.5 are almost the same except for the segment of I_2 when t is small. When $\kappa = 0.1$, the curve of I_2 is concave, which implies that virus 2 does not exhibit its seasonality before it vanishes. When $\kappa = 0.4$, the curve of I_2 is convex, and it is interpreted that I_2 starts to oscillate but the replacement is so overwhelming that virus 2 vanishes within a period. For I_1 , the amplitude of its oscillation is larger when κ is larger, which is expected from the definition of κ .

5.2.3 Periodic and Alternating Coexistence and Replacement

Fixing parameters $\gamma = 4.6681$, $\delta_1 = 0.0347$, $\delta_2 = 0.0538$, $\beta = 11.5110$, the following series of figures (Figure 5.6-5.9) displays I_1 and I_2 as functions of time with different seasonalities. It is noticed that there is a critical point of $\kappa_0 \approx 0.19$ such that the two viruses vanish temporarily and periodically if $\kappa > \kappa_0$.

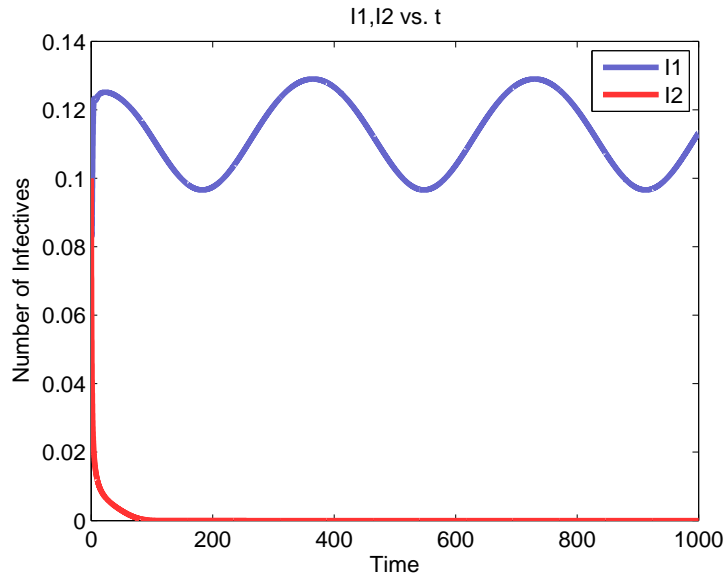
For $\kappa = 0.1$, the curves of I_1 and I_2 are similar to those with constant transmission rate. See Figure 5.6.

For $\kappa = 0.2$, virus 1 vanishes at $t \approx 200$ and resurges at $t \approx 240$. Virus 2 vanishes at $t \approx 175$ and resurges at $t \approx 220$. See Figure 5.7.

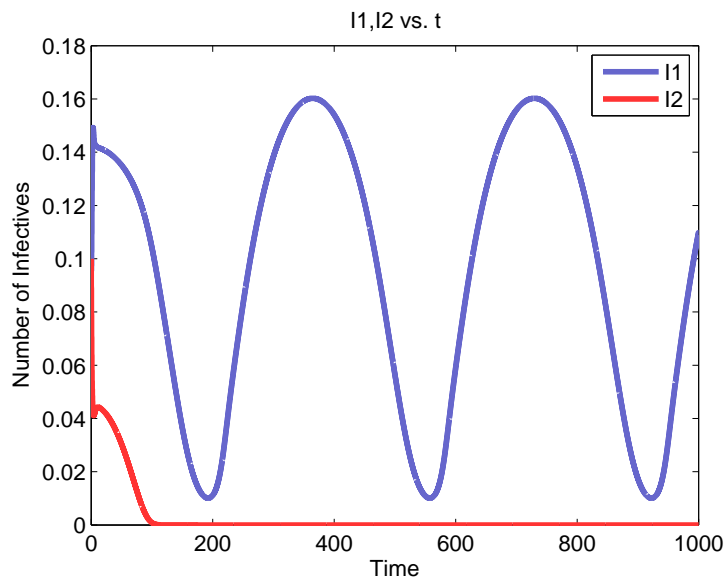
For $\kappa = 0.3$, virus 1 vanishes at $t \approx 150$ and resurges at $t \approx 300$. Virus 2 vanishes at $t \approx 140$ and resurges at $t \approx 250$. See Figure 5.8.

For $\kappa = 0.4$, virus 1 vanishes at $t \approx 125$ and resurges at $t \approx 280$. Virus 2 vanishes at $t \approx 140$ and resurges at $t \approx 315$. See Figure 5.9.

It can be claimed that the larger κ is, the shorter the time a virus exists within a period. Complicated computation and rigorous analysis are needed to prove and interpret this fact. However, it is believed that the periodically temporary vanishment of a virus corresponds to the skip which will be discussed in Section 6.3.3.



(a) $\kappa=0.1$



(b) $\kappa=0.4$

Figure 5.5: Replacement of virus 2 by virus 1 with $\kappa = 0.1$ and $\kappa = 0.4$

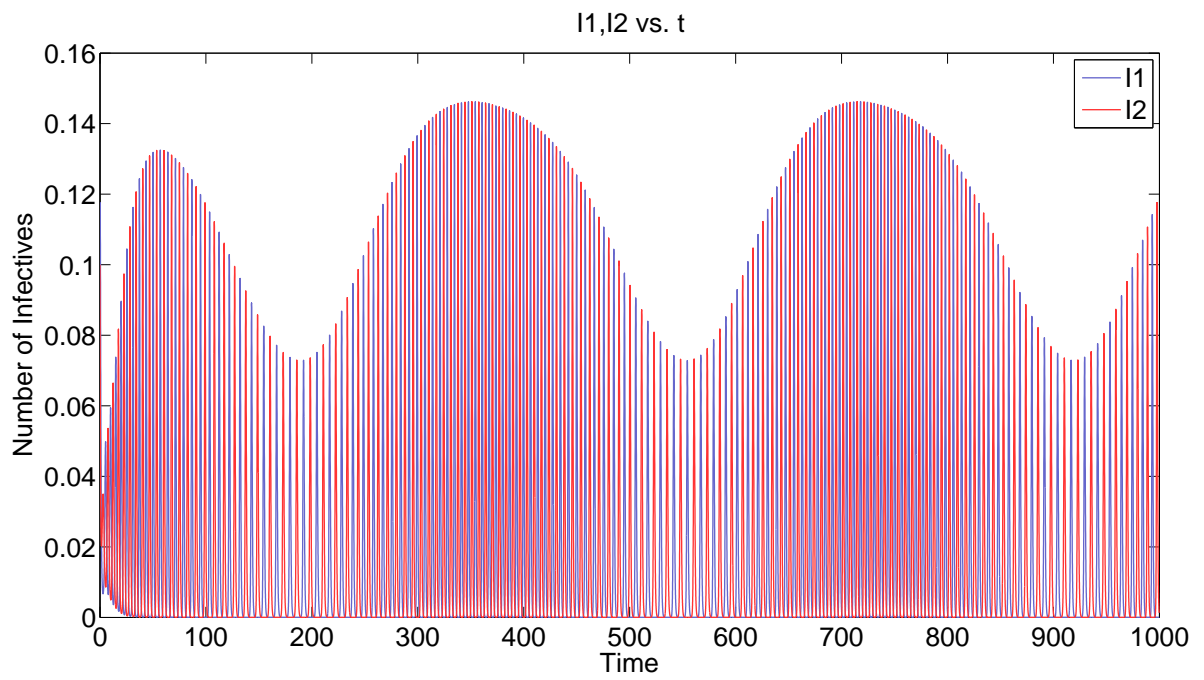
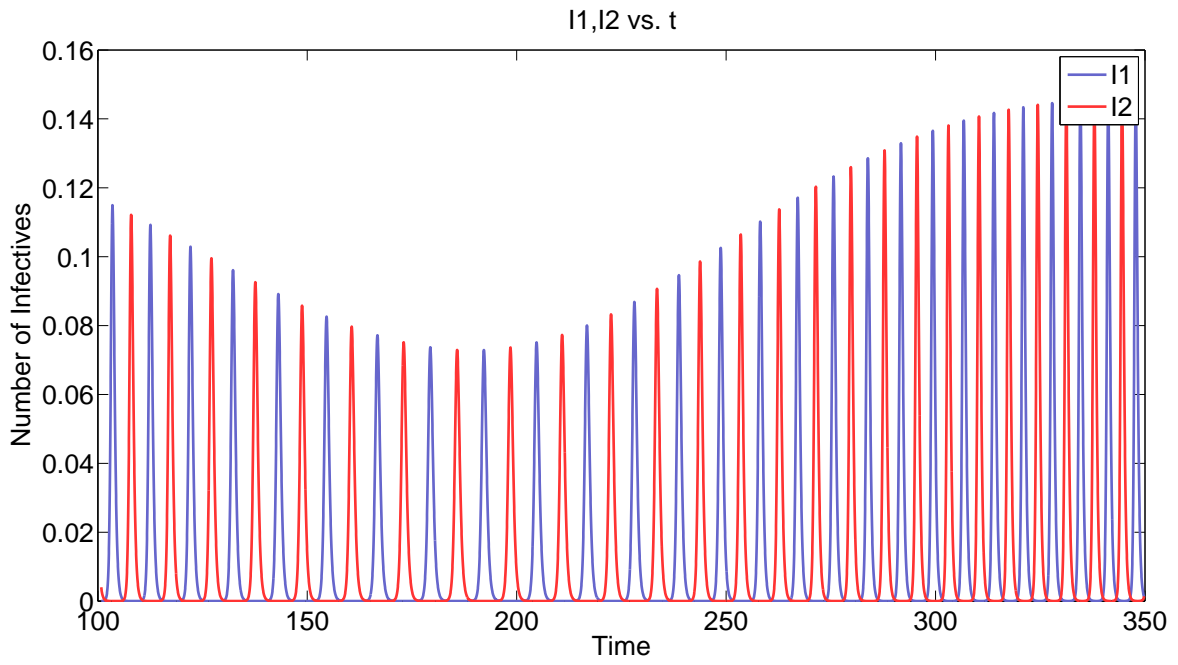


Figure 5.6: Periodic and alternating coexistence and replacement with $\kappa = 0.1$

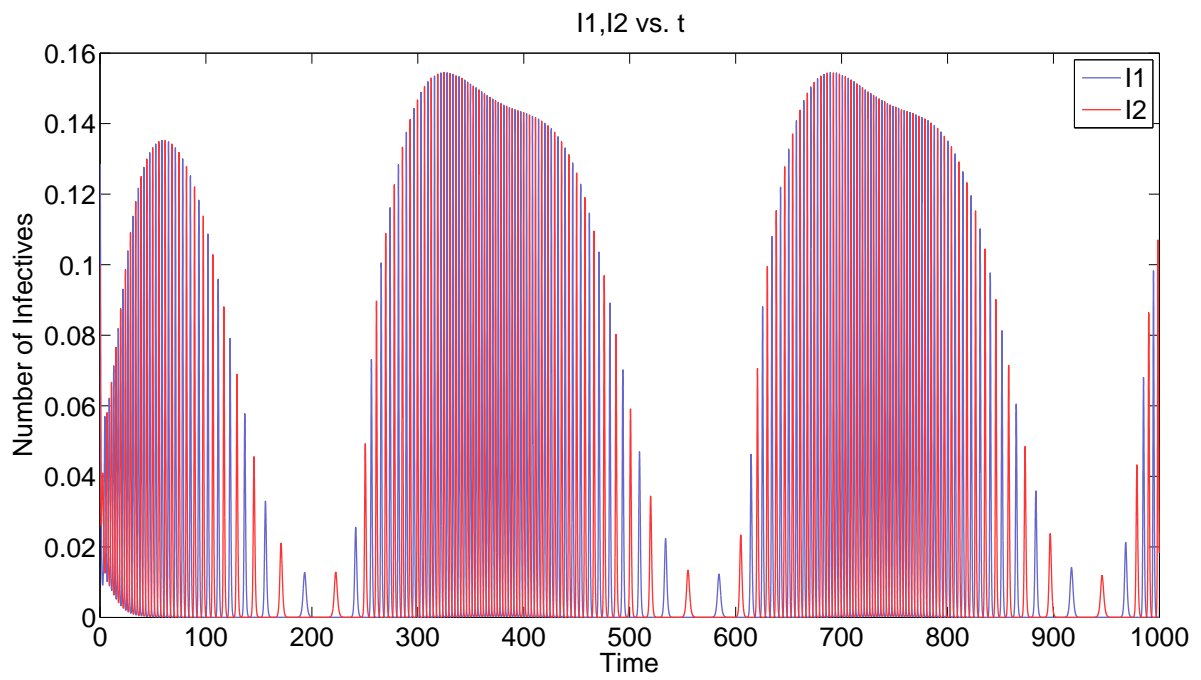
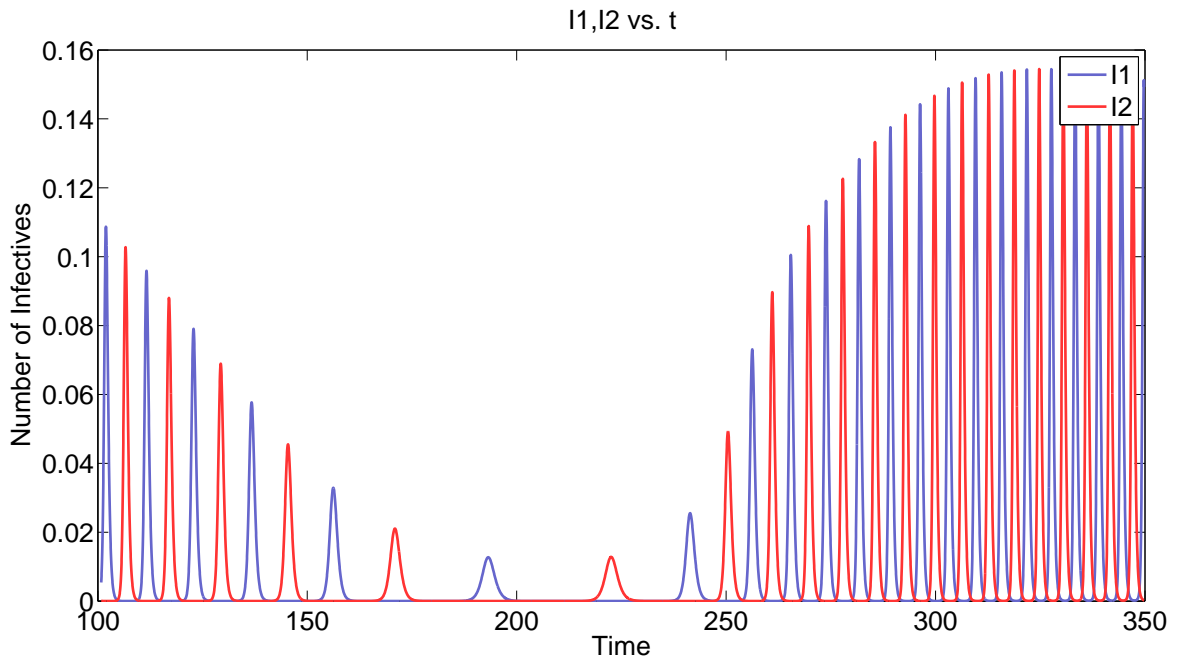


Figure 5.7: Periodic and alternating coexistence and replacement with $\kappa = 0.2$

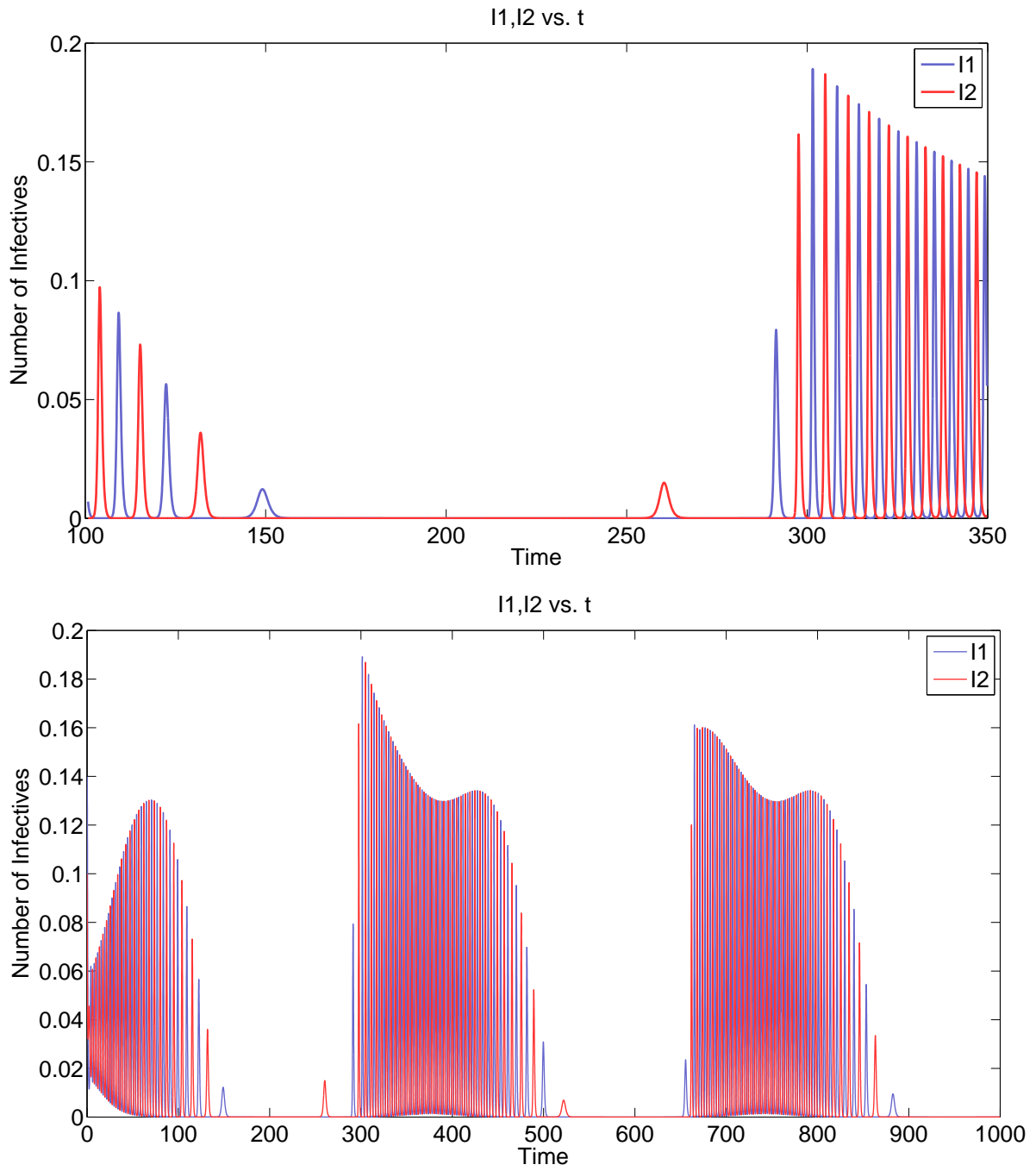


Figure 5.8: Periodic and alternating coexistence and replacement with $\kappa = 0.3$

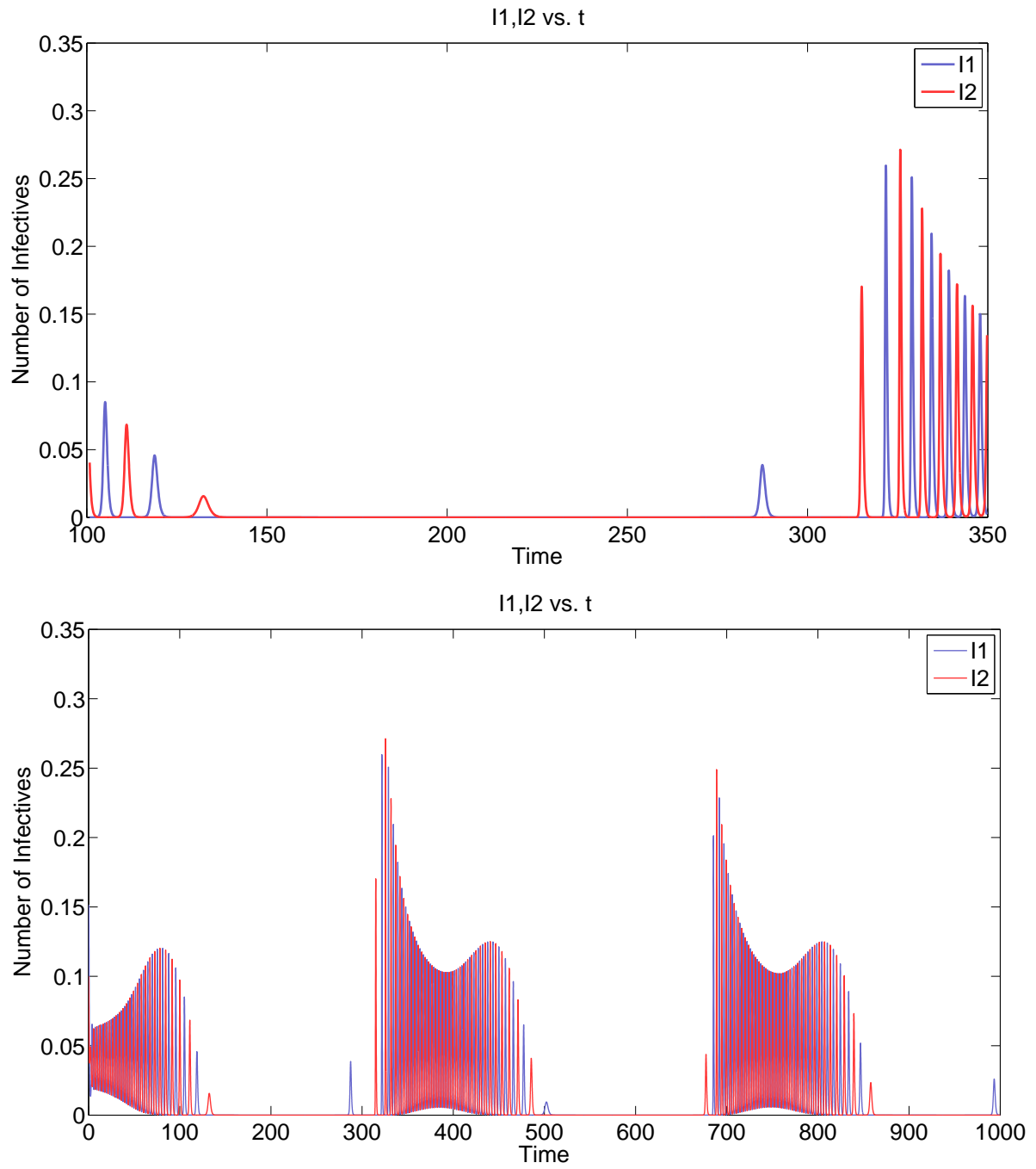


Figure 5.9: Periodic and alternating coexistence and replacement with $\kappa = 0.4$

Chapter 6

Analysis of the WHO Data

In Chapter 3 - 4, the replacement and coexistence of two influenza viruses were studied analytically. From FluNet, one of the major modules under the WHO official website, one can download demographic data on the number of reported infective of a subtype of influenza viruses in a country/region over a specified period. In this chapter, these data will be used to explain the coexistence of H3N2(68) and H1N1(77)/H1N1(09), as well as the replacement of H1N1(77) by H1N1(09).

6.1 Downloading Data from FluNet

To obtain the data of interest, one can follow the detailed instructions.

1. Go to the WHO official website. Under module Programmes, find FluNet and click.
http://www.who.int/influenza/gisrs_laboratory/flunet/en/
2. Click on "Data entry and advanced functions" under FluNet functions.
<http://gamapserver.who.int/GlobalAtlas/home.asp>
3. Click on "DATA QUERY" on the left panel.
4. Select indicators and variables. For the purpose of this study, the number of influenza viruses detected is chosen as the indicator, and A(H1), A(H3) and A(H1N1)pdm09 are the variables. These variables correspond to H1N1(77), H3N2(68), and H1N1(09), respectively.
5. In the next page, select a country / countries and a time range. Caution: it may be out of memory if too many data are requested at one time. To avoid this situation, one can limit the number of countries selected or shorten the time range.
6. In the next page, click on "REPORTS", which is the first option above the chart.
7. Select the report type. To view geographic areas by row and time periods by column, click on the first chart.

8. In the next page, click on "EXPORT TO EXCEL" to download the data as a *.xls file (Excel 97-2003 Workbook). Notice that some browsers do not support this download and thus generate a *.asp file.

After that, one can either manipulate the Excel file manually or write some code to output figures and statistics.

6.2 Interpolation of the Data

Due to the randomness of the infected individuals of a given country, the cubic spline method is applied to interpolate the data: divide the approximation interval into a collection of subintervals and construct a cubic polynomial on each subinterval. For detailed algorithm of cubic spline interpolation, one can refer to Sec. 3.5 in (Burden and Faires, 2009).

Given a subtype of influenza viruses and a country/region, the node and node values were built up as follows.

1. With 469 weeks from January 1, 2005 to December 31, 2013, the nodes are chosen to be $x_i = 13i + 1$, $i = 0, 1, 2, \dots, 36$. Thus, there are 36 subintervals, each containing 13 weeks of data (a three-month period).
2. The node value $f(x_i)$ of the corresponding node is the mean of five observed values, $y_{i-2}, y_{i-1}, y_i, y_{i+1}, y_{i+2}$. For $i = 0$ or $i = 36$, $f(x_i)$ is the mean of the three observed values which are available.
3. Use the Matlab built-in function `spline` to find the values of the underlying function at the values of the interpolant $\mathbf{x} = (x_0, x_1, x_2, \dots, x_{36})$.

Since the corresponding Matlab code is heavily based on the data selected, it will not appear in the Appendix.

6.3 Interpretation of the Data

Three assertions can be made from the Matlab output figures.

6.3.1 Replacement of H1N1(77) by H1N1(09)

On the 200th week (January, 2009), most countries had the first H1N1(09) outbreaks, and after that no outbreaks of H1N1(77) took place. It is believed that H1N1(09) replaced H1N1(77). To illustrate the replacement of H1N1(77) by H1N1(09), data of the following regions are

used. Each region contains a list of countries as follows.

- **East Asia:** China, Japan, Mongolia, and Republic of Korea.
- **Southeast Asia:** Cambodia, Indonesia, Lao People’s Democratic Republic, Malaysia, Philippines, Thailand, and Viet Nam.
- **North Europe:** Denmark, Estonia, Finland, Iceland, Ireland, Latvia, Lithuania, Norway, Sweden, and United Kingdom.
- **South Europe:** Albania, Bosnia and Herzegovina, Croatia, Greece, Italy, Montenegro, Portugal, Serbia, Serbia and Montenegro, Slovenia, Spain, and the former Yugoslav Republic.

The replacement will be shown based on the data of H1N1(77) and H1N1(09) in the above regions from January 1, 2005 to December 31, 2013.

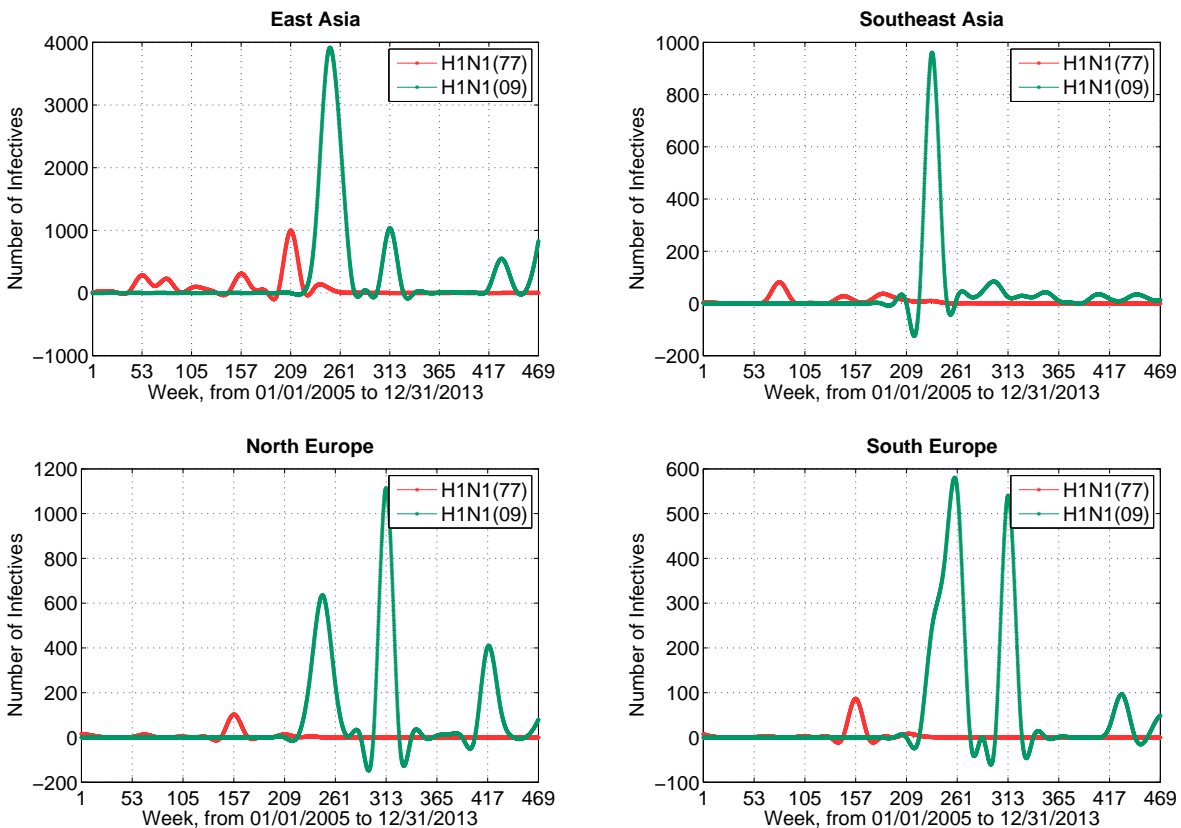


Figure 6.1: Replacement of H1N1(77) by H1N1(09) in some European and Asian regions

From Figure 6.1, it can be seen that all of these four regions had some H1N1(77) cases from 2005, and relatively significant outbreaks (compared to the overall magnitude of the

virus) in around the 150th week (December, 2007). After around the 210th week (January, 2009), there were few H1N1(77) cases. Instead, since then, H1N1(09) surged and soon became a pandemic. It is believed that H1N1(77) was replaced by H1N1(09) due to antigenetic drift.

6.3.2 Coexistence of H1N1 and H3N2(68)

Most countries had H1N1(77) and H3N2(68), or H1N1(09) and H3N2(68) outbreaks at almost the same period of time. It is considered that there is a coexistence of H1N1(77) and H3N2(68), or H1N1(09) and H3N2(68). To illustrate the coexistence of H1N1 and H3N2(68), data of the following regions are used. Each region contains a list of countries as follows.

- **North America:** Canada, Mexico, and United States of America.
- **South America:** Argentina, Bolivia, Brazil, Chile, Colombia, Ecuador, French Guiana, Paraguay, Peru, Suriname, Uruguay, and Venezuela.
- **East Asia:** China, Japan, Mongolia, and Republic of Korea.
- **Southeast Asia:** Cambodia, Indonesia, Lao People's Democratic Republic, Malaysia, Philippines, Thailand, and Viet Nam.

The coexistence will be shown from two aspects.

Coexistence of H1N1(77) and H3N2(68)

Since H1N1(77) was replaced by H1N1(09) in the early 2009, data used in this section are from January 1, 2005 to December 31, 2008.

From Figure 6.2, it can be seen that although different regions suffered outbreaks of H1N1(77) and H3N2(68) at different weeks, the two viruses had the same period of about one year in all regions. Moreover, the two viruses reached their peaks almost simultaneously.

Notice that the purple curve in Figure 6.2(a), which represents the number of infective of H3N2(68) in North America, is very close to the theoretical results in Chapter 2, Figure 2.6.

Coexistence of H1N1(09) and H3N2(68)

Since H1N1(09) did not exist before 2009, data used in this section are from January 1, 2009 to December 31, 2013.

From Figure 6.3, similar conclusion can be drawn that the outbreaks of the two viruses occurred almost simultaneously.

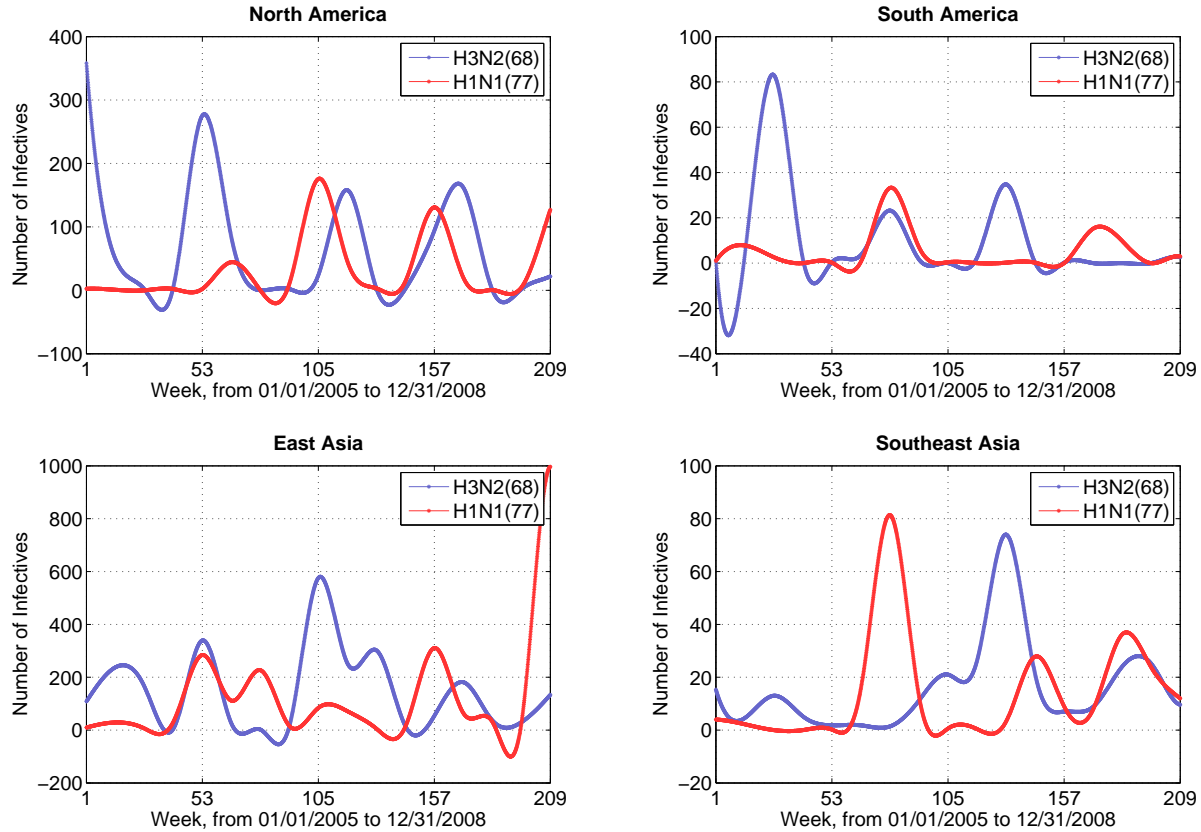


Figure 6.2: Coexistence of H1N1(77) and H3N2(68) in the American regions

Compare with Figure 6.2 and 6.3, it can be seen the pattern of the infective number of H3N2(68) is more regular, and can be reproduced computationally with larger seasonality κ . From the figure, it is hard to tell whether the period of either H3N2(68) or H1N1(77) is about one year. More information, such as health insurance policy and migration, should be taken into consideration to interpret the oscillation.

6.3.3 Skips of H1N1(09) and H3N2(68)

The outbreaks of H1N1(09) happened on the 260th, 320th and 440th week (December, 2009, February, 2011, and June, 2013, respectively). It was expected that an outbreak should have occurred on the 380th week (March, 2012), but there was no outbreak, which is called a skip. The outbreaks of H3N2(68) occurred on the 200th, 380th and 440th week. It was expected that outbreaks should have taken place on the 260th and 320th week, but no outbreaks happened. Subtype H3N2(68) had two skips over the observed period. To illustrate the skips of H1N1(09) and H3N2(68), data from the European regions are used. Each part contains a list of countries as follows.

- **East Europe:** Armenia, Azerbaijan, Belarus, Bulgaria, Czech Republic, Georgia, Hungary, Poland, Republic of Moldova, Romania, Russian Federation, Slovakia, and

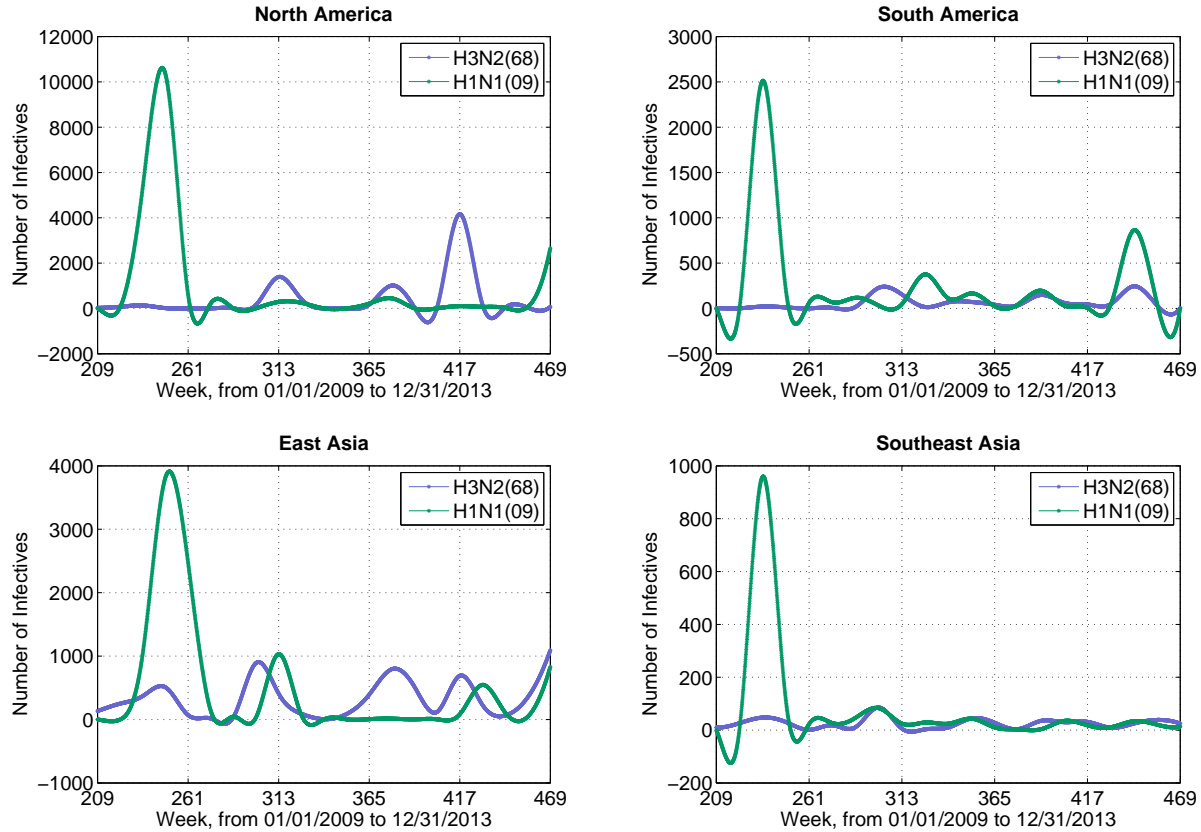


Figure 6.3: Coexistence of H1N1(09) and H3N2(68) in the American regions (Due to the magnitude, the peaks of H3N2(68) are hard to see)

Ukraine.

- **North Europe:** Denmark, Estonia, Finland, Iceland, Ireland, Latvia, Lithuania, Norway, Sweden, and United Kingdom.
- **South Europe:** Albania, Bosnia and Herzegovina, Croatia, Greece, Italy, Montenegro, Portugal, Serbia, Serbia and Montenegro, Slovenia, Spain, and the former Yugoslav Republic.
- **West Europe:** Austria, Belgium, France, Germany, Luxembourg, Netherlands, and Switzerland

The skips will be shown based on the data of H1N1(09) and H3N2(68) in the above regions from January 1, 2009 to December 31, 2013.

From Figure 6.4, it can be seen that all of these four regions had their first H1N1(09) outbreaks in around the 260th week (December, 2009), and the second in the 320th week (February, 2011). If the outbreak of H1N1(09) was considered periodic, the third outbreak should have happened in around the 380th week (March, 2012), indicated by the arrows.

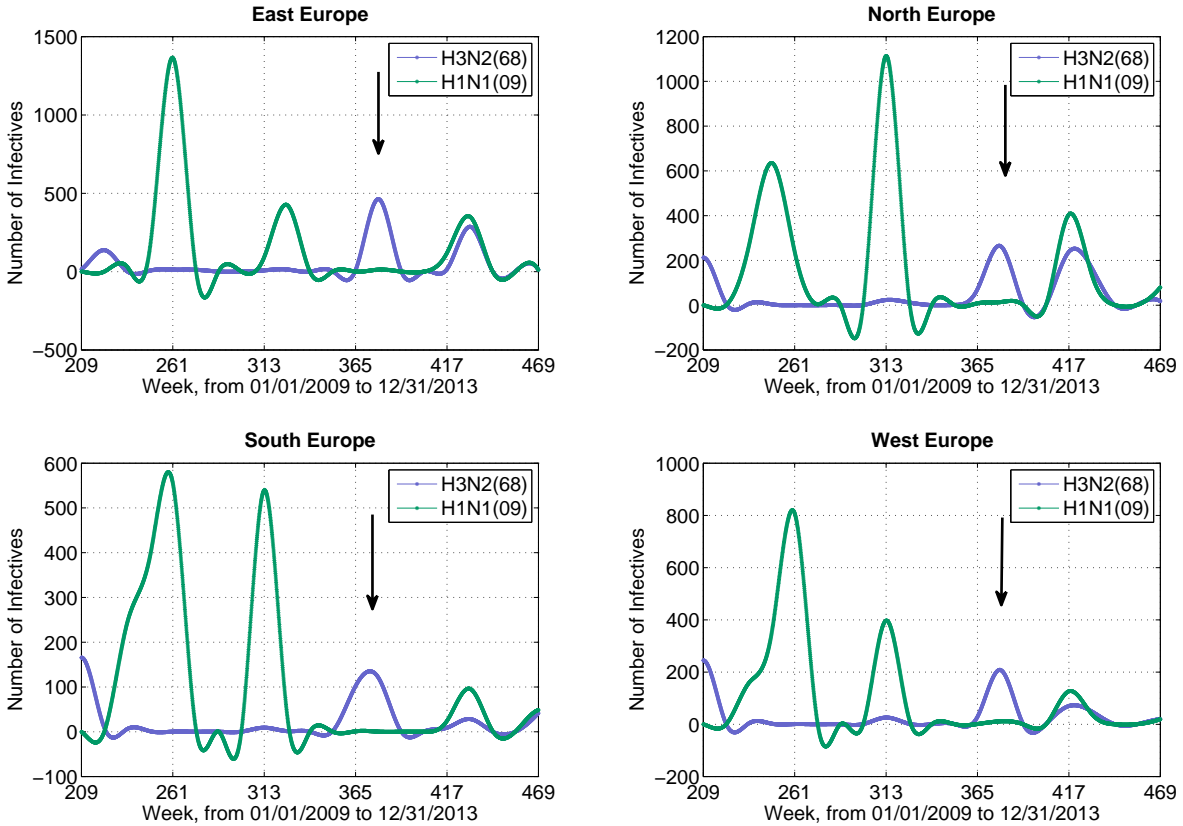


Figure 6.4: Skips of H1N1(09) and H3N2(68) in the European regions

However, there was a skip in that week. After another 60-week period, in the 440th week (June, 2013), there was a resurgence of H1N1(09) as expected.

On the other hand, all of these four regions had their H3N2(68) outbreaks in around the 200th week (January, 2009). There were no significant H3N2(68) outbreaks in Europe until in around the 380th week (March, 2012). Another H3N2(68) outbreak took place in the 440th week (summer of 2012). It is concluded that H3N2(68), with a period of 60 weeks, skipped two outbreaks, one in the 260th week, and the other in the 320th week.

Chapter 7

Conclusion

The field of epidemic models is a large and growing area of applied mathematics. It is being increasingly used to model the transmission of communicable diseases through individuals. In this Major Qualifying Project, we studied three models with constant and periodic transmission rates.

We started this project with the simplest SIR model and its extension, the SEIR model. Since the SIR and SEIR models with constant transmission rates have already been well studied, we focused mainly on the models with periodic transmission rates. With a constant transmission rate in the SIR or SEIR model, the occurrence of an epidemic outbreak depends on the Basic Reproduction Number of the model. With a periodic transmission rate, we showed numerically in Chapter 2 that the small-amplitude periodic solutions of the SIR or SEIR model with periodic transmission rate form a sequence of period-doubling bifurcations. As the seasonality increases, the solution passes from a period 1 cycle to period 2 to period 3 and tends to a chaotic behavior. However, this transition is not stable in the SEIR model, where a period tripling bifurcation may degrade to a period doubling bifurcation.

Then we moved on to the two-strain SIR model, in which two SIR models are coupled together and the revolution and competition parameters δ_i are introduced. By analyzing the four equilibrium points in this model, we found three major relationships between the two viruses: coexistence, replacement, and periodic alternation between coexistence and replacement. When the transmission rate is constant and there is no stable equilibrium point, the model has periodic solutions. In Chapter 5, we examined the effects of periodic transmission rate in the two-strain SIR model on the number of infective individuals. When coexistence or replacement takes place between the two viruses, the periodic transmission rate $\beta(t)$ turns $I_1(t)$ and $I_2(t)$ into trigonometric-like functions with a constant amplitude. When the solution displays an alternating coexistence and replacement, $\beta(t)$ results in transitory extinctions of both viruses in each period, as well as chaotic features in the functions $I_1(t)$ and $I_2(t)$.

Research in the application of the two-strain SIR model is far from complete. There remains a wealth of mathematical problems relating to the model that have yet to be solved. In Chapter 6, we interpreted the data of the infective individuals of H1N1(77), H1N1(09), and H3N2(68) downloaded from WHO. The infective numbers of these viruses display the three

relationships to some extent. We noticed the replacement of H1N1(77) by H1N1(09), the co-existence of H1N1 and H3N2(68), and the skips of H1N1(09) and H3N2(68). Unfortunately, the interpolation results are very different from our simulation results. We have thus summarized some limitations of the two-strain SIR model. First, we assumed that the population is homogeneous in our model, and there is neither birth nor death in the population. However, the population structure in the real life is much more complicated, consisting of different ages, races, and genders. Second, the transmission rate function, $\beta(t)$, used in the model is too simplistic. It may change from year to year and between countries, depending on public health policies and global migrations. In addition, the WHO data may not be accurate, as some countries are reluctant to report their cases.

The followings are some suggestions to improve the two-strain SIR model. First, one can make use of the interpolation polynomial of the infective individuals and extend it to a transmission rate function. Second, since different countries have different health policies, one can add additional parameters to the model such as birth rate, death rate, and government control over health care. Third, to improve the accuracy of the model, one can keep track of each individual's contribution to the spread of viruses by extending the model to a multicity model.

Bibliography

- J.L. Aron and I.B. Schwartz. Seasonally and period-doubling bifurcations in an epidemic model. *Journal of Theoretical Biology*, 110:665–679, 1984.
- R.L. Burden and J.D. Faires. *Numerical Analysis*. Cengage Learning, 9 edition, 2009.
- M. Chan. World now at the start of 2009 influenza pandemic. Technical report, World Health Organization, 2009.
- D.J.D. Earn, J. Dushoff, and S.A. Levin. Ecology and evolution of the flu. *Trends in Ecology and Evolution*, 17:334340, 2002.
- J. Galvin. Spanish flu pandemic: 1918. Technical report, Popular Mechanics.
- J. Greene. *The Bird Flu Pandemic: Can It Happen? Will It Happen? How to Protect Yourself and Your Family If It Does*. St. Martin’s Griffin, 1 edition, 2006.
- J. Greene and K. Moline. *The Bird Flu Pandemic*. St. Martin’s Griffin, 1 edition, 2006.
- A.J. Hay, Gregory V., Douglas A.R., and Lin Y.P. The evolution of human influenza viruses. *Philosophical Transactions of the Royal Society B: Biological*, 356:1861–1870, 2001.
- M.R. Hilleman. Realities and enigmas of human viral influenza: Pathogenesis, epidemiology and control. *Vaccine*, 20:25–26, 2002.
- H. Hong. *Plague, SARS, and the Story of Medicine in Hong Kong*. Hong Kong University Press, 1 edition, 2006.
- K.J. Jakeman, M. Tisdale, S. Russell, A. Leone, and C. Sweet. Efficacy of 2’-deoxy-2’-fluororibosides against influenza a and b viruses in ferrets. *Antimicrobial Agents and Chemotherapy*, 38:1864–1867, 1994.
- Y. Kawaoka. *Influenza Virology: Current Topics*. Caister Academic Press, 1 edition, 2006.
- M.J. Keeling, P. Hohani, and B.T. Grenfell. Seasonally forced disease dynamics explored as switching between attractors. *Physica D*, 148:317–335, 2001.
- M. Mandel. No need to panic. *Toronto Sun*, 2009.

- Y. Matsuzaki, K. Sugawara, K. Mizuta, E. Tsuchiya, Y. Muraki, S. Hongo, H. Suzuki, and K. Nakamura. Antigenic and genetic characterization of influenza c viruses which caused two outbreaks in Yamagata city, Japan, in 1996 and 1998. *Journal of Clinical Microbiology*, 40:422–429, 2002.
- T.C. Mettenleiter and F. Sobrino. *Animal Viruses: Molecular Biology*. Caister Academic Press, 1 edition, 2008.
- O. Narayan and J. Griffin, D.E. and Chase. Antigenic shift of visna virus in persistently infected sheep. *Science*, 197:376–378, 1977.
- A.D. Osterhaus, G.F. Rimmelzwaan, B.E. Martina, T.M. Bestebroer, and Fouchier R.A. Influenza b virus in seals. *Science*, 288:1051–1053, 2000.
- L.S. Ott. The economic impact of an influenza pandemic on the United States. *Economic Information Newsletter*, 2008.
- W.E. Paul. *Fundamental Immunology*. Wolters Kluwer, 6 edition, 2008.
- K. Rogers. Flu shots for everyone. Technical report, Encyclopaedia Britannica, Inc, 2007.
- I.B. Schwartz and H.L. Smith. Infinite subharmonic bifurcation in an SEIR epidemic model. *Journal of Mathematical Biology*, 18:233–253, 1983.
- J.K. Taubenberger and D. Morens. 1918 influenza: the mother of all pandemics. *EID Journal*, 12:15–22, 2006.
- J.K. Taubenberger and D.M. Morens. The pathology of influenza virus infections. *Annual Review of Pathology*, 3:499–522, 2008.
- J. Treanor. Influenza vaccine — outmaneuvering antigenic shift and drift. *New England Journal of Medicine*, 350:218–220, 2004.
- Unknown. World Health Organization issues alert: Mexican president tries to isolate those with swine flu. *Associated Press*, 2009a.
- Unknown. Current WHO global phase of pandemic alert for pandemic (H1N1) 2009. Technical report, World Health Organization, 2009b.
- Unknown. How the flu virus can change: Drift and shift. Technical report, Centers for Disease Control and Prevention, National Center for Immunization and Respiratory Diseases (NCIRD), 2011a.
- Unknown. How the flu virus can change: Drift and shift. Technical report, Centers for Disease Control and Prevention, National Center for Immunization and Respiratory Diseases (NCIRD), 2011b.
- Unknown. Seasonal influenza: Flu basics. Technical report, Centers for Disease Control and Prevention, National Center for Immunization and Respiratory Diseases (NCIRD), 2013a.

- Unknown. Current who global phase of pandemic alert: Avian influenza a(h5n1). Technical report, World Health Organization, 2013b.
- Unknown. Report of hong kong flu. Technical report, U.S. Department of Health and Human Services, 2013c.
- Unknown. History of pandemic. Technical report, U.S. Department of Health and Human Services, 2013d.
- Unknown. About pandemics. Technical report, U.S. Department of Health and Human Services, 2013e.
- Unknown. Pandemics flu history. Technical report, U.S. Department of Health and Human Services, 2013f.
- M.A. Urban. Influenza: Viral infections: Merck manual home edition. Technical report, 2009.
- M.C. Zambon. Epidemiology and pathogenesis of influenza. *Journal of Antimicrobial Chemotherapy*, 44:3–9, 1999.

Appendix A

List of Symbols

Symbol	Description
α	infective rate
β	transmission rate
C	the effective infectee number
δ	revolution and competition parameter
E	the number of people exposed to the virus but not infectious
$\mathbf{E}_1, \mathbf{E}_2, \mathbf{E}_3, \mathbf{E}_4$	equilibrium points of the two-strain SIR model
F_0	critical value that determines the existence of \mathbf{E}_4
γ	recovery rate
I	the number of infected people
κ	seasonality
N	population size
$\mathbf{P}_1, \mathbf{P}_2$	equilibrium points of the SIR model
$\mathbf{Q}_1, \mathbf{Q}_2$	equilibrium points of the SEIR model
R	the number of recovered people
R_0	the basic reproduction number
S	the number of susceptible people
t	time
μ	birth rate, death rate

Appendix B

Matlab Scripts

B.1 SIRperiodic.m

```
1 % This function simulates the SIR model with periodic beta, and
2 % plots the graph of  $-\log(I)$  vs.  $t$  and  $-\log(I)$  vs.  $-\log(S)$ .
3 function SIRperiodic(T,b,c,d)
4 % Input Parameters
5 % T - Times of simulation
6 % b - The contact rate of the periodic beta
7 % c - Starting time of the graph
8 % d - Ending time of the graph
9
10 % Variables
11 global mu gamma beta0 delta
12 mu = 0.02; beta0 = 1800; gamma = 100; delta = b;
13
14 % Initial condition
15 s0 = 0.7; i0 = 0.3; r0 = 0;
16 initdata = [s0,i0,r0];
17
18 % Solving the ODE
19 options = odeset('MaxStep',0.01);
20 [t,x] = ode45(@SIRmodel,[0,T],initdata,options);
21
22 % Plotting
23 figure(1);
24 set(gcf,'DefaultAxesFontSize',12,'Color','white');
25 plot(t(c:d),-log(x(c:d,2)),'LineWidth',2,'Color','red');
26 xlabel('t');ylabel('-log(I)');
27 title('-log(I) vs. t');
28 figure(2);
29 set(gcf,'DefaultAxesFontSize',12,'Color','white');
```

```

30 plot(-log(x(c:d,1)), -log(x(c:d,2)), 'LineWidth', 2, 'Color', 'red');
31 xlabel('-log(S)'); ylabel('-log(I)');
32 title('-log(I) vs. -log(S)');
33
34 % SIR model
35 function dydt = SIRmodel(t,y)
36 global mu gamma beta0 delta
37 s = y(1); i = y(2); r = y(3);
38 beta = beta0*(1+delta*cos(2*pi*t));
39 dydt(1) = mu-mu*s-beta*s*i;
40 dydt(2) = beta*s*i-(mu+gamma)*i;
41 dydt(3) = gamma*i-mu*r;
42 dydt = dydt';

```

B.2 SEIRstable.m

```

1 % This program examines the stability of the nontrivial equilibrium
2 % point of the SEIR model.
3 function SEIRstable(n)
4 counts = 0; countu = 0;
5 for k = 1:n
6     % generate parameters
7     beta = 1000*rand(1); alpha = 100*rand(1);
8     gamma = 10*rand(1); mu = (1/10)*rand(1);
9     beta0 = beta;
10    R0 = alpha*beta0/(mu + gamma)/(mu + alpha);
11    % Jacobian at the nontrivial equilibrium point
12    J = [-mu-beta0*(mu/(mu+alpha)-mu*(mu+gamma)/(alpha*beta0)) ...
13         0 -(mu+gamma)*(mu+alpha)/alpha 0;
14         beta0*(mu/(mu+alpha)-mu*(mu+gamma)/(alpha*beta0)) ...
15         -mu-alpha (mu+gamma)*(mu+alpha)/alpha 0;
16         0 alpha -mu-gamma 0;
17         0 0 gamma -mu];
18    if R0 < 1
19        % the nontrivial equilibrium point does not exist
20        continue
21    else
22        rx = eig(J);
23        countR = countR + 1;
24        if (real(rx(1)) > 0 || real(rx(2)) > 0 || real(rx(3)) > 0
25            || real(rx(4)) > 0)
26            countu = countu + 1; % unstable
27        else
28            counts = counts + 1; % stable
29        end

```



```

29     end
30 end
31 display(countu); display(counts);

```

B.3 SIRSIR.m

```

1  % Simulate the stability of the equilibrium points.
2  function SIRSIR(m)
3  % =====
4  % Initializing variables
5  % =====
6  sign1 = 0; % stability of E1
7  sign2 = 0; % stability of E2
8  sign3 = 0; % stability of E3
9  sign4 = 0; % stability of E4
10 sign = 0; % combined result
11 % 0 = DNE; 1 = stable; 2 = unstable
12 E1st_E4dne = zeros(3,3); % matrix for E1 stable, E4 DNE
13 E1un_E4dne = zeros(3,3); % matrix for E1 unstable, E4 DNE
14 E1st_E4st = zeros(3,3); % matrix for E1 stable, E4 stable
15 E1un_E4st = zeros(3,3); % matrix for E1 unstable, E4 stable
16 E1st_E4un = zeros(3,3); % matrix for E1 stable, E4 unstable
17 E1un_E4un = zeros(3,3); % matrix for E1 unstable, E4 unstable
18
19 for k=1:m
20     % =====
21     % Generating parameters
22     % =====
23     gamma = 22*rand(1);
24     delta1 = rand(1);
25     delta2 = (1+rand(1))*delta1;
26     beta0 = 5*rand(1)*gamma;
27     beta = round(rand(1)*5)*beta0;
28     F0 = (beta-2*gamma)/((abs(delta1-delta2))*(gamma+1));
29     % some values of equilibrium points
30     S11 = delta2/(delta1+delta2);
31     S12 = delta1/(delta1+delta2);
32     I31 = (beta*delta2-gamma*delta2-delta1*gamma)/...
33           (beta*(gamma+delta2+gamma*delta2));
34     S32 = gamma*(beta-gamma+delta1+delta1*gamma)/...
35           (beta*(gamma+delta2+gamma*delta2));
36     S21 = gamma*(beta-gamma+delta2+delta2*gamma)/...
37           (beta*(gamma+delta1+gamma*delta1));
38     I22 = (beta*delta1-gamma*delta1-delta2*gamma)/...
39           (beta*(gamma+delta1+gamma*delta1));

```

```

40
41 % =====
42 % Analysis of E1
43 % =====
44 if ((beta*S12-gamma) < 0 && (beta*S11-gamma) < 0)
45     %if both of the rest two eigenvalues are negative
46     sign1=1; % E1 is stable
47 else
48     % if anyone of these two is positive , E1 is unstable
49     sign1=2;
50 end
51
52 % =====
53 % Analysis of E2
54 % =====
55 % conditions for E2 to exist
56 condition21 = beta-gamma+delta2*(1+gamma);
57 condition22 = beta*delta1-gamma*(delta1+delta2);
58 % coefficients of E2's characteristic polynomial
59 a1=1+beta*I22+delta1+delta2;
60 a2=(gamma+1+delta1)*beta*I22+(delta1+delta2);
61 a3=beta*I22*(gamma+delta1+gamma*delta1);
62 % check conditions for E2 to exist
63 if(condition21 > 0 && condition22 > 0)
64     % if both conditions satisfied , E2 exists
65     % first part of E2's characteristic polynomial
66     p1=[1 -beta*S21+gamma];
67     % second part of E2's characteristic polynomial
68     p2=[1 a1 a2 a3];
69     rx1=roots(p1); % roots of p1
70     rx2=roots(p2); % roots of p2
71     if (real(rx1)<0 && real(rx2(1)) < 0 &&...
72         real(rx2(2)) < 0 && real(rx2(3)) < 0)
73         % if all roots are negative
74         sign2 = 1; % E2 stable
75     else % if anyone of them is positive
76         sign2 = 2; % E2 unstable
77     end
78 else
79     sign2 = 0; % E2 does not exist
80 end
81
82 % =====
83 % Analysis of E3
84 % =====

```

```

85 % conditions for E3 to exist
86 condition31 = gamma*(beta-gamma +delta1+delta1*gamma);
87 condition32 = beta*delta2-gamma*delta1-delta2*gamma;
88 % coefficients of characteristic polynomial
89 b1=1+beta*I31+delta1+delta2;
90 b2=(gamma+1+delta2)*beta*I31+delta1+delta2;
91 b3=beta*I31*(gamma+delta2+gamma*delta2);
92 % check conditions for E3 to exist
93 if condition31 > 0 && condition32 > 0
94 % first part of E2's characteristic polynomial
95 p1=[1 -beta*S32+gamma];
96 % second part of E2's characteristic polynomial
97 p2=[1 b1 b2 b3];
98 rx1=roots(p1); % roots of p1
99 rx2=roots(p2); % roots of p2
100 if (real(rx1)< 0 && real(rx2(1)) < 0 &&...
101     real(rx2(2)) < 0 && real(rx2(3)) < 0)
102     % if all roots are negative
103     sign3 = 1; % E3 stable
104 else
105     sign3 = 2; % E3 unstable
106 end
107 else
108     sign3 = 0;
109 end
110
111 % =====
112 % Analysis of E4
113 % =====
114 % E4 exists when F0 > 1
115 if F0 > 1
116     R1 = (beta-2*gamma+(delta2-delta1)*(gamma+1))/(2+2*gamma);
117     R2 = (beta-2*gamma+(delta1-delta2)*(gamma+1))/(2+2*gamma);
118     % coefficients of characteristic polynomial
119     c1 = (2+delta1+delta2)+(R1+R2);
120     c2 = 1+2*delta1+2*delta2+2*R1+delta2*R1+gamma*R1 ...
121         +2*R2+delta1*R2+gamma*R2+R1*R2;
122     c3 = delta1+delta2+(2*delta2+2*gamma+1+delta2*gamma)*R1 ...
123         +(2*delta1+2*gamma+1+delta1*gamma)*R2+(1+gamma)*R1*R2;
124     c4 = (delta2+gamma+delta2*gamma)*R1+(delta1+gamma+...
125         delta1*gamma)*R2+(4*gamma+1+gamma^2)*R1*R2;
126     c5 = 2*gamma*(1+gamma)*R1*R2;
127 % construct E4's characteristic polynomial
128 p4=[1 c1 c2 c3 c4 c5];
129 rx4 = roots(p4); % roots of E4's characteristic polynomial

```

```

130     if(real(rx4(1)) > 0 || real(rx4(2)) > 0 || real(rx4(3))...
131         > 0 || real(rx4(4)) > 0 || real(rx4(5)) > 0)
132         % if one of the eigenvalues is positive, E4 unstable
133         sign4 = 2;
134     else
135         sign4 = 1; % all eigenvalues are negative, E4 stable
136     end
137 else
138     sign4=0; % F0 < 1, E4 does not exist
139 end
140
141 % =====
142 % Analysis of existence and stability
143 % =====
144 sign = sign1*1000+sign2*100+sign3*10+sign4;
145 % Case 1: E1 stable, E4 DNE
146 if sign == 1000 % E1 stable, E2 DNE, E3 DNE, E4 DNE
147     E1st_E4dne(1,1) = E1st_E4dne(1,1)+1;
148 elseif sign == 1010 % E1 stable, E2 DNE, E3 stable, E4 DNE
149     E1st_E4dne(2,1) = E1st_E4dne(2,1)+1;
150 elseif sign == 1020 % E1 stable, E2 DNE, E3 unstable, E4 DNE
151     E1st_E4dne(3,1) = E1st_E4dne(3,1)+1;
152 elseif sign == 1100 % E1 stable, E2 stable, E3 DNE, E4 DNE
153     E1st_E4dne(1,2) = E1st_E4dne(1,2)+1;
154 elseif sign == 1110 % E1 stable, E2 stable, E3 stable, E4 DNE
155     E1st_E4dne(2,2) = E1st_E4dne(2,2)+1;
156 elseif sign == 1120 % E1 stable, E2 stable, E3 unstable, E4 DNE
157     E1st_E4dne(3,2) = E1st_E4dne(3,2)+1;
158 elseif sign == 1200 % E1 stable, E2 unstable, E3 DNE, E4 DNE
159     E1st_E4dne(1,3) = E1st_E4dne(1,3)+1;
160 elseif sign == 1210 % E1 stable, E2 unstable, E3 stable, E4 DNE
161     E1st_E4dne(2,3) = E1st_E4dne(2,3)+1;
162 elseif sign == 1220 % E1 stable, E2 unstable, E3 unstable, E4
163     DNE
164     E1st_E4dne(3,3) = E1st_E4dne(3,3)+1;
165 end
166 % Case 2: E1 unstable, E4 DNE
167 if sign == 2000 % E1 unstable, E2 DNE, E3 DNE, E4 DNE
168     E1un_E4dne(1,1) = E1un_E4dne(1,1)+1;
169 elseif sign == 2010 % E1 unstable, E2 DNE, E3 stable, E4 DNE
170     E1un_E4dne(2,1) = E1un_E4dne(2,1)+1;
171 elseif sign == 2020 % E1 unstable, E2 DNE, E3 unstable, E4 DNE
172     E1un_E4dne(3,1) = E1un_E4dne(3,1)+1;
173 elseif sign == 2100 % E1 unstable, E2 stable, E3 DNE, E4 DNE
174     E1un_E4dne(1,2) = E1un_E4dne(1,2)+1;

```

```

174 elseif sign == 2110 % E1 unstable , E2 stable , E3 stable , E4 DNE
175     E1un_E4dne(2,2) = E1un_E4dne(2,2)+1;
176 elseif sign == 2120 % E1 unstable , E2 stable , E3 unstable , E4
    DNE
177     E1un_E4dne(3,2) = E1un_E4dne(3,2)+1;
178 elseif sign == 2200 % E1 unstable , E2 unstable , E3 DNE, E4 DNE
179     E1un_E4dne(1,3) = E1un_E4dne(1,3)+1;
180 elseif sign == 2210 % E1 unstable , E2 unstable , E3 stable , E4
    DNE
181     E1un_E4dne(2,3) = E1un_E4dne(2,3)+1;
182 elseif sign == 2220 % E1 unstable , E2 unstable , E3 unstable , E4
    DNE
183     E1un_E4dne(3,3) = E1un_E4dne(3,3)+1;
184 end
185 % Case 3: E1 stable , E4 stable
186 if sign == 1001 % E1 stable , E2 DNE, E3 DNE, E4 stable
187     E1st_E4st(1,1) = E1st_E4st(1,1)+1;
188 elseif sign == 1011 % E1 stable , E2 DNE, E3 stable , E4 stable
189     E1st_E4st(2,1) = E1st_E4st(2,1)+1;
190 elseif sign == 1021 % E1 stable , E2 DNE, E3 unstable , E4 stable
191     E1st_E4st(3,1) = E1st_E4st(3,1)+1;
192 elseif sign == 1101 % E1 stable , E2 stable , E3 DNE, E4 stable
193     E1st_E4st(1,2) = E1st_E4st(1,2)+1;
194 elseif sign == 1111 % E1 stable , E2 stable , E3 stable , E4
    stable
195     E1st_E4st(2,2) = E1st_E4st(2,2)+1;
196 elseif sign == 1121 % E1 stable , E2 stable , E3 unstable , E4
    stable
197     E1st_E4st(3,2) = E1st_E4st(3,2)+1;
198 elseif sign == 1201 % E1 stable , E2 unstable , E3 DNE, E4 stable
199     E1st_E4st(1,3) = E1st_E4st(1,3)+1;
200 elseif sign == 1211 % E1 stable , E2 unstable , E3 stable , E4
    stable
201     E1st_E4st(2,3) = E1st_E4st(2,3)+1;
202 elseif sign == 1221 % E1 stable , E2 E3 unstable , E4 stable
203     E1st_E4st(3,3) = E1st_E4st(3,3)+1;
204 end
205 % Case 4: E1 unstable , E4 stable
206 if sign == 2001 % E1 unstable , E2DNE, E3 DNE, E4 stable
207     E1un_E4st(1,1) = E1un_E4st(1,1)+1;
208 elseif sign == 2011 % E1 unstable , E2 DNE, E3 stable , E4 stable
209     E1un_E4st(2,1) = E1un_E4st(2,1)+1;
210 elseif sign == 2021 % E1 unstable , E2 DNE, E3 unstable , E4
    stable
211     E1un_E4st(3,1) = E1un_E4st(3,1)+1;

```

```

212 elseif sign == 2101 % E1 unstable , E2 stable , E3 DNE, E4
    stable
213     E1un_E4st(1,2) = E1un_E4st(1,2)+1;
214 elseif sign == 2111 % E1 unstable , E2 stable , E3 stable , E4
    stable
215     E1un_E4st(2,2) = E1un_E4st(2,2)+1;
216 elseif sign == 2121 % E1 E3 unstable , E2 stable , E4 stable
    E1un_E4st(3,2) = E1un_E4st(3,2)+1;
217
218 elseif sign == 2201 % E1 unstable , E2 unstable , E3 DNE, E4
    stable
219     E1un_E4st(1,3) = E1un_E4st(1,3)+1;
220 elseif sign == 2211 % E1 E2 unstable , E3 stable , E4 stable
    E1un_E4st(2,3) = E1un_E4st(2,3)+1;
221
222 elseif sign == 2221 % E1 E2 E3 unstable , E4 stable
    E1un_E4st(3,3) = E1un_E4st(3,3)+1;
223
224 end
225 % Case 5: E1 stable , E4 unstable
226 if sign == 1002 % E1 stable , E2 DNE, E3 DNE, E4 unstable
    E1st_E4un(1,1) = E1st_E4un(1,1)+1;
227
228 elseif sign == 1012 % E1 stable , E2 DNE, E3 stable , E4 unstable
    E1st_E4un(2,1) = E1st_E4un(2,1)+1;
229
230 elseif sign == 1022 % E1 stable , E2 DNE, E3 unstable , E4
    unstable
231     E1st_E4un(3,1) = E1st_E4un(3,1)+1;
232 elseif sign == 1102 % E1 stable , E2 stable , E3 DNE, E4 unstable
    E1st_E4un(1,2) = E1st_E4un(1,2)+1;
233
234 elseif sign == 1112 % E1 stable , E2 stable , E3 stable , E4
    unstable
235     E1st_E4un(2,2) = E1st_E4un(2,2)+1;
236 elseif sign == 1122 % E1 stable , E2 stable , E3 E4 unstable
    E1st_E4un(3,2) = E1st_E4un(3,2)+1;
237
238 elseif sign == 1202 % E1 stable , E2 unstable , E3 DNE, E4
    unstable
239     E1st_E4un(1,3) = E1st_E4un(1,3)+1;
240 elseif sign == 1212 % E1 stable , E3 stable , E2 E4 unstable
    E1st_E4un(2,3) = E1st_E4un(2,3)+1;
241
242 elseif sign == 1222 % E1 stable , E2 E3 E4 unstable
    E1st_E4un(3,3) = E1st_E4un(3,3)+1;
243
244 end
245 % Case 6: E1 unstable , E4 unstable
246 if sign == 2002 % E1 unstable , E2DNE, E3 DNE, E4 unstable
    E1un_E4un(1,1) = E1un_E4un(1,1)+1;
247
248 elseif sign == 2012 % E1 unstable , E2 DNE, E3 stable , E4
    unstable
249     E1un_E4un(2,1) = E1un_E4un(2,1)+1;

```

```

250     elseif sign == 2022 % E1 unstable, E2 DNE, E3 unstable, E4
        unstable
251         E1un_E4un(3,1) = E1un_E4un(3,1)+1;
252     elseif sign == 2102 % E1 unstable, E2 stable, E3 DNE, E4
        unstable
253         E1un_E4un(1,2) = E1un_E4un(1,2)+1;
254     elseif sign == 2112 % E1 E4 unstable, E2 stable, E3 stable
        E1un_E4un(2,2) = E1un_E4un(2,2)+1;
255     elseif sign == 2122 % E1 E3 E4 unstable, E2 stable
        E1un_E4un(3,2) = E1un_E4un(3,2)+1;
256     elseif sign == 2202 % E1 unstable, E2 unstable, E3 DNE, E4
        unstable
257         E1un_E4un(1,3) = E1un_E4un(1,3)+1;
258     elseif sign == 2212 % E1 E2 E4 unstable, E3 stable
        E1un_E4un(2,3) = E1un_E4un(2,3)+1;
259     elseif sign == 2222 % all unstable
        E1un_E4un(3,3) = E1un_E4un(3,3)+1;
260     end
261 end % end of for k=1:m loop
262
263 %fprintf('F0 > 1 : %d\n', a000);
264 display(E1st_E4dne);
265 disp('E2    DNE;    stable;    unstable');
266 display(E1un_E4dne);
267 disp('E2    DNE;    stable;    unstable');
268 display(E1st_E4st);
269 disp('E2    DNE;    stable;    unstable');
270 display(E1st_E4un);
271 disp('E2    DNE;    stable;    unstable');
272 display(E1un_E4st);
273 disp('E2    DNE;    stable;    unstable');
274 display(E1un_E4un);
275 disp('E2    DNE;    stable;    unstable');
276 end

```

B.4 SIRSIRplot.m

```

1 % Plot the trajectory of 2-strain SIR model.
2 function [t,y] = SIRSIRplot(T)
3 global delta1 delta2 gamma beta0 E1 E2 E3 E4
4 % =====
5 % Data for different cases
6 % =====
7 % Case1000: E1 stable; E2 not exist; E3 not exist; E4 DNE
8 % gamma=17.5047; delta1=0.7801; delta2=0.9553; beta0=27.7309;

```

```

9 % Case2010: E1 unstable; E2 not exist; E3 stable; E4 DNE
10 % gamma=9.7299; delta1=0.5402; delta2=0.8004; beta0=18.4107;
11 % Case2210: E1 unstable; E2 unstable; E3 stable; E4 DNE
12 % gamma=1.5499; delta1=0.8473; delta2=1.4234; beta0=4.2359;
13 % Case 2221 E1 unstable, E2 unstable, E3 unstable, E4 stable:
14 % gamma=3.4675; delta1=0.9706; delta2=1.8996; beta0=33.6607;
15 % Case 2222 E1 unstable, E2 unstable, E3 unstable, E4 unstable:
16 % gamma=3.5244; delta1=0.0356; delta2=0.0394; beta0=10.7309;
17 % Case 2021 E1 unstable, E2 DNE, E3 unstable, E4 stable:
18 % gamma=1.4878; delta1=0.1818; delta2=0.3080; beta0=3.5196;
19 % Case 2022 E1 unstable, E2 DNE, E3 unstable, E4 unstable:
20 gamma=4.6681; delta1=0.0347; delta2=0.0538; beta0=11.5110;
21
22 % =====
23 % Solving the system of ODE
24 % =====
25 s10 = .2; i10 = 10/1e3; r10 = 2*s10; s20 = .2;
26 i20 = 10/(3e2); r20 = 1-s10-i10-r10-s20-i20;
27 initdata = [s10,i10,r10,s20,i20,r20];
28 eqpts;
29 [t,y] = ode45(@twostrain,[0,T],initdata);
30 y(end,:);
31
32 % =====
33 % Plotting the solutions
34 % =====
35 % Figure 1: S1-S2
36 figure(1);
37 set(gcf,'DefaultAxesFontSize',12,'Color','white');
38 plot(y(:,1),y(:,4),'LineWidth',2);
39 hold on;
40 plot(s10,s20,'*r');
41 hold on;
42 scatter(E1(1),E1(4),'c','fill','LineWidth',2);
43 hold on;
44 scatter(E2(1),E2(4),'k','fill','LineWidth',2);
45 hold on;
46 scatter(E3(1),E3(4),'g','fill','LineWidth',2);
47 hold on;
48 scatter(E4(1),E4(4),'m','fill','LineWidth',2);
49 xlabel('S1');ylabel('S2');
50 title('S1-S2');
51 % Figure 2: I1-I2
52 figure(2);
53 set(gcf,'DefaultAxesFontSize',12,'Color','white');

```



```

54 plot(y(:,2),y(:,5), 'LineWidth',2);
55 hold on;
56 plot(i10,i20, '*r');
57 hold on;
58 scatter(E1(2),E1(5), 'c', 'fill', 'LineWidth',2);
59 hold on;
60 scatter(E2(2),E2(5), 'k', 'fill', 'LineWidth',2);
61 hold on;
62 scatter(E3(2),E3(5), 'g', 'fill', 'LineWidth',2);
63 hold on;
64 scatter(E4(2),E4(5), 'm', 'fill', 'LineWidth',2);
65 xlabel('I1');ylabel('I2');
66 title('I1-I2');
67 % Figure 3: R1-R2
68 figure(3);
69 set(gcf, 'DefaultAxesFontSize',12, 'Color', 'white');
70 plot(y(:,3),y(:,6), 'LineWidth',2);
71 hold on;
72 plot(r10,r20, '*r');
73 hold on;
74 scatter(E1(3),E1(6), 'c', 'fill', 'LineWidth',2);
75 hold on;
76 scatter(E2(3),E2(6), 'k', 'fill', 'LineWidth',2);
77 hold on;
78 scatter(E3(3),E3(6), 'g', 'fill', 'LineWidth',2);
79 hold on;
80 scatter(E4(3),E4(6), 'm', 'fill', 'LineWidth',2);
81 xlabel('R1');ylabel('R2');
82 title('R1-R2');
83 % Figure 4: S1-I1-R1
84 figure(4);
85 set(gcf, 'DefaultAxesFontSize',12, 'Color', 'white');
86 plot3(y(:,1),y(:,2),y(:,3), 'LineWidth',2);
87 hold on;
88 plot3(s10,i10,r10, '*r');
89 hold on;
90 scatter3(E1(1),E1(2),E1(3), 'c', 'fill', 'LineWidth',2);
91 hold on;
92 scatter3(E2(1),E2(2),E2(3), 'k', 'fill', 'LineWidth',2);
93 hold on;
94 scatter3(E3(1),E3(2),E3(3), 'g', 'fill', 'LineWidth',2);
95 hold on;
96 scatter3(E4(1),E4(2),E4(3), 'm', 'fill', 'LineWidth',2);
97 xlabel('S1');ylabel('I1');zlabel('R1');
98 title('S1-I1-R1');

```

```

99 % Figure 5: S2-I2-R2
100 figure(5);
101 set(gcf, 'DefaultAxesFontSize', 12, 'Color', 'white');
102 plot3(y(:,4), y(:,5), y(:,6), 'LineWidth', 2);
103 hold on;
104 plot3(s20, i20, r20, '*r');
105 hold on;
106 scatter3(E1(4), E1(5), E1(6), 'c', 'fill', 'LineWidth', 2);
107 hold on;
108 scatter3(E2(4), E2(5), E2(6), 'k', 'fill', 'LineWidth', 2);
109 hold on;
110 scatter3(E3(4), E3(5), E3(6), 'g', 'fill', 'LineWidth', 2);
111 hold on;
112 scatter3(E4(4), E4(5), E4(6), 'm', 'fill', 'LineWidth', 2);
113 xlabel('S2'); ylabel('I2'); zlabel('R2');
114 title('S2-I2-R2');
115
116 display(E1); display(E2); display(E3); display(E4);
117
118 % =====
119 % 2-strain SIR model
120 % =====
121 function dydt = twostrain(~, y)
122 global delta1 delta2 gamma beta0
123 s1 = y(1); i1 = y(2); r1 = y(3); s2 = y(4); i2 = y(5); r2 = y(6);
124 dydt(1) = r2 - beta0*s1*i1 - delta1*s1 + delta2*s2;
125 dydt(2) = beta0*s1*i1 - gamma*i1;
126 dydt(3) = gamma*i1 - r1;
127 dydt(4) = r1 - beta0*s2*i2 - delta2*s2 + delta1*s1;
128 dydt(5) = beta0*s2*i2 - gamma*i2;
129 dydt(6) = gamma*i2 - r2;
130 dydt = dydt';
131
132 % =====
133 % function of the parameter
134 % =====
135 function eqpts
136 global delta1 delta2 gamma beta0 E1 E2 E3 E4
137 % E1
138 S11 = delta2 / (delta1 + delta2); I11 = 0; R11 = 0;
139 S12 = delta1 / (delta1 + delta2); I12 = 0; R12 = 0;
140 % E2
141 S21 = gamma * (beta0 - gamma + delta2 + delta2 * gamma) / ...
142     (beta0 * (gamma + delta1 + gamma * delta1));
143 I21 = 0; R21 = 0;

```

```

144 S22 = gamma/beta0;
145 I22 = (beta0*delta1-gamma*delta1-delta2*gamma) / ...
146       (beta0*(gamma+delta1+gamma*delta1));
147 R22 = gamma*I22;
148 % E3
149 S31 = gamma/beta0;
150 I31 = (beta0*delta2-gamma*delta2-delta1*gamma) / ...
151       (beta0*(gamma+delta2+gamma*delta2));
152 R31 = gamma*I31;
153 S32 = gamma*(beta0-gamma+delta1+delta1*gamma) / ...
154       (beta0*(gamma+delta2+gamma*delta2));
155 I32 = 0; R32 = 0;
156 % E4
157 D = 2*beta0*(1+gamma);
158 R41 = (gamma/D)*((beta0-2*gamma)+(delta2-delta1)*(1+gamma));
159 R42 = (gamma/D)*((beta0-2*gamma)+(delta1-delta2)*(1+gamma));
160 S41 = gamma/beta0; S42 = gamma/beta0;
161 I41 = R41/gamma; I42 = R42/gamma;
162 % equilibrium points
163 E1 = [S11 , I11 , R11 , S12 , I12 , R12];
164 E2 = [S21 , I21 , R21 , S22 , I22 , R22];
165 E3 = [S31 , I31 , R31 , S32 , I32 , R32];
166 E4 = [S41 , I41 , R41 , S42 , I42 , R42];

```

B.5 simulateE4.m

```

1 % This function evaluates roots of the characteristic polynomial
2 % of E4, distributes them to different cases, counts the number
3 % of occurrence of each case, and give an sample for each case.
4 function simulateE4(n)
5 % Input Parameters
6 %   n - Times of simulation
7
8 % The countsigns is a 20*2 matrix. Each element of the second
9 % column stands for a case of combination of positive/negative
10 % real/complex roots, and the first column is the number of
11 % occurrence of the corresponding case.
12 countsigns=zeros(20,1);
13 % These are the symbols of cases. The first digit is the number
14 % of positive real roots in the roots of the polynomial, the second
15 % digit the number of negative real roots, the third digit the
16 % number of positive complex roots, and the last digit the number of
17 % negative complex roots. There are 20 conditions in total.
18 countsigns(1,2)=5000; countsigns(2,2)=4100;
19 countsigns(3,2)=3200; countsigns(4,2)=2300;

```

```

20 countsigns(5,2)=1400; countsigns(6,2)=0500;
21 countsigns(7,2)=3020; countsigns(8,2)=3002;
22 countsigns(9,2)=2120; countsigns(10,2)=2102;
23 countsigns(11,2)=1220; countsigns(12,2)=1202;
24 countsigns(13,2)=0320; countsigns(14,2)=0302;
25 countsigns(15,2)=1040; countsigns(16,2)=1004;
26 countsigns(17,2)=1022; countsigns(18,2)=0140;
27 countsigns(19,2)=0104; countsigns(20,2)=0122;
28
29 for k=1:n
30     % =====
31     % Parameters
32     % =====
33     rp = 0; % number of real positive root
34     rn = 0; % number of real negative root
35     cp = 0; % number of complex positive root
36     cn = 0; % number of complex negative root
37     % Generate gamma, delta1, delta2 and beta.
38     gamma = 22*rand(1);
39     delta1 = rand(1);
40     delta2 = rand(1);
41     beta0 = 5*gamma*rand(1);
42     beta = round(rand(1)*5)*beta0;
43     % The polynomial
44     R0 = (beta - 2*gamma)/((abs(delta1-delta2))*(gamma+1));
45     r1 = (beta-2*gamma+(delta2-delta1)*(1+gamma))/(2+2*gamma);
46     r2 = (beta-2*gamma+(delta1-delta2)*(1+gamma))/(2+2*gamma);
47     c1 = 2+delta1+delta2+r1+r2;
48     c2 = 1+2*delta1+2*delta2+(2+delta2+gamma)*r1 + ...
49         (2+delta1+gamma)*r2+r1*r2;
50     c3 = delta1+delta2+(2*delta2+2*gamma+1+delta2*gamma)*r1+ ...
51         (2*delta1+2*gamma+1+delta1*gamma)*r2+(1+gamma)*r1*r2;
52     c4 = (delta2+gamma+delta2*gamma)*r1+(delta1+gamma+...
53         delta1*gamma)*r2+(1+gamma^2+4*gamma)*r1*r2;
54     c5 = 2*gamma*(1+gamma)*r1*r2;
55
56     % =====
57     % Calculation
58     % =====
59     % If R0 < 1, then E4 does not exist.
60     if(R0 < 1)
61         continue;
62     % solve the polynomial
63     else
64         p = [1, c1, c2, c3, c4, c5];

```

```

65     rx = roots(p);
66     % identify the roots.
67     for i = 1:5
68         if (isreal(rx(i)) == 1 && sign(real(rx(i))) == 1)
69             rp = rp + 1;
70         elseif (isreal(rx(i)) == 1 && sign(real(rx(i))) == -1)
71             rn = rn + 1;
72         elseif (isreal(rx(i)) == 0 && sign(real(rx(i))) == 1)
73             cp = cp + 1;
74         elseif (isreal(rx(i)) == 0 && sign(real(rx(i))) == -1)
75             cn = cn + 1;
76         end
77     end
78     sign1 = rp*1000+rn*100+cp*10+cn;
79     % identify the case
80     for n = 1:20
81         if (sign1 == countsigns(n,2))
82             countsigns(n,1) = countsigns(n,1) + 1;
83         end
84     end
85 end
86 end
87
88 display(countsigns);
89 end

```

B.6 E4root.m

```

1 % This function can evaluate the roots of the characteristic
2 % polynomial of E4 with dynamically changing beta, and plot
3 % the graph for all roots in complex coordinate
4 function E4root(m, n)
5 % Input Parameters
6 % m - Times of simulation
7 % n - step size of beta
8
9 % variables of five cases
10 display('case 0500')
11 % gamma=0.163493; beta=0.572847; delta1=0.827510; delta2=0.931735;
12 % display('case 0320')
13 % gamma=2.767152; beta=5.980414; delta1=0.016157; delta2=0.011327;
14 % display('case 0302')
15 % gamma=0.233436; beta=1.120709; delta1=0.919705; delta2=0.469961;
16 % display('case 0122')
17 % gamma=5.030269; beta=49.974446; delta1=0.337011; delta2=0.125742;

```

```

18 % display('case 0104')
19 gamma=7.523786; beta=20.519838; delta1=0.835185; delta2=0.364033;
20
21 rx1=zeros(m,2); rx2=zeros(m,2); rx3=zeros(m,2);
22 rx4=zeros(m,2); rx5=zeros(m,2);
23
24 for k=1:m
25     rp = 0; % number of roots that are real and positive
26     rn = 0; % number of roots that are real and negative
27     cp = 0; % number of roots that are complex and positive
28     cn = 0; % number of roots that are complex and negative
29
30     % =====
31     % Solve for the roots
32     % =====
33     r1 = (beta-2*gamma+(delta2-delta1)*(1+gamma))/(2+2*gamma);
34     r2 = (beta-2*gamma+(delta1-delta2)*(1+gamma))/(2+2*gamma);
35     c1 = 2+delta1+delta2+r1+r2;
36     c2 = 1+2*delta1+2*delta2+(2+delta2+gamma)*r1+...
37         (2+delta1+gamma)*r2+r1*r2;
38     c3 = delta1+delta2+(2*delta2+2*gamma+1+delta2*gamma)*r1+ ...
39         (2*delta1+2*gamma+1+delta1*gamma)*r2+(1+gamma)*r1*r2;
40     c4 = (delta2+gamma+delta2*gamma)*r1+(delta1+gamma+...
41         delta1*gamma)*r2+(1+gamma^2+4*gamma)*r1*r2;
42     c5 = 2*gamma*(1+gamma)*r1*r2;
43     D3 = c1*(c5-c1*c4)+c3*(c1*c2-c3);
44     D4 = c5*(c1*c4-c5)-c5*c2*(c1*c2-c3)+c4*D3;
45     p = [1, c1, c2, c3, c4, c5];
46     rx = roots(p);
47
48     % identify the case
49     for i = 1:5
50         if (isreal(rx(i)) == 1 && sign(real(rx(i))) == 1)
51             rp = rp + 1;
52         elseif (isreal(rx(i)) == 1 && sign(real(rx(i))) == -1)
53             rn = rn + 1;
54         elseif (isreal(rx(i)) == 0 && sign(real(rx(i))) == 1)
55             cp = cp + 1;
56         elseif (isreal(rx(i)) == 0 && sign(real(rx(i))) == -1)
57             cn = cn + 1;
58         end
59     end
60     signnew = rp*1000+rn*100+cp*10+cn; % sign for all roots
61
62     % If the sign changes, print out the old roots and new roots

```

```

63     if k>1
64         if signold ~= signnew
65             display(k);
66             fprintf('betaold=%f, beta=%f\n', betaold, beta);
67             fprintf('Delta3old=%f, Delta3=%f\n', D3old, D3);
68             fprintf('Delta4old=%f, Delta4=%f\n', D4old, D4);
69             display(rxold);
70             display(rx);
71         end
72     end
73
74     % Make the new ones be the old ones in next loop
75     rx1(k,1)=real(rx(1)); rx1(k,2)=imag(rx(1));
76     rx2(k,1)=real(rx(2)); rx2(k,2)=imag(rx(2));
77     rx3(k,1)=real(rx(3)); rx3(k,2)=imag(rx(3));
78     rx4(k,1)=real(rx(4)); rx4(k,2)=imag(rx(4));
79     rx5(k,1)=real(rx(5)); rx5(k,2)=imag(rx(5));
80
81     betaold=beta;
82     beta = beta+n;
83     D3old=D3; D4old=D4;
84     signold = signnew; rxold=rx;
85 end
86
87 % =====
88 % Plot the graph
89 % =====
90 set(gcf, 'DefaultAxesFontSize',18, 'Color', 'white');
91 plot(rx1(:,1), rx1(:,2), 'r*', 'MarkerSize',3);
92 hold on
93 plot(rx2(:,1), rx2(:,2), 'k*', 'MarkerSize',3);
94 hold on
95 plot(rx3(:,1), rx3(:,2), 'b*', 'MarkerSize',3);
96 hold on
97 plot(rx4(:,1), rx4(:,2), 'g*', 'MarkerSize',3);
98 hold on
99 plot(rx5(:,1), rx5(:,2), 'm*', 'MarkerSize',3);
100 hold on
101 xlabel('Real Axis');
102 ylabel('Imaginary Axis');
103 title('Trace of Roots');
104 legend('root 1', 'root 2', 'root 3', 'root 4', 'root 5');

```